

ERDC/GSL TR-04-16

Geotechnical and Structures Laboratory



**US Army Corps  
of Engineers®**  
Engineer Research and  
Development Center

*Infrastructure Technologies Research Program*

## **Seismic Analysis of Intake Towers Considering Multiple-Support Excitation and Soil-Structure Interaction Effects**

Aidcer L. Vidot, Luis E. Suárez, Enrique E. Matheu, and  
Michael K. Sharp

September 2004

20041117 076

# **Seismic Analysis of Intake Towers Considering Multiple-Support Excitation and Soil-Structure Interaction Effects**

Aidcer L. Vidot and Luis E. Suárez

*Department of Civil and Environmental Engineering  
University of Puerto Rico  
Mayagüez Campus  
Mayagüez, PR 00681*

Enrique E. Matheu and Michael K. Sharp

*Geotechnical and Structures Laboratory  
U.S. Army Engineer Research and Development Center  
3909 Halls Ferry Road  
Vicksburg, MS 39180-6199*

Final report

Approved for public release; distribution is unlimited

**ABSTRACT:** This report investigates the seismic response of intake-outlet towers. The effect of different ground accelerations at the supports of the tower and inspection bridge is examined. The water outside and inside the tower is accounted for by added masses. The accelerations at the bridge support and tower base are obtained from a finite element model of the dam and soil foundation. The other effect examined is the soil-structure interaction. First, a direct approach based on a finite element model of the tower, bridge, and dam with the earthquake motion applied at the bedrock is used. The second approach uses a frame model of the tower and bridge with springs and dashpots accounting for the soil-structure interaction. This simple model provides reasonable results if adequate values of the torsional spring are used. The effects of the soil-structure interaction proved to be much more important than the multiple-support excitation.

**DISCLAIMER:** The contents of this report are not to be used for advertising, publication, or promotional purposes. Citation of trade names does not constitute an official endorsement or approval of the use of such commercial products. All product names and trademarks cited are the property of their respective owners. The findings of this report are not to be construed as an official Department of the Army position unless so designated by other authorized documents.

**DESTRUCTION NOTICE:** For classified documents, follow the procedures in DoD 5200.22-M, Industrial Security Manual, Section II-19, or DoD 5200.1-R, Information Security Program Regulation, Chapter IX. For unclassified, limited documents, destroy by any method that will prevent disclosure of contents or reconstruction of the document.

# Contents

---

Conversion Factors, Non-SI to SI Units of Measurement .....	viii
Preface .....	ix
1—Introduction .....	1
Problem Description .....	1
Justification .....	2
Contribution to the State of the Art .....	3
Report Organization .....	4
2—Literature Review .....	6
Intake-Outlet Towers .....	6
Seismic Response of Intake-Outlet Towers .....	7
Multiple-Support Seismic Excitation .....	8
3—General Methodology .....	13
Selection of the Case Study .....	14
Summary .....	23
4—Finite Element Models .....	25
Brief Description of the Computer Program SAP2000 .....	25
Brief Description of the Computer Program QUAD4M .....	26
Finite Element Models .....	26
Summary .....	32
5—The MATLAB-Based Program .....	33
Multiple-Support Excitation Formulation .....	33
Simplified Procedure for Added Hydrodynamic Masses .....	38
Soil-Structure Interaction .....	46
Summary .....	49
6—Numerical Results .....	51
Seismic Input .....	51
Multiple-Support Excitation Analysis .....	56
Soil-Structure Interaction .....	60
Response Spectrum Analysis .....	79
Summary .....	82



7—Conclusions and Recommendations .....	84
Summary and Conclusions .....	84
Recommendations for Further Studies .....	86
References .....	88
SF 298	

## List of Figures

---

Figure 1.	Model of the intake-outlet tower plus the access bridge .....	3
Figure 2.	Typical section of an intake-outlet tower .....	6
Figure 3.	Two-dimensional model of a pipeline system .....	12
Figure 4.	Location of Arkabutla Dam .....	15
Figure 5.	Shear curves .....	16
Figure 6.	Damping curves .....	17
Figure 7.	Distribution of the soil layers in Arkabutla Dam .....	21
Figure 8.	Dimensions of Arkabutla Dam .....	22
Figure 9.	Cross section and front view of the typical intake-outlet tower (units in feet) .....	23
Figure 10.	Simplified model of the intake-outlet tower using SAP2000 .....	27
Figure 11.	Finite element model of Arkabutla Dam using QUAD4M .....	28
Figure 12.	Finite element model of Arkabutla Dam using SAP2000 .....	29
Figure 13.	Finite element model of Arkabutla Dam plus its intake using SAP2000 .....	30
Figure 14.	Spring-dashpot model of the typical intake tower using SAP2000 .....	31
Figure 15.	Plot for normalized outside hydrodynamic added mass for circular cylindrical towers .....	41
Figure 16.	Properties of "equivalent" circular cylindrical towers corresponding to uniform elliptical towers associated with added hydrodynamic mass due to surrounding water .....	42
Figure 17.	Normalized outside hydrodynamic added mass for an infinitely long tower .....	43
Figure 18.	Plot for normalized inside hydrodynamic added mass for circular cylindrical towers .....	45
Figure 19.	Acceleration time-history of the El Centro earthquake .....	52

Figure 20.	Acceleration time-history of the Loma Prieta earthquake at Gilroy Building .....	52
Figure 21.	Smoothed Fourier spectrum of the El Centro earthquake .....	53
Figure 22.	Smoothed Fourier spectrum of the Loma Prieta earthquake at Gilroy Building .....	53
Figure 23.	Raw and smoothed Fourier spectra for El Centro earthquake.....	54
Figure 24.	Raw and smoothed Fourier spectra of the Loma Prieta earthquake at Gilroy Building .....	54
Figure 25.	Arias intensity for El Centro earthquake.....	55
Figure 26.	Arias intensity for Loma Prieta earthquake at Gilroy Building .....	55
Figure 27.	Acceleration at the tower base and bridge support (El Centro).....	57
Figure 28.	Acceleration at the tower base and bridge support (Loma Prieta) .....	57
Figure 29.	Relative displacements (El Centro).....	58
Figure 30.	Relative displacements (Loma Prieta).....	58
Figure 31.	Relative displacements obtained with the frame model with MSE effects and with the dam plus tower finite element model (El Centro).....	59
Figure 32.	Relative displacements obtained with the frame model with MSE effects and with the dam plus tower finite element model (Loma Prieta) .....	60
Figure 33.	Accelerations at the tower base and bridge support obtained with the dam plus intake tower finite element model (El Centro) .....	61
Figure 34.	Accelerations at the tower base and bridge support obtained with the dam plus intake tower finite element model (Loma Prieta) .....	61
Figure 35.	Accelerations at the base of the dam obtained with the dam plus intake tower and the dam alone finite element models (El Centro) .....	62
Figure 36.	Accelerations at the base of the dam obtained with the dam plus intake tower and the dam alone finite element models (Loma Prieta) .....	62
Figure 37.	Nodes of the finite element model selected to calculate the acceleration .....	63
Figure 38.	Acceleration time-histories at two nodes at the free surface on opposite sides of the dam .....	63
Figure 39.	Acceleration time-histories at a node at the tower base and on the free surface .....	64
Figure 40.	Displacements at the top of the tower for the dam plus tower and the frame with spring-dashpot models (El Centro) .....	66

Figure 41.	Displacements at the top of the tower for the dam plus tower and the frame with spring-dashpot models (Loma Prieta) .....	66
Figure 42.	Displacements at the top of the tower for the dam plus tower and the frame with spring-dashpot models (Coalinga) .....	67
Figure 43.	Displacements at the top of the tower for the dam plus tower and the frame with spring-dashpot models (Anza) .....	67
Figure 44.	Displacements obtained with the dam plus tower and spring-dashpot models with frequency independent and dependent coefficients (Coalinga) .....	69
Figure 45.	Mode shape obtained with the dam plus tower and bridge finite element model .....	72
Figure 46.	Mode shape obtained with the dam plus tower finite element model without the bridge .....	72
Figure 47.	Relative displacements obtained with the dam plus tower and the new spring-dashpot models including all modes (Anza) .....	75
Figure 48.	Relative displacements obtained with the dam plus tower and the new spring-dashpot models considering only the first mode of vibration (Anza) .....	75
Figure 49.	Relative displacements obtained with the dam plus tower and the new spring-dashpot models including all modes (Coalinga) .....	76
Figure 50.	Relative displacements obtained with the dam plus tower and the new spring-dashpot models considering only the first mode of vibration (Coalinga) .....	76
Figure 51.	Relative displacements obtained with the dam plus tower and the new spring-dashpot models including all vibration modes (El Centro) .....	77
Figure 52.	Relative displacements obtained with the dam plus tower and the new spring-dashpot models considering only the first mode of vibration (El Centro) .....	77
Figure 53.	Acceleration response spectra for the El Centro earthquake .....	81
Figure 54.	Acceleration response spectra for the Loma Prieta earthquake .....	81

## List of Tables

---

Table 1.	Properties of the Soil Layers of Arkabutla Dam .....	16
Table 2.	Degradation Curves of the Soils in Arkabutla Dam .....	17
Table 3.	Parameters of the Intake Towers of the USACE Inventory .....	22
Table 4.	Final Parameters of the Typical Intake-Outlet Tower .....	22

Table 5.	Properties of Rigid Circular Plate on Surface of Half-Space.....	32
Table 6.	Strong Motion Duration, Predominant Periods, and Frequencies for Several Earthquakes.....	68
Table 7.	Natural Periods of the Simplified Intake Tower Model.....	70
Table 8.	Modal Frequencies for the Simplified Intake Tower Model.....	70
Table 9.	Natural Periods and Frequencies for the Dam Plus Tower Model .....	71
Table 10.	Stiffness Coefficients for the Spring-Dashpot Model.....	73
Table 11.	Natural Periods for the Simplified Intake Tower Model with the New Coefficients .....	74
Table 12.	Natural Frequencies for the Simplified Intake Tower Model with the New Coefficients .....	74
Table 13.	Base Shears and Overturning Moments for El Centro and Loma Prieta Earthquakes (Response Spectrum Analysis).....	81
Table 14.	Base Shears and Overturning Moments for El Centro and Loma Prieta Earthquakes (Time-History Analysis).....	81
Table 15.	Base Shears and Overturning Moments for El Centro and Loma Prieta Spectrum-Compatible Accelerograms (Response Spectrum Analysis).....	82
Table 16.	Base Shears and Overturning Moments for El Centro and Loma Prieta Spectrum-Compatible Accelerograms (Time- History Analysis) .....	82

# Conversion Factors, Non-SI to SI Units of Measurement

---

Multiply	By	To Obtain
cubic feet	0.02831685	cubic meters
feet	0.3048	meters
inches	25.4	millimeters
kips (force)	4.448222	kilonewtons
kips (mass)	453.5924	kilograms
miles (U.S. statute)	1.609347	kilometers
square feet	0.09290304	square meters

# Preface

---

The work described herein was sponsored by Headquarters, U.S. Army Corps of Engineers (HQUSACE), as part of the Infrastructure Technologies Research Program. The Program Manager was Ms. Yazmin Seda-Sanabria, Geosciences and Structures Division (GSD), Geotechnical and Structures Laboratory (GSL), U.S. Army Engineer Research and Development Center (ERDC). The research was performed under Work Unit 33013, "Rehabilitation of Concrete Hydraulic Structures Under Extreme Loads," for which Dr. Enrique E. Matheu, Geotechnical and Earthquake Engineering Branch (GEEB), GSD, was the Principal Investigator. The HQUSACE Program Monitor was Ms. Anjana Chudgar, CECW-EW.

The research described herein was conducted by Ms. Aidcer L. Vidot and Prof. Luis E. Suárez, Department of Civil Engineering and Surveying, University of Puerto Rico at Mayagüez, and by Drs. Matheu and Michael K. Sharp, GEEB, GSL. This publication was prepared under the general supervision of Dr. David W. Pittman, Acting Director, GSL; Dr. Robert L. Hall, Chief, GSD; and Dr. Joseph P. Koester, Chief, GEEB.

COL James R. Rowan, EN, was Commander and Executive Director of ERDC, and Dr. James R. Houston was Director.

# 1 Introduction

---

## Problem Description

Outlet works consist of a combination of structures designed to control the release of water from the reservoir as required for project purposes or operation. Outlet works structures are typically found in embankment dams, although in some cases concrete dams may exhibit outlet works detached from the dam. Outlet works are used to pass diversion flows during construction, regulate flood flows, support water supply and power generation operations, aid in emptying the reservoir in an emergency condition, and permit reservoir lowering for inspections and special repairs. In many dams, outlet works provide the only means of lowering the reservoir and thereby providing a means of minimizing the risk of catastrophic failure in the event of an earthquake. Their proper functioning immediately after an earthquake is very important, since the controlled release of the reservoir could help to prevent additional propagation of damage by reducing the hydrostatic loads.

Typically, outlet works consist primarily of an intake structure and a conduit or tunnel, in addition to other features necessary for operation, such as control gates, approach and discharge channels, and energy dissipaters (Headquarters, U.S. Army Corps of Engineers 2003). The intake structure may exhibit multiple openings with the corresponding valves or gates, to allow for more effective control of the flow of water. The control mechanisms are typically located within the intake tower, although configurations with control gates within the conduit or at the downstream end of the conduit are also possible. Intake towers can be separated into two broad categories: free-standing (vertical structure, typically with a service bridge at the top) and inclined (structure supported against the abutment). This research work will concentrate on free-standing intake towers, since they constitute the most common structural configuration.

The dynamic response of an intake tower during an earthquake may present quite complex characteristics due to many factors. The water, inside and outside of the tower, plays an important role in the modification of the response of the structure. In addition, the complexity of the analysis is increased by important soil-structure interaction effects. In addition, although this effect is generally neglected, the intake structure is actually subjected to multiple-support excitations. Although a free-standing intake tower is basically a hollow column, it exhibits an inspection bridge that connects the top of the tower to the dam or abutment. Therefore, the intake-outlet tower and bridge system has two

well-separated supports. Different local soil conditions, traveling wave effects, phase difference in the seismic motions, and other factors can cause a spatial variability of the ground motion at the supports. These multiple-support excitation effects can be important in the calculation of the seismic response of the system. Therefore, and because of the lack of previous investigations dealing with these effects, there is a need to study in more detail their influence on the dynamic response of the intake tower.

The main objective of the research described herein was to calculate the dynamic response of the intake-outlet tower under earthquake excitations, giving proper consideration to multiple-support effects and soil-structure interaction phenomena. Several alternative methods were considered for the analyses in order to compare the results obtained with a simplified model of the tower-bridge system with those generated using more refined finite element models. It is advantageous to show that the results from a simplified model are comparable to those from the more accurate finite element models, since practicing engineers will in all likelihood make use of the simplified model.

## **Justification**

Several natural hazards affect both human lives and properties. Earthquake ground motions are one of the most destructive hazards, and this threat is increased by its random nature. Earthquakes affect all human-made structures founded on ground or buried. The failure of certain structures also compromises the lives of many people living in the surrounding areas. Dams are among these critical structures; thus, they have been and remain the object of attention of the structural and geotechnical engineering community. Intake-outlet towers could play an important role in preventing the catastrophic failure of a dam after an earthquake, by providing a means of controlling the water level and reducing the corresponding hydrostatic pressure. The structural safety of these towers and their functional capability in the event of a major earthquake are crucial.

As pointed out by Dove (1996), many intake towers under the responsibility of the U.S. Army Corps of Engineers (USACE) are located in areas associated with high seismic activity. Therefore, the analysis of the structural safety and functional capability of these towers in the event of a major earthquake reaches paramount importance. Observations during past earthquakes demonstrated the importance of the effects of multiple excitations in some extended structures, such as bridges, pipelines, and dams (Der Kiureghian and Neuenhofer 1991). In studies that are currently performed for the analysis, design, and verification of intake towers, these multiple excitation effects are not considered. This fact increases the need to develop better procedures for the accurate prediction of the dynamic response of these structures. This report intends to address this concern by developing a relatively simple model to perform seismic response analysis of free-standing intake towers considering the spatial variability of the ground motion and soil-structure interaction effects. In addition, this report will evaluate the importance of considering these two effects in the analysis.



## Contribution to the State of the Art

To the authors' knowledge, all previous studies dealing with free-standing intake towers did not consider the effects of attached structures such as the access bridge (Figure 1), and the models used in the analyses were limited to the towers themselves. In general engineering practice, a typical "stick model" is used to study these towers when the geometry of the tower is relatively simple and the bridge has a light weight. However, it is reasonable to expect that the bridge can have an effect on the response of the tower. Whether the effect of the bridge is such that it reduces or magnifies the seismic response is not clear. Thus, a model of the bridge will be included to calculate the seismic response in order to assess its importance.

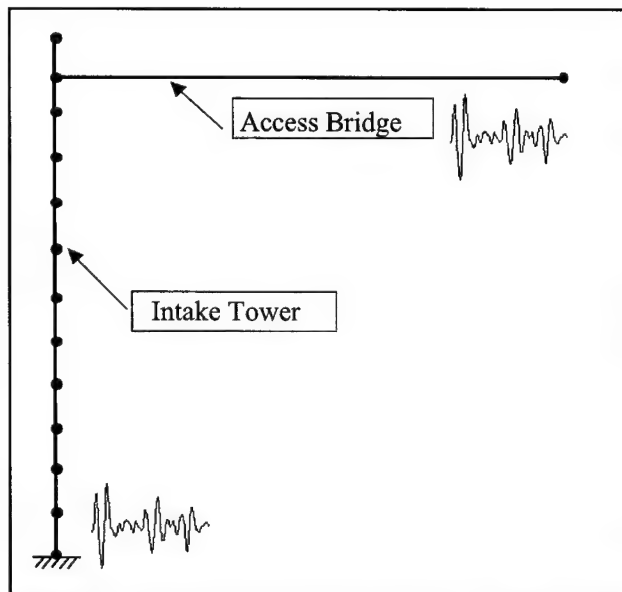


Figure 1. Model of the intake-outlet tower plus the access bridge

The inclusion of a model of a bridge can be easily accomplished either by modeling the bridge as a flexural beam that is rigid in the axial direction or by using frame elements including axial deformation. Appropriate definition of the ground acceleration is more complex. It is reasonable to expect that the absolute acceleration at the base of the tower may not be the same as that experienced by the tower at the elevation where the bridge connection is made. Therefore, the effects of traveling waves, lack of coherence, and other phenomena associated with multiple-support excitations must be considered.

One could argue that these effects may not be important since the distances between the supports of the tower and bridge are not substantial. This may be true in some cases, but the fact that the supports are at different elevations can heighten the dissimilar character of the ground acceleration. The ground acceleration could suffer amplification or attenuation depending on the soil properties,

the height of the dam, and the frequency content of the excitation. The previous studies dealing with multiple-support excitations considered that the supports of the extended structure were well separated in space but at the same elevation. This is the case of the highway bridges and pipeline systems. Therefore, one of the areas that will be studied is the case in which the supports are at different levels. In addition, other analyses will be performed considering the soil-structure interaction effects to obtain a better insight into the dynamic response of this type of structure.

The first step undertaken to consider the multiple-support excitation will be to prepare a finite element model of the topography of the earthen dam. This model will be used to calculate the response at the location of the bridge. The records of the absolute acceleration at the latter point and at the base are used as input for a combined model of the bridge and tower. A computer program will be developed to account for the effects of the multiple-support excitations and the soil-structure interaction in the tower and access structure.

## Report Organization

Chapter 1 contains a general introduction. The justification of the research and the problem description are briefly discussed. The chapter includes a discussion of the specific contribution to the state of the art.

Chapter 2 contains a brief literature review related to the topics of the research. The first section of this chapter presents information regarding studies of intake-outlet towers. The seismic response of these towers is discussed in the second section. This section explains the factors that affect the response of this type of structure, such as the fluid-structure and soil-structure interaction and multiple-support excitation effects. The third section is devoted to the general concepts and a review of the most relevant works on the subject of multiple-support excitation effects. Also included is a brief review of several investigations related to soil-structure interaction effects in structures such as intake-outlet towers.

Chapter 3 describes the general methodology used to accomplish the goals of this report. The chapter starts with an introduction of the assumptions and considerations taken into account during the research. There is a brief description of the finite element models and computer programs developed for this research. There is also a description of the procedure followed to select the specific tower used in the study. Drawings showing the final intake-outlet tower selected for the case study are presented in this section.

Chapter 4 is devoted to the description of the finite element models developed during this research and previously mentioned in the general methodology (Chapter 3). The chapter includes descriptions of the SAP2000 and QUAD4M computer programs, which are the principal tools for the finite element analyses used in this research. The rest of the chapter contains detailed information

regarding the finite element models developed during the study, such as dimensions, boundary conditions, and input data.

Chapter 5 contains the description of the computer program developed in the MATLAB computational environment, which is the main tool used in this research. The formulations upon which this computer program is based are discussed in several sections. First, the multiple-support excitation formulation is presented in detail. The simplified approach developed by Goyal and Chopra (1989a) for the calculation of the added hydrodynamic masses along the height of the tower is also included. The procedure to account for the soil-structure interaction effects in the towers is also presented in this chapter. Furthermore, information concerning the numerical integration and time-history analysis performed by the computer program is provided at the end of the chapter.

Chapter 6 presents the most important results of all the analyses undertaken during this research. In particular, the results obtained with the finite element models and with the computer program developed for this research are presented. A comparison of the results is also included. The results are presented in the form of graphs and tables. The chapter ends with a discussion of the results obtained.

Chapter 7 contains the conclusions and recommendations. A summary of the main findings and achievements is discussed. A list of recommendations is included, to provide guidance for further studies.

## 2 Literature Review

---

### Intake-Outlet Towers

For most earthen, and some concrete, dams the release of water is controlled through concrete intake-outlet towers. They form the entrance to the reservoir outlet works (Daniell and Taylor 1994). The intake-outlet towers contain the equipment necessary for the controlled discharge of impounded water to accommodate flood operation demands or to fulfill services such as water supply or power generation. They stand above the outlet tunnel or conduit used to transport water out of the reservoir. A system of valves and gates is used to control the flow of the water through the outlet (Figure 2). These towers could play an important role in preventing the catastrophic failure of a dam after an earthquake by controlling the water level and reducing the corresponding hydrostatic pressure. Several configurations of intake-outlet towers are found, such as free-standing towers with uniform or tapered cross section, and inclined towers supported on the rock abutments (such as in the Cerrillos Dam, Puerto Rico). The construction of inclined towers is recommended in high seismic zones or in areas with soil stability problems.

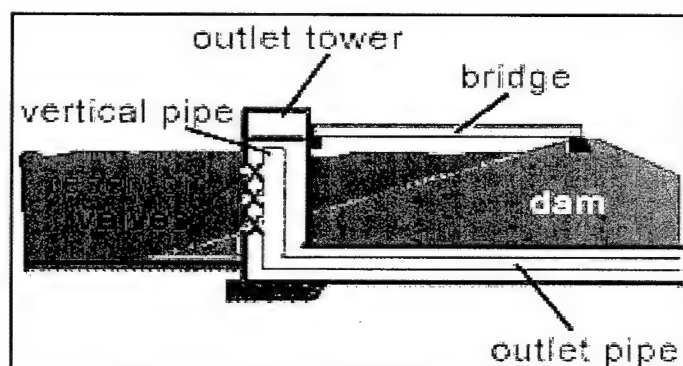


Figure 2. Typical section of an intake-outlet tower

The USACE conducted an inventory of the towers under its jurisdiction in the United States during the period 1993-1997 (Dove 1996) identifying approximately 77 towers located in seismic zones 2 or greater, as defined by the Uniform

Building Code (International Conference of Building Officials, ICBO 1997). The majority of these towers are very lightly reinforced structures. A later USACE study (Dove 1998) concentrated efforts on the evaluation of the ductility characteristics of these towers. The final goal was to develop nonlinear analysis techniques to estimate the ductility and to determine the ability of these towers to resist the earthquake demand. An additional objective was to identify the possible failure mechanisms in these towers by means of laboratory-scale tests (Dove 2000).

The cost of retrofitting an existing tower has been estimated to be between \$5 million and \$100 million depending on the work required (Dove 2000). Therefore, an accurate estimation of the seismic performance could potentially lead to significant savings. Nevertheless, the retrofitting is an expensive process, and it causes disruptions to the operation of the dam. To avoid these problems, intake towers in seismically active regions should be designed to withstand earthquakes using rational analytical methods based on a thorough understanding of the dynamic behavior of such towers (Daniell and Taylor 1994). The success of a given tower in resisting a seismic event depends on the magnitude of the loads imposed by the earthquake and the structural details that control the characteristics of the nonlinear dynamic response. It has been argued that the techniques currently used for dynamic analysis of intake towers may not properly include these factors (Dove 1996).

## **Seismic Response of Intake-Outlet Towers**

According to previous studies, the response of an intake tower under dynamic loading can be strongly influenced by its interaction with the surrounding outside and inside water (Daniell and Taylor 1994). It is now accepted that the surrounding water modifies the dynamic properties of the tower and causes additional dynamic forces (Chopra and Liaw 1975). One of the leading authorities on the subject, Prof. Anil Chopra, has shown that the water acts as an incompressible fluid in the important modes of vibration of the tower. The hydrodynamic interaction effects can then be represented by equivalent added masses along the height of the tower. These effects are taken into account exactly by added-mass functions if the tower is uniform, and quite accurately if the cross-sectional dimensions of the tower vary along its height (Goyal and Chopra 1989b). The surrounding water tends to lower the vibration frequencies and to modify the mode shapes (Chopra and Liaw 1975). The simple approach based on added masses may introduce errors at higher vibration modes, but for a response dominated by the fundamental vibration modes, it is adequate to adopt this simplified procedure. Williams (1990) analyzed the seismic response of intake-outlet towers using a more sophisticated approach, i.e., Green's functions to obtain the response of the towers. Williams placed special emphasis on the study of squat towers (towers with larger diameter to water depth ratios). In his investigation, Williams demonstrated that, for both slender and squat towers, the interior surrounding water tends to lower the natural frequencies of the system compared with those predicted by including only the exterior surrounding water. The proper consideration of the fluid-structure interaction effects is important to understand

the behavior of the intake towers during the event of an earthquake. Although important, this topic is not the primary focus of this research. For the analyses to be undertaken, the hydrodynamic interaction will be considered using accepted modern procedures.

It was also demonstrated that the earthquake response of intake towers can be computed with enough accuracy by considering only the contribution of the first natural vibration modes (Goyal and Chopra 1989c). This is acceptable when their fundamental vibration periods are located in the acceleration or velocity-controlled regions of the earthquake response spectrum. In another study, the same authors (Goyal and Chopra 1989b) demonstrated that the influence of the shear deformations and rotatory inertia should be considered in the analysis of squat towers when only the first two vibration modes are taken into account.

Soil-structure interaction effects constitute another important factor that may have a significant influence on the seismic response of intake towers. The tower-foundation-soil interaction increases the fundamental natural period and the effective damping at this period. These effects are the consequence of the flexibility and energy dissipation in the foundation-soil region (Goyal and Chopra 1989c). The dissipation of energy through radiation (and to a lesser extent, the material damping) has a significant effect in the response. The tower-foundation interaction effects are stronger for stiff structures and for those with large tower height to footing radius ratio. The influence of this effect depends on several factors such as the flexibility of the foundation soil and the slenderness ratio, and it becomes smaller in the presence of water.

## **Multiple-Support Seismic Excitation**

Free-standing intake towers are typically connected to an access bridge, and this feature may influence their response during an earthquake. This response occurs because the supports of the tower and bridge are located at different elevations and thus may experience different ground accelerations. Therefore, to carry out a more rigorous analysis of structures, it is necessary to consider the effects of the spatially varying ground motions at the supports.

The effects of the variation of the support motions on the response of extended structures have been investigated for some time. The principal causes of the spatial variation in seismic ground motions are (Der Kiureghian and Neuenhofer 1991) the difference in the arrival times of seismic waves, the loss of coherency of the motions due to reflections and refractions of the waves in the medium where they travel, and the difference in the local soil conditions at each support location. Observations during past earthquakes, for example the Loma Prieta earthquake of 17 October 1989, demonstrated the importance of the effects of multiple excitations in the supports of some extended structures such as bridges. The failure of several extended structures during the Loma Prieta earthquake highlighted the need for a better understanding of this response (Der Kiureghian and Neuenhofer 1991).

To understand the response of structures subjected to multiple-support excitations, it is necessary to introduce the equation of motion for these types of systems. The equation of motion for a structure subjected to multiple-support excitations can be approximated by Equation 1 (Rutenberg and Heidebrecht 1988):

$$M\ddot{u} + C\dot{u} + Ku = -MR\ddot{u}_g(t) \quad (1)$$

where

$M$  = mass matrix (lumped or consistent) associated with active (or dynamic) degrees of freedom (dofs)

$u$  = relative displacement vector

$C$  = damping matrix

$K$  = stiffness matrix

$R$  = quasi-static influence matrix (given by Equation 2)

$\ddot{u}_g$  = seismic acceleration vector of support points

$$R = -K_{ii}^{-1} K_{ib} \quad (2)$$

In Equation 2,  $K_{ii}^{-1}$  is the inverse of the stiffness matrix related to the motion at the interior dofs, and  $K_{ib}$  is the stiffness matrix whose rows are associated with the interior dofs and its columns with the motions of the supports.

Several methods and procedures have been developed to account for the multiple-support excitation effects in extended structures such as bridges, dams, and pipeline systems. To select the proper approach for the analysis of intake towers subjected to multiple-support excitation, a survey of the available procedures was performed. The most relevant methods are briefly reviewed in the following paragraphs.

Various approaches, such as response spectrum and time-history methods, were used to evaluate the response of multi-degree of freedom (MDF) systems to multiple-support excitations (Yamamura and Tanaka 1990). One of the disadvantages of the time-history method is that the results from the analysis are specific to the set of selected time-histories. Also, this method requires extensive computational effort (Der Kiureghian and Neuenhofer 1991). However, if the motions at all the supports of the structure are available as a function of time, this method accounts for the effect in an exact way. Moreover, it is easy to understand, and its implementation is not very difficult.

Another method used for the analysis of systems subjected to spatially varying ground motion is the random vibration approach. This method accounts for the effects in the correlation between support motions by means of the corresponding power spectral density and correlation functions. This approach is based on the statistical characterization of a set of ground motions between the

different supports of a structural system (Der Kiureghian and Neuenhofer 1991). However, this method is not presently used by practicing engineers.

Der Kiureghian and Neuenhofer (1991) proposed a response spectrum method that properly includes the effects of the variability in ground motions that arise from the wave passage effect, the incoherence effect, and the local soil conditions. This method is based on the random vibration theory. The procedure requires the calculation of cross-mode correlation coefficients, influence and modal participation factors, and peak ground response at each station corresponding to each modal damping and frequency. In theory, the method is straightforward because it employs a simple combination rule. However, it requires extensive computation and the knowledge of many factors that, in the majority of the cases, are unknown.

Another study by Harichandran and Wang (1988), confirmed that the response of long structures (such as bridges, dams, and pipeline systems) to earthquake ground excitation is sensitive to traveling wave effects as well as spatial correlation effects of ground accelerations. The same authors (Harichandran and Wang 1989) examined the effects of the spatial variation of the ground motion on an indeterminate structure using as an example a two-span beam model. This study also showed that it is important to consider the spatial variation of earthquake ground motion in the analysis of long, statically indeterminate structures.

Zerva (1991) studied the effects of the spatial variability and propagation of seismic ground motions in lifeline systems. He indicated that the variability of ground motions between supports may be attributed to the loss of coherence and phase difference of the seismic motions. The loss of coherence may result from the variability in the rupture process and discontinuities in the travel path of the seismic waves from the source to the site (Zerva 1991). The same author (Zerva 1988) had previously examined the vertical response of a two-span bridge due to the spatial variation of ground motion. The analysis was made using the power spectral density of the acceleration and the correlation function. This study showed that the assumption of equal support motion in the seismic evaluation of bridges may underestimate the response. The same author (Zerva 1992) also presented a review of the techniques used for the modeling of the spatial variability of the seismic ground motions. Zerva described in this paper the procedure for the stochastic analysis and assigned special importance to the following tasks:

- a. The definition of the smoothed cross covariance functions of the motion between two stations.
- b. The evaluation of the smoothed cross spectrum by the Fourier transform.
- c. The estimation of the coherency (a complex number) and the coherence (a real number between 0 and 1). The coherency is a measure of similarity in the seismic motions. For uncorrelated motions, its value is equal to zero.



- d. The estimation of the lagged coherency, which describes the phase variability in the acceleration time series.

The study also presented several empirical coherency models. The majority of these models are event-specific and time-consuming, and hence their use is limited in earthquake engineering. For these reasons, the models will not be considered for this investigation.

Rutenberg and Heidebrecht (1988) also proposed a response spectrum analysis for multiple-support excitations in bridges using a traveling wave approach. Their method approximates the modal displacement time-history plot near its peak using a sine curve. It was observed that the accuracy of the results obtained with this method depends on the transit time of the wave and the natural period. A good agreement in the results was found in the range of  $\tau_{\max} < 0.25T$  and  $T > 0.1$  sec, where  $\tau_{\max}$  is the transit time and  $T$  is the lowest natural period affecting the displacement response.

Loh and Ku (1995) developed another method to calculate the structural response for multiple-support seismic excitations, based on the studies of Der Kiureghian and Neuenhofer (1991). Loh and Ku (1995) emphasized the importance of the spatial variation of the ground motion and the procedures for combining the responses. This method simplifies the power spectral density of the ground motion and system transfer function in order to evaluate analytically the frequency integrals that define the cross-correlation coefficients. The authors pointed out that they were able to achieve a great reduction in the computational time of the response. Also, they mentioned that even though they neglected the cross-correlation effects between quasi-static and dynamic responses, this did not introduced significant errors.

Shaw (1975) studied the seismic response of nuclear plant equipment accounting for multiple-support excitations. Pieces of equipment such as pipelines are subjected to spatial variation in the acceleration of the supports during seismic excitation. Shaw proposed a response spectrum analysis based in the typical equations of motion. The proposed method decomposes the multiple-support excitation problem into a series of problems subject to a single support excitation. Afterwards, the individual responses are combined using the square root of the sum of the squares (SRSS) rule.

Loh (1991) studied the spatial variability of ground motion in buried pipelines. In this study, he put special emphasis on the differences in soil stiffness and the variations in seismic waves along the segments of the pipelines. He used a two-dimensional model to represent the pipeline system subjected to different seismic waves (Figure 3). In this model  $K_p$  and  $m$  represent the stiffness and mass of the pipeline, respectively, and  $K_{g1}$  and  $K_{g2}$  are the stiffness of the soil at each segment. Loh demonstrated the importance of considering the variability in soil stiffness to calculate the response of this type of system. He indicated that this effect is more significant than the spatial variation in the seismic waves.

A more recent study by Zembaty and Rutenberg (2002) focused on the local site amplification effects on the seismic response of multi-support structures. The

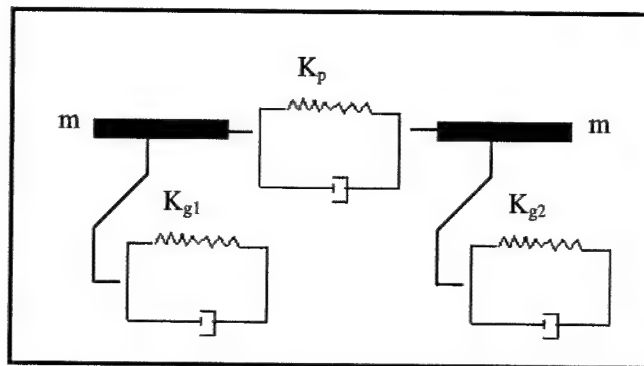


Figure 3. Two-dimensional model of a pipeline system (adapted from Loh 1991)

authors recognized the importance of three main sources of spatial variability: the complexity of the seismic source, the velocity of propagation of waves, and the geological and geometrical heterogeneities of the ground. The effects of the first two sources on the structural response increase for structures with larger dimensions. However, the third source can be important at short distances. The local soil conditions amplify the structural response and may contribute substantially to the overall spatial seismic effects. The authors cited the collapse of the Cypress Street Viaduct during the 1989 Loma Prieta earthquake as an example of spatial variability of the motion at the supports. It is now believed that the significant variation in local soil conditions along the viaduct generated different excitations at the supports, causing its collapse. They adopted for their study a complex coherency model in order to measure the similarity between motions. These authors proposed a simplified response spectrum approach that considered the local variations in site amplification based on the studies by Safak (1995). This model properly reflects the physics of soil amplification resulting from the reflections of the shear waves. The study by Zembaty and Rutenberg (2002) demonstrated the importance of the site amplification effects in the response of multi-supported structures. These effects significantly modify the seismic response of such structures. Zembaty and Rutenberg's study serves as additional motivation and justification for this technical report.

After examining the literature on the subject, it was decided to carry out a time-history analysis of the tower plus bridge system in which the different excitations at their two supports are considered. This will allow us to assess the importance of the effect for the particular case under study. Although all the previously mentioned investigations concluded that the influence of the multiple-support excitations on the response is important, they dealt primarily with spatially extended structures. The tower plus bridge system is not quite a spatially extended system; the difference in the support motions will arise from the fact that the supports are at different elevations along the dam. As shown in Figure 2, the base of the intake tower is near the toe of the dam, and the abutment of the bridge is close to the crest.

### 3 General Methodology

---

An overview of the general methodology and a brief description of the finite element models used during this research are presented in this chapter. Several analytical tools were used to accomplish the objectives. The study began with a review of the methods currently available for the analysis of structures with multiple-support excitations. This study was done to find the most practical method for the analysis of the system formed by the intake tower and the bridge. A review of the studies related to intake-outlet towers and access structures was also performed. This study was used to obtain general knowledge about the factors that affect the seismic response of this structural system. These factors included the hydrodynamic and soil-structure interaction effects. This review was also intended to identify methods for the analysis and computer modeling of these towers. A typical existing intake-outlet tower was selected for the case study.

The next step of the research was the development of several finite element models. The finite element models were created using the SAP2000 (CSI 2000) and QUAD4M (Idriss et al. 1973) computer programs. These models included

- a. A frame model of the intake tower using SAP2000.
- b. A finite-element model of the earthen dam using QUAD4M.
- c. A finite-element model of the earthen dam using SAP2000.
- d. A finite-element model of the combined dam-tower system using SAP2000.
- e. A frame model of the intake tower with added springs and dashpots representing soil-structure effects using SAP2000.

The finite element models were used for the seismic response analysis of the intake tower and bridge system. An acceleration time-history was applied to the base of each finite element model. The same boundary conditions were applied to each model to compare the results. These models were developed to obtain the acceleration time-histories at the base of the tower and at the support of the inspection or access bridge. Detailed information about the conditions used in each model will be discussed in the next chapter. Only a brief description of the models is presented in this chapter as part of the general methodology used.

Another tool developed during this investigation was a computer program for the analysis of intake-outlet towers created using the MATLAB (MathWorks 2000) computational environment. The program can account for the effects of multiple-support excitations by means of a time-history analysis. It reads the earthquake accelerograms at two different locations in the horizontal and vertical directions. The formulation for the response calculation is based on the relative displacements formulation of the equations of motion. The program also includes the water-tower interaction effects using the formulation developed by Goyal and Chopra (1989b), which introduces the concept of added hydrodynamic masses along the height of the tower. The program can include the access structure using truss or frame elements. In the last phase of the research, the soil-structure interaction effects were included in this computer program. The problem of soil-structure interaction was introduced by adding the springs and dashpots at the base of the tower and at the support of the bridge.

The results obtained with the MATLAB computer program and with the more comprehensive finite element models were examined and compared. The absolute acceleration and relative and absolute displacement time-histories were compared. Conclusions and recommendations for the seismic analysis of the towers, including the importance of considering the bridge and the multiple-support excitations, were drawn based on the results.

## **Selection of the Case Study**

A specific case study was needed as framework for this research effort, and the earthen dam selected was Arkabutla Dam. This example was selected based on recommendations from personnel at the U.S. Army Engineer Research and Development Center (ERDC) during a summer internship that the primary author completed at the ERDC Geotechnical and Structures Laboratory (GSL) in Vicksburg, MS.

Arkabutla Dam is located in northern Mississippi, 30 miles<sup>1</sup> south of Memphis, TN, west of Interstate 55 (Figure 4). The dam is of a rolled earth fill, approximately 11,500 ft long with an average height of 66 ft. It was constructed during the period 1940 to 1943. The dam is founded in a valley filled with alluvium. The alluvium consists of a top stratum of fine-grained sediments and a substratum of predominantly coarse-grained sediments (Chang 1990). The fine-grained sediments consist of clays, silts, and some fine sands.

The soil properties vary along the length of the dam. The soil strata were divided into 17 layers to obtain a better representation of the dam in the finite element model. These properties were obtained from USACE data available in the GSL. Table 1 presents the values for the shear modulus ( $G$ ), shear wave velocity ( $V_s$ ), unit weights ( $\gamma$ ), and the number of shear and damping curves used in the analysis for the different types of soils. The modulus and damping degradation curves are presented in Figures 5 and 6, respectively. These plots show,

---

<sup>1</sup> A table of factors for converting non-SI units of measurement to SI units is presented on page viii.



Figure 4. Location of Arkabutla Dam

respectively, how the modulus decreases and the damping ratio increases, due to the nonlinear behavior of the soil. These plots were obtained from the values shown in Table 2. This table shows the values of ratio  $G/G_{max}$  and damping ratio  $\zeta$  as a function of the shear strain  $\gamma$  used as input to the model developed in QUAD4M for all the types of soil that comprise the dam.

The finite element model of the embankment was developed using these soil properties in two computer programs, SAP2000 and QUAD4M. Figure 7 shows the soil strata in the finite element model of the Arkabutla Dam identified according to the material number listed in Table 1.

Initially, the real intake-outlet tower of the Arkabutla Dam was chosen for the analysis. However, because the geometry of this tower is quite complex, a typical intake-outlet tower representative of the existing tower inventory in the United States was finally used. In addition, using this typical tower allows a general understanding of the dynamic behavior of the whole population of USACE towers. The dimensions were chosen based on data available from the Corps' inventory (Figure 8).

Dove (1996) conducted a comprehensive study aimed at identifying the most important structural characteristics of intake towers in the USACE inventory. This study focused on 162 intake towers. A summary of the results is presented in Table 3, highlighting the mean value and standard deviation of some of the main geometric properties of these towers (Dove and Matheu 2000a,b). Based on these dimensions, typical tower and access structures were defined to use in conjunction with the analyses of Arkabutla Dam. Table 4 summarizes the final

**Table 1**  
**Properties of the Soil Layers of Arkabutla Dam**

Number	Material Type	Shear Curve No.	Damp Curve No.	$\gamma$ kip/ft <sup>3</sup>	$\nu$	G kip/ft <sup>2</sup>	$V_s$ ft/sec
1	Sand upper bound	5	5	0.120	0.35	1,073	600
2	Sand upper bound	5	5	0.120	0.35	1,908	800
3	Sand average	4	4	0.120	0.35	1,722	760
4	Sand average	4	4	0.120	0.35	604	450
5	Clay 20 - 40 <sup>1</sup>	9	7	0.120	0.35	1,461	700
6	Clay 10 -20	8	8	0.120	0.35	477	400
7	Clay 20 - 40	9	8	0.120	0.35	1,461	700
8	Clay 20 - 40	9	8	0.120	0.35	604	450
9	Clay 20 - 40	9	8	0.120	0.35	1,461	700
10	Clay 20 - 40	9	8	0.120	0.35	604	450
11	Clay 20 - 40	9	8	0.120	0.35	1,814	780
12	Clay 20 - 40	9	8	0.120	0.35	477	400
13	Clay 20 - 40	9	8	0.120	0.35	1,461	700
14	Sand upper bound	5	5	0.120	0.35	1,583	700
15	Clay 20 - 40	9	8	0.120	0.35	1,461	700
16	Rock	1	1	0.150	0.38	93,168	5,000
17	Sand upper bound	5	5	0.120	0.35	2,981	1,000

<sup>1</sup> The number 20-40 or 10-20 indicates the plasticity index (PI) of the clay soil.

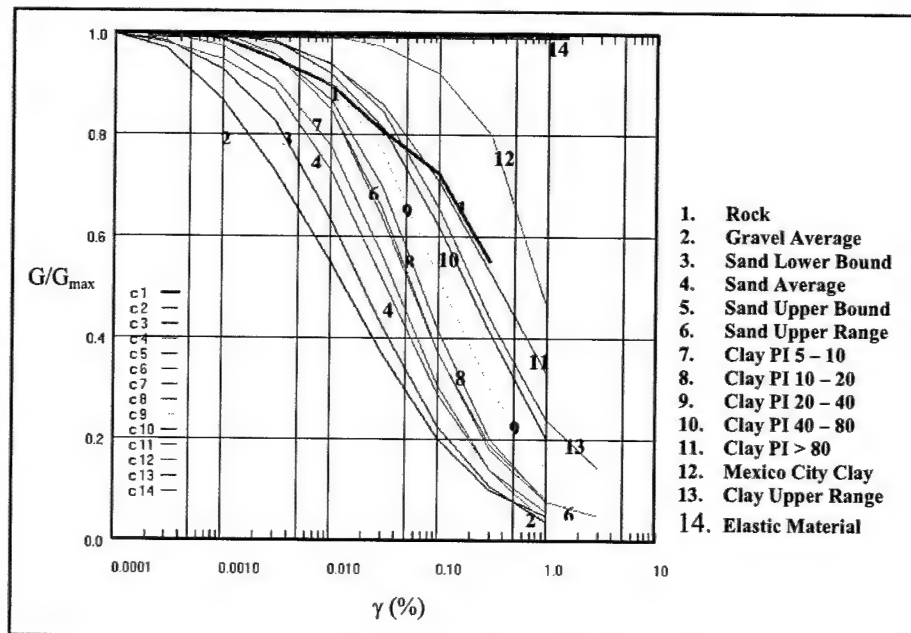


Figure 5. Shear curves

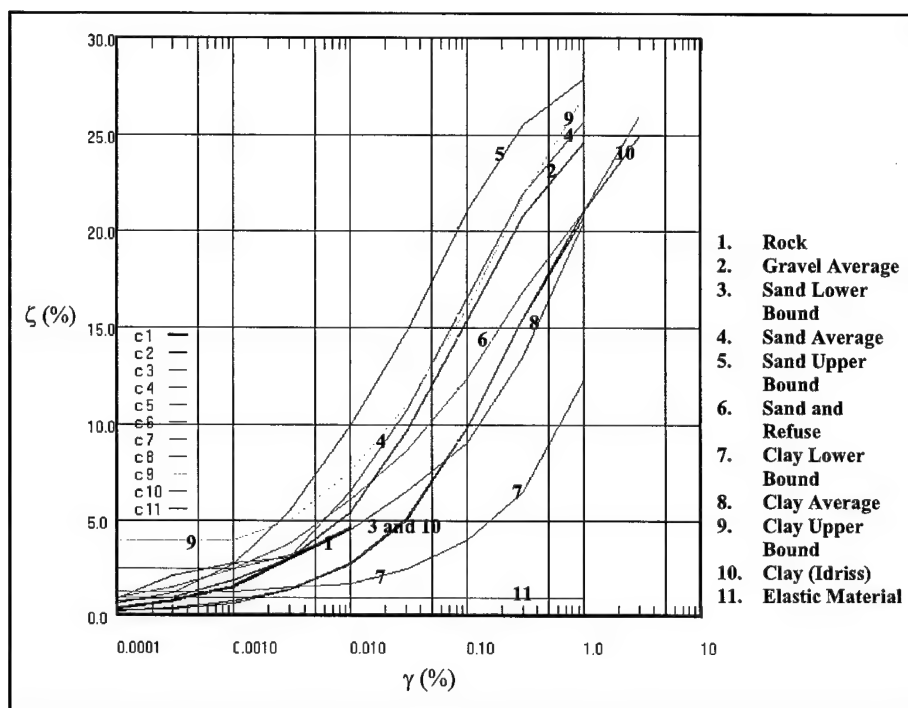


Figure 6. Damping curves

**Table 2**  
**Degradation Curves of the Soils in Arkabutla Dam**

**Curve #1      Modulus Reduction SAND Upper Bound (Seed and Idriss 1970)**

Strain, $\gamma$ (%)	0.0001	0.0003	0.001	0.003	0.01	0.03	0.01	0.3	1
$G/G_{max}$	1	1	0.99	0.96	0.85	0.655	0.37	0.19	0.085

**Curve #1      Damping      SAND Upper Bound (Seed and Idriss 1970)**

Strain, $\gamma$ (%)	0.0001	0.0003	0.001	0.003	0.01	0.03	0.01	0.3	1
$\zeta$ (%)	0.7	1.2	2.7	5.5	9.9	14.8	21	25.5	27.9

**Curve #2      Modulus Reduction SAND Upper Bound (Seed and Idriss 1970)**

Strain, $\gamma$ (%)	0.0001	0.0003	0.001	0.003	0.01	0.03	0.01	0.3	1
$G/G_{max}$	1	1	0.99	0.96	0.85	0.655	0.37	0.19	0.085

**Curve #2      Damping      SAND Upper Bound (Seed and Idriss 1970)**

Strain, $\gamma$ (%)	0.0001	0.0003	0.001	0.003	0.01	0.03	0.01	0.3	1
$\zeta$ (%)	0.7	1.2	2.7	5.5	9.9	14.8	21	25.5	27.9

(Sheet 1 of 4)

**Table 2 (Continued)**

**Curve #3 Modulus Reduction SAND Average (Seed and Idriss 1970)**

Strain, $\gamma$ (%)	0.0001	0.0003	0.001	0.003	0.01	0.03	0.01	0.3	1
$G/G_{max}$	1	0.98	0.95	0.89	0.73	0.52	0.29	0.14	0.06

**Curve #3 Damping SAND Average (Seed and Idriss 1970)**

Strain, $\gamma$ (%)	0.0001	0.0003	0.001	0.003	0.01	0.03	0.01	0.3	1
$\zeta$ (%)	0.9	2.1	2.8	3.1	6.5	10.7	16.5	21.9	25.7

**Curve #4 Modulus Reduction SAND Average (Seed and Idriss 1970)**

Strain, $\gamma$ (%)	0.0001	0.0003	0.001	0.003	0.01	0.03	0.01	0.3	1
$G/G_{max}$	1	0.98	0.95	0.89	0.73	0.52	0.29	0.14	0.06

**Curve #4 Damping SAND Average (Seed and Idriss 1970)**

Strain, $\gamma$ (%)	0.001	0.0003	0.001	0.003	0.01	0.03	0.01	0.3	1
$\zeta$ (%)	0.9	2.1	2.8	3.1	6.5	10.7	16.5	21.9	25.7

**Curve #5 Modulus Reduction CLAY (PI=20 Sun et al. 1988)**

Strain, $\gamma$ (%)	0.0001	0.0003	0.001	0.003	0.01	0.03	0.01	0.3	1
$G/G_{max}$	1	1	1	0.97	0.9	0.77	0.52	0.3	0.4

**Curve #5 Damping CLAY Lower Bound (Seed and Idriss 1970)**

Strain, $\gamma$ (%)	0.0001	0.0003	0.001	0.003	0.01	0.03	0.01	0.3	1
$\zeta$ (%)	1.3	1.3	1.3	1.5	1.7	2.5	4	6.5	12.3

**Curve #6 Modulus Reduction CLAY (PI=20-40 Sun et al. 1988)**

Strain, $\gamma$ (%)	0.0001	0.0003	0.001	0.003	0.01	0.03	0.01	0.3	1
$G/G_{max}$	1	1	1	0.96	0.87	0.7	0.415	0.2	0.08

**Curve #6 Damping CLAY Average (Seed and Idriss 1970)**

Strain, $\gamma$ (%)	0.0001	0.0003	0.001	0.003	0.01	0.03	0.01	0.3	1
$\zeta$ (%)	2.5	2.5	2.5	3.2	4.5	6.5	9	13.5	20.5

**Curve #7 Modulus Reduction CLAY (PI=20-40 Sun et al. 1988)**

Strain, $\gamma$ (%)	0.0001	0.0003	0.001	0.003	0.01	0.03	0.01	0.3	1
$G/G_{max}$	1	1	1	0.97	0.9	0.77	0.52	0.3	0.14

**Curve #7 Damping CLAY Average (Seed and Idriss 1970)**

Strain, $\gamma$ (%)	0.0001	0.0003	0.001	0.003	0.01	0.03	0.01	0.3	1
$\zeta$ (%)	2.5	2.5	2.5	3.2	4.5	6.5	9	13.5	20.5

(Sheet 2 of 4)



**Table 2 (Continued)****Curve #8 Modulus Reduction CLAY (PI=20-40 Sun et al. 1970)**

Strain, $\gamma$ (%)	0.0001	0.0003	0.001	0.003	0.01	0.03	0.01	0.3	1
G/G <sub>max</sub>	1	1	1	0.97	0.9	0.77	0.52	0.3	0.14

**Curve #8 Damping SAND Average (Seed and Idriss 1970)**

Strain, $\gamma$ (%)	0.0001	0.0003	0.001	0.003	0.01	0.03	0.01	0.3	1
$\zeta$ (%)	2.5	2.5	2.5	3.2	4.5	6.5	9	13.5	20.5

**Curve #9 Modulus Reduction CLAY (PI=20-40 Sun et al. 1988)**

Strain, $\gamma$ (%)	0.0001	0.0003	0.001	0.003	0.01	0.03	0.01	0.3	1
G/G <sub>max</sub>	1	1	1	0.97	0.9	0.77	0.52	0.3	0.14

**Curve #9 Damping CLAY Average (Seed and Idriss 1970)**

Strain, $\gamma$ (%)	0.0001	0.0003	0.001	0.003	0.01	0.03	0.01	0.3	1
$\zeta$ (%)	2.5	2.5	2.5	3.2	4.5	6.5	9	13.5	20.5

**Curve #10 Modulus Reduction CLAY (PI=20-40 Sun et al. 1988)**

Strain, $\gamma$ (%)	0.0001	0.0003	0.001	0.003	0.01	0.03	0.01	0.3	1
G/G <sub>max</sub>	1	1	1	0.97	0.9	0.77	0.52	0.3	0.14

**Curve #10 Damping CLAY Average (Seed and Idriss 1970)**

Strain, $\gamma$ (%)	0.0001	0.0003	0.001	0.003	0.01	0.03	0.01	0.3	1
$\zeta$ (%)	2.5	2.5	2.5	3.2	4.5	6.5	9	13.5	20.5

**Curve #11 Modulus Reduction CLAY (PI=20-40 Sun et al. 1988)**

Strain, $\gamma$ (%)	0.0001	0.0003	0.001	0.003	0.01	0.03	0.01	0.3	1
G/G <sub>max</sub>	1	1	1	0.97	0.9	0.77	0.52	0.3	0.14

**Curve #11 Damping CLAY Average (Seed and Idriss 1970)**

Strain, $\gamma$ (%)	0.0001	0.0003	0.001	0.003	0.01	0.03	0.01	0.3	1
$\zeta$ (%)	2.5	2.5	2.5	3.2	4.5	6.5	9	13.5	20.5

**Curve #12 Modulus Reduction CLAY (PI=20-40 Sun et al. 1988)**

Strain, $\gamma$ (%)	0.0001	0.0003	0.001	0.003	0.01	0.03	0.01	0.3	1
G/G <sub>max</sub>	1	1	1	0.97	0.9	0.77	0.52	0.3	0.14

**Curve #12 Damping CLAY Average (Seed and Idriss 1970)**

Strain, $\gamma$ (%)	0.0001	0.0003	0.001	0.003	0.01	0.03	0.01	0.3	1
$\zeta$ (%)	2.5	2.5	2.5	3.2	4.5	6.5	9	13.5	20.5

(Sheet 3 of 4)

**Table 2 (Concluded)****Curve #13 Modulus Reduction CLAY (PI=20-40 Sun et al. 1988)**

Strain, $\gamma$ (%)	0.0001	0.0003	0.001	0.003	0.01	0.03	0.01	0.3	1
G/G <sub>max</sub>	1	1	1	0.97	0.9	0.77	0.52	0.3	0.14

**Curve #13 Damping CLAY Average (Seed and Idriss 1970)**

Strain, $\gamma$ (%)	0.0001	0.0003	0.001	0.003	0.01	0.03	0.01	0.3	1
$\zeta$ (%)	2.5	2.5	2.5	3.2	4.5	6.5	9	13.5	20.5

**Curve #14 Modulus Reduction SAND Upper Bound (Seed and Idriss 1970)**

Strain, $\gamma$ (%)	0.0001	0.0003	0.001	0.003	0.01	0.03	0.01	0.3	1
G/G <sub>max</sub>	1	1	0.99	0.96	0.85	0.655	0.37	0.19	0.085

**Curve #14 Damping CLAY Average (Seed and Idriss 1970)**

Strain, $\gamma$ (%)	0.0001	0.0003	0.001	0.003	0.01	0.03	0.01	0.3	1
$\zeta$ (%)	0.7	1.2	2.7	5.5	9.9	14.8	21	25.5	27.9

**Curve #15 Modulus Reduction CLAY (PI=20-40 Sun et al. 1988)**

Strain, $\gamma$ (%)	0.0001	0.0003	0.001	0.003	0.01	0.03	0.01	0.3	1
G/G <sub>max</sub>	1	1	1	0.97	0.9	0.77	0.52	0.3	0.14

**Curve #15 Damping CLAY Average (Seed and Idriss 1970)**

Strain, $\gamma$ (%)	0.0001	0.0003	0.001	0.003	0.01	0.03	0.01	0.3	1
$\zeta$ (%)	2.5	2.5	2.5	3.2	4.5	6.5	9	13.5	20.5

**Curve #16 Modulus Reduction ROCK (Schnabel et al. 1972)**

Strain, $\gamma$ (%)	0.0001	0.0003	0.001	0.003	0.01	0.03	0.1	0.3
G/G <sub>max</sub>	1	1	0.99	0.95	0.9	0.81	0.725	0.55

**Curve #16 Damping ROCK (Schnabel et al. 1972)**

Strain, $\gamma$ (%)	0.0001	0.0003	0.001	0.003	0.01
$\zeta$ (%)	0.4	0.8	1.5	3	4.6

**Curve #17 Modulus Reduction SAND Upper Bound (Seed and Idriss 1970)**

Strain, $\gamma$ (%)	0.0001	0.0003	0.001	0.003	0.01	0.03	0.01	0.3	1
G/G <sub>max</sub>	1	1	0.99	0.96	0.85	0.655	0.37	0.19	0.085

**Curve #17 Damping SAND Upper Bound (Seed and Idriss 1970)**

Strain, $\gamma$ (%)	0.0001	0.0003	0.001	0.003	0.01	0.03	0.01	0.3	1
$\zeta$ (%)	0.7	1.2	2.7	5.5	9.9	14.8	21	25.5	27.9

(Sheet 4 of 4)

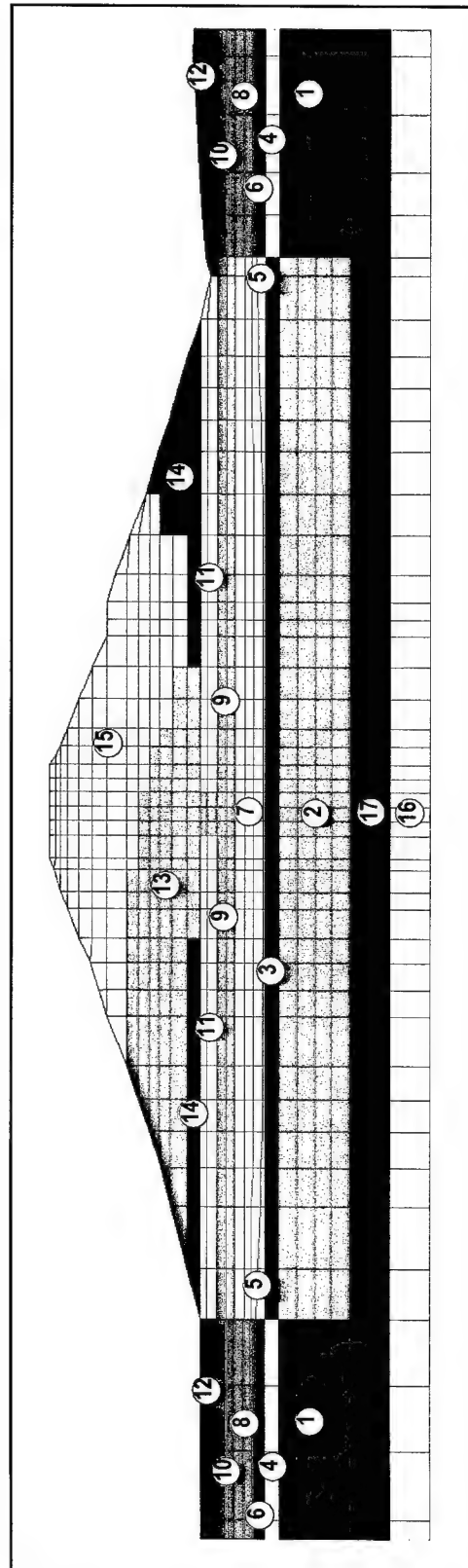


Figure 7. Distribution of the soil layers in Arkabutla Dam

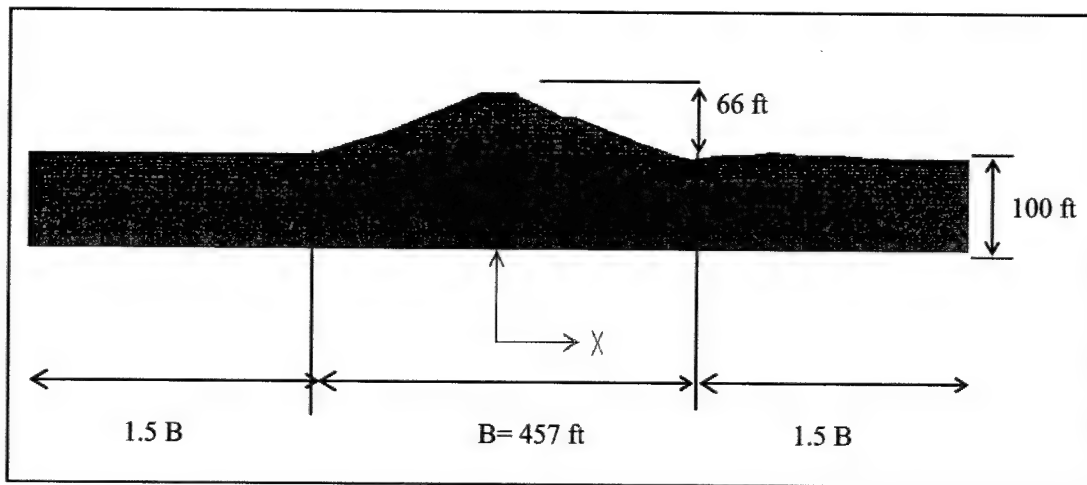


Figure 8. Dimensions of Arkabutla Dam

**Table 3**  
**Parameters of the Intake Towers of the USACE Inventory**

Parameter	Mean Value	Std Deviation
Total structural height, ft	163.31	19.31
Section width (parallel to flow), ft	32.86	3.91
Section width (perpendicular to flow), ft	35.69	3.88
Thickness of the walls (parallel to flow), ft	3.21	0.64
Thickness of the walls (perpendicular to flow), ft	3.28	0.63
Vertical steel reinforcement (walls parallel to flow), %	0.273	0.178
Vertical steel reinforcement (walls perpendicular to flow), %	0.275	0.166

**Table 4**  
**Final Parameters of the Typical Intake-Outlet Tower**

Parameter	Value
Total structural height, ft	75.00
Section width (parallel to flow), ft	30.00
Section width (perpendicular to flow), ft	30.00
Thickness of the walls, ft	3.00
Height of the outside water, ft	57.00
Height of the inside water, ft	57.00
Height of the crest dam, ft	66.00

parameters and dimensions selected for the case study used in this research. The final access bridge selected was longer than the actual bridge of the dam: it has an approximate length of 202.0 ft. The actual access bridge is a truss-type

structure; an equivalent rectangular section was chosen for the bridge in order to simplify the analysis and to generate the computer models in two dimensions. The intake-outlet tower selected has a prismatic hollow square section along its height. The materials of the tower and service bridge are concrete and steel, respectively. Figure 9 shows the cross section and front view of the tower selected.

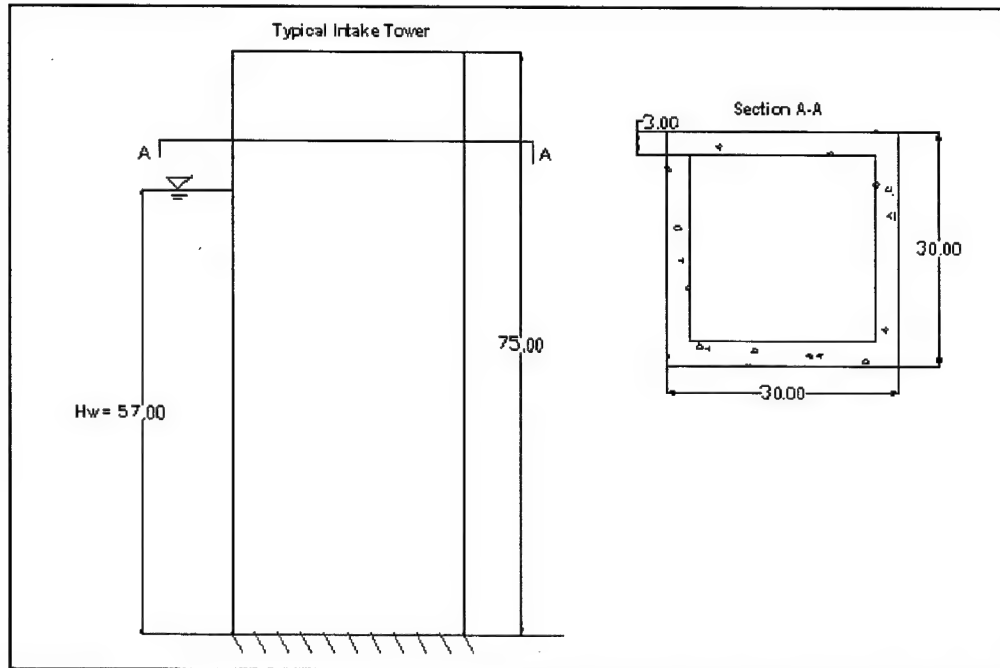


Figure 9. Cross section and front view of the typical intake-outlet tower (units in feet)

As mentioned previously, this tower was used in all the finite element and frame models developed for this investigation. It is expected that this case study will allow a better understanding of the dynamic behavior of intake-outlet towers with similar characteristics. This analysis also intends to identify the factors that have more influence on the seismic response of this type of structural system.

## Summary

This chapter presented a brief description of the methodology used in this research. Basically, this methodology can be divided into four phases: literature review, definition and development of the finite element models, generation of the computer program using the MATLAB computational environment, and analysis of the results. In the next chapter, a detailed description of the conditions used in each finite element model will be presented.

The selection of the particular case study for this investigation was also presented in this chapter. The intake-outlet tower selected was based on typical dimensions found in an inventory of the towers under USACE jurisdiction. The dam selected for this study was Arkabutla Dam in the state of Mississippi. This dam was chosen because of the interest of the Corps in its study. Special considerations were taken to adjust the typical tower and access structure to the dimensions of Arkabutla Dam.

## 4 Finite Element Models

---

This chapter presents a description of the finite element models developed for this investigation. The parameters, boundary conditions, type of analyses, and input data used in each model are also described. The finite element models as described in the previous chapter included (a) a frame model of the stand-alone intake-outlet tower, (b) a model of the Arkabutla Dam using the program QUAD4M, (c) a model of the Arkabutla Dam using the program SAP2000, (d) a model of the Arkabutla Dam plus the intake-outlet tower using SAP2000, and (e) a spring-dashpot model of the tower in SAP2000 and MATLAB. Each model was analyzed to identify the importance of the multiple-support excitation effects and other factors in the response of these towers. Moreover, descriptions of the computer programs SAP2000 and QUAD4M are presented for informative purposes.

### Brief Description of the Computer Program SAP2000

Several commercial software packages have been developed for the analysis and design of all types of civil engineering structures. The Structural Analysis Program (SAP) is one of them. This program was originally developed by Prof. Edward Wilson at the University of California at Berkeley in the 1970s. It was later updated and commercialized by Computers and Structures, Inc., of Berkeley, CA. The most recent version, SAP2000, is among the most powerful and versatile programs available on the market. Some of the program features include static and dynamic analysis, linear and nonlinear analysis, dynamic seismic analysis, static pushover and P-Delta analysis, bridge analysis, nonlinear links, spring elements, multiple coordinate systems, many types of constraints, and several other features (CSI 2000). The majority of the models can be created using the SAP2000 graphical user interface. This graphical interface makes the program very user friendly. For all these reasons, this computer program was selected as the main tool for the analyses performed during this research.

## **Brief Description of the Computer Program QUAD4M**

The program QUAD4M was used during this research to develop one of the finite element models of Arkabutla Dam. QUAD4M is a modification of the QUAD4 program, which was developed in 1973 by researchers at the Department of Civil Engineering, University of California at Berkeley (Idriss et al. 1973). The computer programs QUAD4 and QUAD4M were developed to evaluate the seismic response of soil structures using finite element procedures. The modifications included in the QUAD4M were the implementation of transmitting boundaries and the improvement of the time-stepping algorithm and seismic coefficient calculations (Hudson et al. 1994). The formulation of the program includes a variable damping finite element procedure. This feature permits the accurate analysis of soil structures with irregular boundary conditions and variations in material properties. The irregular boundary conditions, when present, cause the strains developed in each element to vary considerably compared with one-dimensional models such as those used in the SHAKE program. Because the damping in soils is strain dependent, the damping value should be based on the strain developed in each element. Thus, the use of a constant damping value can lead to inaccurate results for some of those conditions. In addition, this procedure allows for the incorporation of both stiffness and damping values that are strain dependent, for each element (Idriss et al. 1973). QUAD4M considers the nonlinear behavior of the soils in an approximate way using the Equivalent Linear Method. The output from the program includes acceleration, displacement, and shear strain time-histories. Because the program is very powerful for analyzing soil structures, it was used to develop the first finite element model of Arkabutla Dam.

## **Finite Element Models**

Five analysis cases were considered in this research to evaluate the effects of the multiple-support excitations in these towers. Other factors were also considered to obtain a complete panorama of the dynamic behavior of this structural system. These factors included the hydrodynamic and soil-structure interaction effects.

First, a simplified model of the intake-outlet tower was developed. This model is very simple and consists of only the tower itself modeled using frame elements. In the current engineering practice, similar column models are used to study intake towers when their geometry is relatively simple. This model was done only for preliminary analysis; it provides an overview of the response of the tower without the effects of the access bridge. Moreover, the model was also used to assess the importance of the inclusion of the access bridge in the analysis of the towers and the effects of the spatial variability of the ground motions at the supports. The model of the tower was created using SAP2000.

The simplified model was developed according to the geometry described in Chapter 3, corresponding to a prismatic hollow section along the height of the



tower with top and base slabs. The two-dimensional model (ZX plane) was discretized using a total of 12 frame elements and 13 nodes. The boundary conditions imposed at the end of the tower were fixed in three directions (translations in X and Z, and rotation around Y) whereas the other points of the tower were free to move. Figure 10 shows the resulting simplified model obtained from SAP2000.

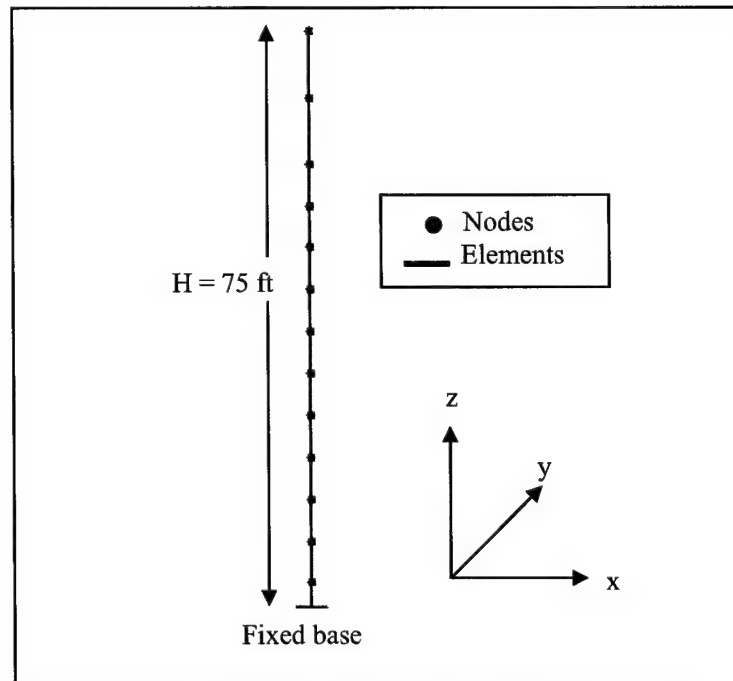


Figure 10. Simplified model of the intake-outlet tower using SAP2000

Other considerations were taken into account for the development of this model. For example, shear deformations and rotational inertia were neglected in the analysis. These effects were neglected in order to compare the results with the MATLAB-based program developed for this investigation. The formulation of the MATLAB program is based in Bernoulli beam elements: these are the simplest beam elements and do not take into account the effects of the shear deformation and rotational inertia. The beam elements in SAP2000 are based in the Timoshenko beam theory, and thus the frame and beam elements include these two special effects.

Fluid-structure interaction effects were included in the model using the concept of hydrodynamic added masses. It was assumed that the water acts as an incompressible fluid. The simplified procedure developed by Goyal and Chopra (1989a) was used to obtain these added masses. A brief description of this procedure is presented in Chapter 5. The input used in the program was an acceleration time-history in the horizontal direction. Vertical acceleration time-histories were not considered in the analyses done with this simple model. The effects of the vertical acceleration in intake-outlet towers are neglected in the majority of the

cases, and this is justified because these structures are extremely rigid in axial direction.

To evaluate the response of the towers subjected to seismic excitation, a time-history analysis was done. The relative and absolute displacement time-histories were obtained from the analysis. First, a modal analysis of the simplified model was performed. From the modal analysis, the mode shapes, modal periods, and frequencies of the tower were obtained.

The principal objective of this research was to examine and establish the importance of the effects of the multiple-support excitations in the intake-outlet towers. For this reason, a finite element model of Arkabutla Dam was created. To obtain reliable results, it is important to choose a tool that is developed specifically for soil structures such as earthen dams and that can provide accurate results. Therefore, the program QUAD4M was used to develop the first model of Arkabutla Dam. QUAD4M analyzes soil structures in a more refined fashion than other general-purpose finite element programs, and it also includes a variable damping finite element procedure. This model was used to calibrate the third model developed with SAP2000. Figure 11 shows the mesh of the finite element model of the dam developed in QUAD4M.

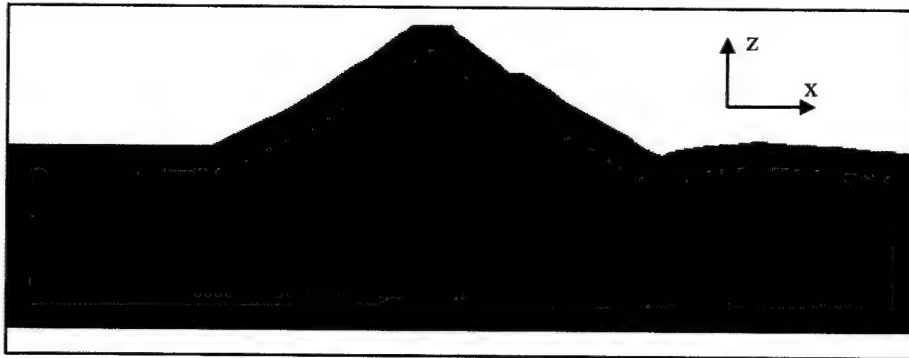


Figure 11. Finite element model of Arkabutla Dam using QUAD4M

The finite element model of the dam consists of 1,404 elements and 1,479 nodes. Plane strain elements were used in the model. The boundary conditions imposed at the base of the embankment were fixed in the two directions (translation in the horizontal X axis and in the vertical Z axis). At the side nodes of the dam foundation, only the vertical translation (Z direction) was restricted for the case of horizontal seismic motion. This condition was achieved with rollers in the horizontal direction. The model was divided into 17 zones representing the different soil layers (see Chapter 3). The input used for the program was a site-specific acceleration time-history.

This model was developed to obtain the absolute accelerations at the top of the dam (point of contact of the access bridge) and at the base of the tower. The dynamic analysis starts with an eigenvalues analysis (modal analysis) of the dam for the determination of the modal periods, frequencies, and modes. Then, a

time-history analysis is performed to calculate the acceleration time-histories at the required locations.

The third finite element model created also corresponds to Arkabutla Dam, but now uses SAP2000. The geometry of the model is identical to the model developed with QUAD4M. The creation of another identical finite element model was needed because QUAD4M cannot consider frame structures such as the intake towers. As was mentioned before, the program was developed to evaluate and analyze soil structures. SAP2000, on the other hand, can combine plane strain elements (such as the dam) with frame elements (such as the intake-outlet tower). The first analyses of the dam using QUAD4M were done because the program is able to provide a better approximation of the seismic response of earth structures. This situation occurs, in part, because of the model's consideration of the nonlinear behavior of the soil and the use of absorbing boundaries. Therefore, the SAP2000 model was calibrated to obtain acceleration time-histories similar to the ones obtained with QUAD4M. The calibration was accomplished by adjusting the value of the modal damping parameter. A damping ratio of 24.5 percent was obtained from the calibration. This value was used for all the modes included in the time-history analysis performed with SAP2000 because this program does not permit assigning different damping values to the elements. Figure 12 illustrates the finite element model generated with SAP2000.

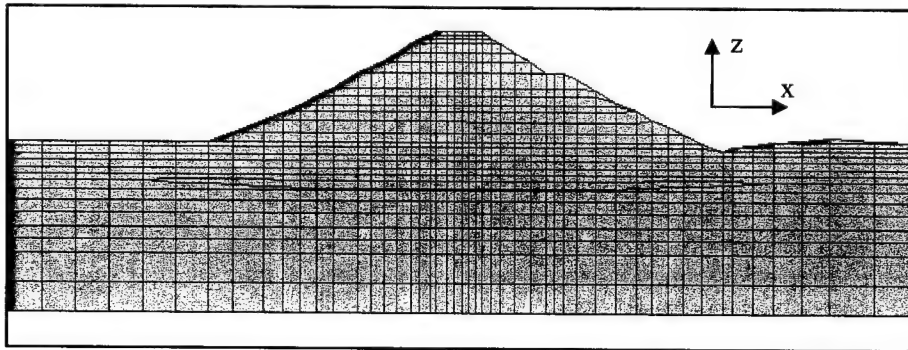


Figure 12. Finite element model of Arkabutla Dam using SAP2000

The model was done in Z-X plane (2-D). The same boundary conditions as previously described for the QUAD4M model were applied to the base of the embankment. The nodal points at the base of the foundation were fixed both in the vertical and horizontal directions. Similar to the other model, horizontal rollers were attached to the nodes at the two sides. Here again, only horizontal acceleration time-histories were used as input.

The two models of the dam just described permit the study of the dynamic behavior of the dam alone. To evaluate and investigate the response of the dam with the intake-outlet tower, it is necessary to use a finite element model that contains both structures. This combined model can be used to analyze the effects of having different excitations at the supports, which is the main objective of the research. In addition, the tower plus dam model is useful to consider the

soil-structure interaction. The mesh, boundary conditions, materials, and input accelerations used in this model were the same as those considered previously for the dam alone. The only modification was the inclusion of the intake tower. Figure 13 illustrates the finite element model of the Arkabutla Dam plus the intake tower.

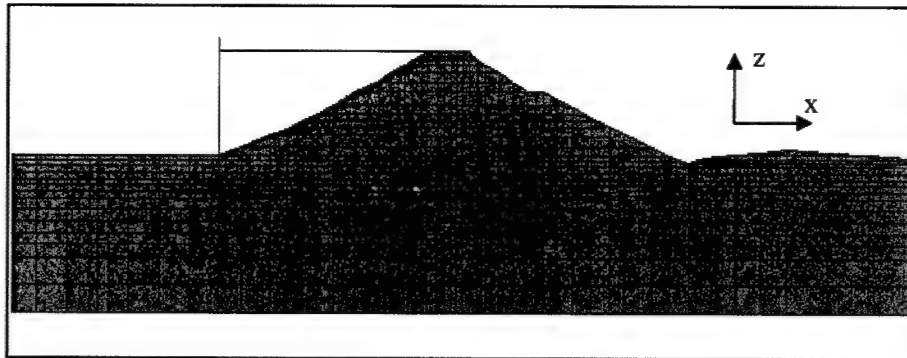


Figure 13. Finite element model of Arkabutla Dam plus its intake using SAP2000

The properties of the tower were described in Chapter 3. The tower was divided into 12 frame elements and 13 nodes. The access bridge was modeled as a long truss element, whose properties were presented in Chapter 3. End releases for the moments were imposed to join the frame element in the access bridge to the truss element. The access bridge is connected at the crest of the dam; its elevation from the base of the tower is 66 ft. A massless and very rigid frame element was embedded into the dam from the base of the tower in order to model more accurately the fixed base condition between the dam and tower.

The output obtained from this model essentially consists of the absolute acceleration, relative and absolute displacement time-histories, and modal periods and frequencies of the combined system.

A model of the intake tower consisting of a frame structure with springs and dashpots at the base was developed in the last phase of this research. This model was used to take into account the soil-structure interaction effects in a simpler way than in the tower-dam model. This phenomenon is caused by the contact stresses between soil and foundation, which are responsible for the deformations in the soil (Newmark and Rosenblueth 1971). Generally, the soil-structure interaction has little effect on the dynamic response of many structures and foundation systems. In other cases, particularly when massive structures are founded in soft soils, this interaction effect can be significant (Kramer 1996). Initially, it was not planned to consider this effect in the study. However, when the results of the fixed-base model created in MATLAB were compared with the SAP2000 finite element model, there were discrepancies that could be attributed only to the soil-structure interaction. A detailed and comprehensive evaluation of the results obtained with this model is discussed in Chapter 7. Figure 14 shows the frame with springs-dashpots model of the intake tower that was created to approximately account for the soil-structure interaction.

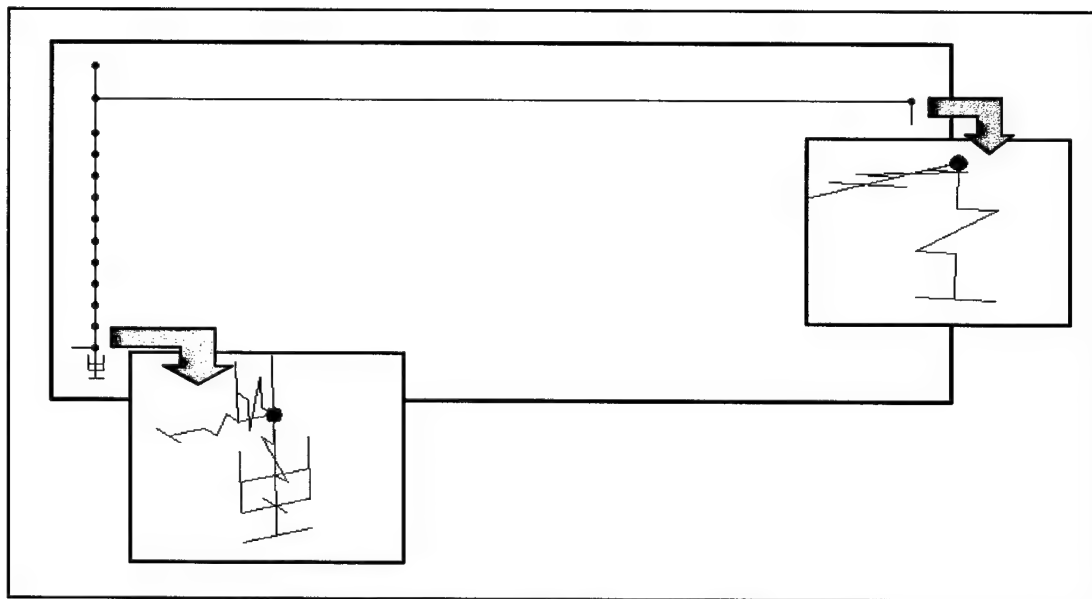


Figure 14. Spring-dashpot model of the typical intake tower using SAP2000

Linear springs (which represent the flexibility of the soil) were attached to the base of the tower and at the end of the access bridge in three degrees of freedom (horizontal and vertical translation and rocking). Viscous dashpots were attached at the base of the tower in the horizontal and vertical directions. Another dashpot in the direction of the rocking motion was also inserted at the base. No dashpots were placed at the base of the bridge. This was done because there is no information in the literature to define the damping constants of the dashpots that represent the radiation damping at the crest of a dam. All the dashpot coefficients available in papers and textbooks were obtained for a uniform or layered half-space.

The stiffness and damping constants for the elements at the base of the tower were calculated from the solutions available in the literature. The first systematic solution of the problem of defining these values was obtained by Lysmer (1965). He developed the stiffness and damping constants for the vertical motion of a rigid circular plate on a half-space taking into account the proper distribution of contact stresses. Later on, other researchers proposed similar coefficients for other types of motion, and for embedded foundations, foundations with other shapes, and foundations on layered soil deposits. The expressions for the stiffness and damping coefficients used in this report were taken from the technical report for SAP2000 (CSI 2000). These solutions were adapted from those published in the book *Fundamentals of Earthquake Engineering* (Newmark and Rosenblueth 1971). Table 10 of the book displays the stiffness and damping coefficients for the spring-dashpot model used in this research. These constants are valid for a rigid circular plate lying on the surface of a half-space and are independent of the frequency of vibration.

In Table 5,  $G$  is the small strain shear modulus of the soil,  $r$  represents the plate radius, and  $\nu$  and  $\rho$  are the Poisson's ratio and mass density of the soil, respectively. When a noncircular foundation is considered, an equivalent radius must be defined in order to use these equations. In the present study, the equivalent radius was obtained by equating the area of a circular plate to the square plate and solving for  $r$ . These constants were introduced to the spring-dashpot model developed in SAP2000 and in MATLAB.

<b>Table 5</b> <b>Properties of Rigid Circular Plate on Surface of Half-Space</b>		
<b>Direction</b>	<b>Stiffness</b>	<b>Damping</b>
Vertical	$K = \frac{4Gr}{1-\nu}$	$C = 1.79\sqrt{K\rho r^3}$
Horizontal	$K = 18.2Gr \frac{(1-\nu^2)}{(2-\nu)^2}$	$C = 1.08\sqrt{K\rho r^3}$
Rocking	$K = 2.7Gr^3$	$C = 0.47\sqrt{K\rho r^3}$

As it was done previously for the other cases, a time-history and modal analysis were performed using this model. Absolute acceleration and absolute and relative displacement time-histories were obtained. Special attention was paid to the time-histories at the top of the tower to compare the results with those of the full tower plus dam model.

## Summary

This chapter presented a description of the finite element models developed for this investigation. Five models were presented, with a description of the boundary conditions, properties, and other features of each model. For all the models, a time-history and modal (eigenvalue) analysis were done. These analyses allow one to understand the seismic response of the tower and dam and to establish some patterns in the behavior. The configurations of the tower and earthen dam (described in Chapter 3) were the same in all models. The results of the analyses will be presented in Chapter 6 where a detailed discussion of the most important findings of this research is also included.

## 5 The MATLAB-Based Program

---

The primary goal of this research was to perform an analysis of a typical intake-outlet tower considering the multiple-support excitation effects. As mentioned, other effects such as the soil-structure interaction were studied to obtain a better understanding of the dynamic behavior of these towers. Several tools were used to analyze the towers considering some or all of these effects. One of the tools used during this research was a MATLAB-based program.

The finite element model of the tower, bridge, dam, and soil foundation accounts for the two effects to be studied. However, this model is relatively complicated to develop, and thus a simpler model was sought. This model can be especially useful when one wants to perform the seismic evaluation of many towers in an inventory. Therefore, it was decided that MATLAB would be the best platform to develop the program to study the seismic response of the tower-bridge system. This chapter presents a description of the formulation used in this program to account for the multiple-support excitation, and the hydrodynamic and soil-structure interaction effects.

### Multiple-Support Excitation Formulation

Several methods and procedures have been developed to account for the multiple-support excitation effects in extended structures such as bridges, dams, and pipeline systems. Some methods include the effects of the local soil conditions, others the effects of traveling waves, etc. (see Chapter 2). The computer program developed for this study in MATLAB includes the effects of multiple-support excitations by means of time-history analysis. It begins with the formulation of the stiffness matrices for a plane frame element. The plane frame element has three degrees of freedom per node (the axial displacements are included). The local stiffness matrix of each element is given by

$$\bar{K} = \frac{E}{L} \begin{bmatrix} -A & 0 & 0 & A & 0 & 0 \\ 0 & \frac{12I}{L^2} & \frac{6I}{L} & 0 & -\frac{12I}{L^2} & \frac{6I}{L} \\ 0 & \frac{6I}{L} & 4I & 0 & -\frac{6I}{L} & 2I \\ -A & 0 & 0 & A & 0 & 0 \\ 0 & -\frac{12I}{L^2} & -\frac{6I}{L} & 0 & \frac{12I}{L^2} & -\frac{6I}{L} \\ 0 & \frac{6I}{L} & 2I & 0 & -\frac{6I}{L} & 4I \end{bmatrix} \quad (3)$$

where

$E$  = modulus of elasticity

$L$  = length of the element

$A$  = cross-sectional area

$I$  = moment of inertia

The local stiffness matrices are assembled into the global stiffness matrix using typical matrix structural analysis procedures. The local element stiffness matrix can be transformed into the global coordinate system using

$$K = T^T \bar{K} T \quad (4)$$

in which  $T$  is the transformation matrix and  $T^T$  is its transpose and is obtained from following the expression:

$$T = \begin{bmatrix} \cos \theta & \sin \theta & 0 & 0 & 0 & 0 \\ -\sin \theta & \cos \theta & 0 & 0 & 0 & 0 \\ 0 & 0 & 1 & 0 & 0 & 0 \\ 0 & 0 & 0 & \cos \theta & \sin \theta & 0 \\ 0 & 0 & 0 & -\sin \theta & \cos \theta & 0 \\ 0 & 0 & 0 & 0 & 0 & 1 \end{bmatrix} \quad (5)$$

where  $\theta$  is the angle between the global horizontal axis and a local axis along the element.

The program also makes use of the consistent mass matrix of plane frame element, i.e.,



$$M = \rho AL \begin{bmatrix} \frac{1}{3} & 0 & 0 & \frac{1}{6} & 0 & 0 \\ 0 & \frac{13}{35} & \frac{11L}{210} & 0 & \frac{9}{70} & -\frac{13L}{420} \\ 0 & \frac{11L}{210} & \frac{L^2}{105} & 0 & \frac{13L}{420} & \frac{L^2}{140} \\ \frac{1}{6} & 0 & 0 & \frac{1}{3} & 0 & 0 \\ 0 & \frac{9}{70} & \frac{13L}{420} & 0 & \frac{13}{35} & -\frac{11L}{210} \\ 0 & -\frac{13L}{420} & \frac{L^2}{140} & 0 & -\frac{11L}{210} & \frac{L^2}{105} \end{bmatrix} \quad (6)$$

The consistent matrix includes the dynamic coupling that exists between the transverse displacements and rotations. The simplest form of the mass matrix obtained from the concentration of masses on each node of the element (lumped mass matrix) ignores this effect. This matrix contains off-diagonal terms, whereas the lumped mass matrix has only diagonal terms (Paz 1997). It is called "consistent" because the same displacement shape functions that are used for deriving the stiffness matrix are used for the derivation of the mass matrix. Finally, the local mass matrix is assembled into the global mass matrix following the same procedure for the assembling of the global stiffness matrix.

The first step in the analysis of a structure subjected to multiple-support excitations is the determination of the pseudo-static displacements. By definition, the pseudo-static displacements are the sum of the displacements of the structure caused by a slow independent motion of each of the supports of the structure. To calculate them, it is necessary to have the full stiffness matrix of the system. The displacements are then divided into interior and boundary degrees of freedom. The stiffness and mass matrices are next divided in the same way. In the case of multiple-support excitations, the boundary dofs are those whose motion will be that of the ground caused by the earthquake. For the tower plus bridge model, the program reads earthquake acceleration histories in the horizontal and vertical directions at two nodes. The remaining dofs are referred to as interior dofs, which in this case are also the pseudo-static displacements. The divided stiffness matrix is given by the following expression:

$$\begin{bmatrix} K_{ii} & K_{ib} \\ K_{bi} & K_{bb} \end{bmatrix} \begin{Bmatrix} u_i \\ u_b \end{Bmatrix} = \begin{Bmatrix} 0 \\ R_b \end{Bmatrix} \quad (7)$$

in which,  $u_i$  and  $u_b$  are the vectors of interior and boundary displacements, respectively. It will be assumed that there are  $ni$  interior dofs and  $nb$  boundary dofs. In the submatrices of  $K$ , the subscripts  $i$  and  $b$  represent the terms related to interior and boundary dofs.

Solving for the interior (pseudo-static) displacements from the first  $ni$  equations leads to

$$u_i = -K_{ii}^{-1} K_{ib} u_b \quad (8)$$

where  $K_{ii}^{-1}$  is the inverse of the submatrix that contains all the degree of freedom associated with the interior displacements (upper-left matrix), and  $K_{ib}$  is the upper-right matrix that results after the division of the total stiffness matrix. Introducing a  $ni \times nb$  matrix,  $R$  is defined as

$$R = -K_{ii}^{-1} K_{ib} \quad (9)$$

in which the pseudo-static displacements can be expressed as

$$u_i = R u_b \quad (10)$$

The matrix  $R$  is called the influence matrix because it describes the influence of the support displacements on the structural displacements. It is important to emphasize that  $R$  represents a matrix, not a vector as in the case of identical support motions. In the latter case,  $R$  becomes the vector of influence coefficients and  $u_b$  is a scalar, i.e., the ground displacement. In the case of multiple-support excitations, each element of  $u_b$  is a displacement time function induced by the earthquake. Here, each column of matrix  $R$  represents an influence vector associated with the support displacements  $u_b$ . The reactions at the supports can be calculated using the relation between the interior displacements  $u_i$  and the prescribed displacements  $u_b$ . First, from the lower part of the system of Equation 7,

$$R_b = K_{bi} u_i + K_{bb} u_b \quad (11)$$

Substituting  $u_i$  from Equation 8 into 11,  $R_b$  can be expressed as

$$R_b = [K_{bb} - K_{bi} K_{ii}^{-1} K_{ib}] u_b \quad (12)$$

Usually the ground motion is defined in terms of acceleration time-histories. Therefore, to obtain the prescribed displacements, a numerical integration has to be done. The method for numerical integration used in the program is the trapezoidal rule. The program reads the acceleration time-histories at the different support locations as input data. Then it determines the displacement time-histories at each support of the structural system by numerical integration.

Once this is done, the program calculates the dynamic displacements of the structure. To do that, it is necessary to calculate the modal participation factors. As it is well known, these factors give a measure of the degree to which the  $n^{th}$  mode participates in the response of the structural system and are given by

$$\Gamma_n = \frac{L_n}{M_n} \quad ; \quad n = 1, \dots, ni \quad (13)$$

$$; \quad l = 1, \dots, nb$$

Note that, opposite to the case of uniform base motion, there are  $ni \times nb$  participation factors. That is, they vary not only with the mode number but also with the particular support. The quantity  $L_{nl}$  is

$$L_{nl} = \phi_n^T M_{ii} R_l \quad (14)$$

where

$\phi_n^T$  = transpose of the  $n^{th}$  vibration mode (the  $n^{th}$  column of the vibration mode matrix)

$M_{ii}$  = submatrix of the mass matrix that corresponds to the terms associated with the interior dofs

$R_l$  = corresponding column in the influence matrix  $R$  associated with the motion of the support  $l$

Variable  $M_n$  in Equation 13 is the generalized modal mass and is expressed by

$$M_n = \phi_n^T M_{ii} \phi_n \quad (15)$$

Due to the orthogonality property of the modes,

$$\phi_k^T M_{ii} \phi_j = \begin{cases} 0 & ; k \neq j \\ M_j & ; k = j \end{cases} \quad (16)$$

If the vibration modes are normalized with respect to the mass matrix,  $M_n$  is equal to one. In this way, the program normalizes the vibration modes; thus, there is no need to determine  $M_n$ .

The determination of the displacements that consider multiple-support excitations follows a procedure similar to the one used for the case of identical support motions. The basic difference is that the total dynamic response of the system is a superposition of the individual responses due to each support motion. To determine these displacements, it is necessary to solve the equations of motion transformed in modal coordinates. The modal equation of motion is then expressed as follows:

$$\ddot{q}_n + 2\zeta_n \omega_n \dot{q}_n + \omega_n^2 q_n = - \sum_{l=1}^{nb} \Gamma_{nl} \ddot{u}_{gl} \quad ; \quad n = 1, \dots, ni \quad (17)$$

where

$q_n$  = modal coordinate

$\zeta_n$  = modal damping ratio

$\omega_n$  = natural frequency of the  $n^{th}$  vibration mode

$nb$  = total number of supports in the system

$\ddot{u}_{gl}$  = ground acceleration at the support  $l$

The right-hand side of Equation 17 is the equivalent modal force, given by

$$N_{nl} = - \sum_{l=1}^{nb} \Gamma_{nl} \ddot{u}_{gl} \quad (18)$$

Each equation of motion is solved for the modal coordinate  $q_n$  using the Duhamel integral. The modal coordinate  $q_n$  represents the deformation response of the  $n^{th}$  mode due to the sum of all the support excitations  $\ddot{u}_{gl}$ . Once the solution for the modal coordinates  $q_n$  is obtained, the physical dynamic displacements can be determined. The dynamic displacements at the interior degrees of freedom are obtained combining the modal coordinates, that is,

$$u_d(t) = \sum_{n=1}^N \phi_n q_n(t) \quad (19)$$

where  $N$  is the total number of modes considered in the analysis.

The total displacement response of the system is the combination of two parts. It is the sum of the dynamic displacements and the pseudo-static displacements given by Equation 10. Combining the two parts leads to

$$u_t(t) = \sum_{l=1}^{nb} R_l u_{gl}(t) + \sum_{n=1}^N \phi_n q_n(t) \quad (20)$$

In this equation,  $u_{gl}(t)$  is the  $l^{th}$  element of the vector  $u_b$ .

## Simplified Procedure for Added Hydrodynamic Masses

It is recognized that the seismic response of structures submerged or partially surrounded by water is influenced by the surrounding water. The interaction with the water imposes additional dynamic forces on the structure and also modifies its dynamic properties (Liaw and Chopra 1974). Some of the effects of the water surrounding the outside and on the inside of the tower include the reduction of the resonant frequencies (or equivalently, the increase in the resonant periods), especially at the higher modes. Also, in some case studies, the hydrodynamic interaction affects the displacements of the tower; as a consequence, the maximum shear and bending moments along the height of the tower also increase, but to a greater extent (Goyal and Chopra 1989a). This was the case, for example, of the Briones Dam intake tower located east of San Francisco Bay (Goyal and Chopra 1989b).

The effect of surrounding water has been studied for decades since Westergaard (1933) first proposed the concept of added hydrodynamic masses for the seismic analysis of dams impounding water. The idea behind this concept is that

the hydrodynamic effect of the fluid is equivalent to an additional water pressure imposed on the structure due to a unit acceleration of the base of the structure. The determination of the added mass is based on the assumptions that the structure is rigid and the water is incompressible with viscous effects neglected.

It has been shown that the compressibility of the water is of no practical significance in determining the dynamic response of slender towers. The errors become significant only for the higher vibration modes of squat towers (Liaw and Chopra 1974). Neglecting the viscosity is also a common and accepted assumption when the liquid is water. The effect of the surface waves was shown to be of little consequence in the earthquake response of towers surrounded by water (Liaw and Chopra 1974). Moreover, the effect of the vertical components of the ground motion is ignored, since the stresses in slender towers are caused primarily by lateral flexural deformations.

The rigid structure assumption was examined by Liaw and Chopra (1974). They found that the magnitude and distribution of the additional mass depend on the deflected shape during the vibration. They developed a method that includes the shape of the vibration mode on the added mass. However, they had to consider a single mode to determine the new added mass; it is not possible to account for all the important modes of vibration of the tower. Therefore, they recommended using the traditional definition of added mass and, hence, in subsequent papers, Chopra and co-workers (Goyal and Chopra 1989a,b,c) adopted this concept to study different aspects of the seismic response of intake towers.

With the assumptions previously mentioned, it is possible to obtain added hydrodynamic mass functions that account for the water outside and inside the tower for cylindrical towers with circular cross sections in a relatively simple way.

The expressions for the added masses developed by Goyal and Chopra (1989b) were obtained based on the analytical solution of the Laplace equation. Equation 20 shows the three-dimensional Laplace equation in polar coordinates used for the analysis of the surrounding (outside) water domain. This equation represents the irrotational motion of the water surrounding the tower. The hydrodynamic pressure in the water surrounding the tower is generated by the acceleration of the outside surface of the tower and the vertical acceleration of the reservoir bottom.

$$\frac{\partial^2 p}{\partial r^2} + \frac{1}{r} \frac{\partial p}{\partial r} + \frac{1}{r^2} \frac{\partial^2 p}{\partial \theta^2} + \frac{\partial^2 p}{\partial z^2} = 0 \quad (21)$$

The solution of the Laplace equation governing the behavior of the surrounding outside water provides the following expression for the corresponding added mass for circular cylindrical towers (Goyal and Chopra 1989b):

$$m_a^o(z) = (\rho_w \pi r_o^2) \left[ \frac{16 H_o}{\pi^2 r_o} \sum_{m=1}^{\infty} \frac{(-1)^{m-1}}{(2m-1)^2} E_m(\alpha_m r_o / H_o) \cos(\alpha_m z / H_o) \right] \quad (22)$$

where

- $z$  = distance above the base of the tower
- $\rho_w$  = mass density of water
- $r_o$  = radius of the outside surface of the tower
- $H_o$  = depth of the surrounding water
- $\alpha_m = (2m-1)\pi/2$

and

$$E_m(\alpha_m r_o/H_o) = \frac{K_1(\alpha_m r_o/H_o)}{K_o(\alpha_m r_o/H_o) + K_2(\alpha_m r_o/H_o)} \quad (23)$$

in which  $K_n$  is the modified Bessel function of order  $n$  of the second kind.

For an infinitely long uniform tower with the same circular cross section, the added mass per unit height is

$$m_\infty^o = \rho_w \pi r_o^2 \quad (24)$$

Note that  $m_\infty^o$  is equal to the added mass of the water displaced by the tower (per unit height).

Figure 15 displays the normalized added mass associated with the outside water as a function of  $z/H_o$  for a range of values of  $r_o/H_o$ , the ratio of the outside radius to the depth of the outside water. The different curves in Figure 15 are obtained from Equation 22 for given values of  $H_o/r_o$  and dividing the results by  $m_\infty^o$ . When the ratio  $H_o/r_o$  tends to infinity (that is, for an infinitely slender cylindrical tower), the normalized added mass becomes unity. As the slenderness ratio  $H_o/r_o$  decreases, i.e., as the tower becomes squatter, the ratio  $m_a^o(z)/m_\infty^o$  decreases.

Goyal and Chopra (1989b) also studied the evaluation of added hydrodynamic masses for towers with noncircular cross sections. They found that the normalized added mass for a uniform tower of arbitrary cross section is essentially the same as that of an equivalent elliptical tower. They defined a slenderness ratio  $H_o/\bar{a}_o$  and a plan dimensions ratio  $\bar{a}_o/\bar{b}_o$  of the equivalent elliptical tower in terms of the corresponding ratios for the actual tower, as follows:

$$\frac{H_o}{\bar{a}_o} = \frac{H_o}{\sqrt{A_o/\pi}} \sqrt{\frac{\bar{b}_o}{a_o}} \quad (25)$$

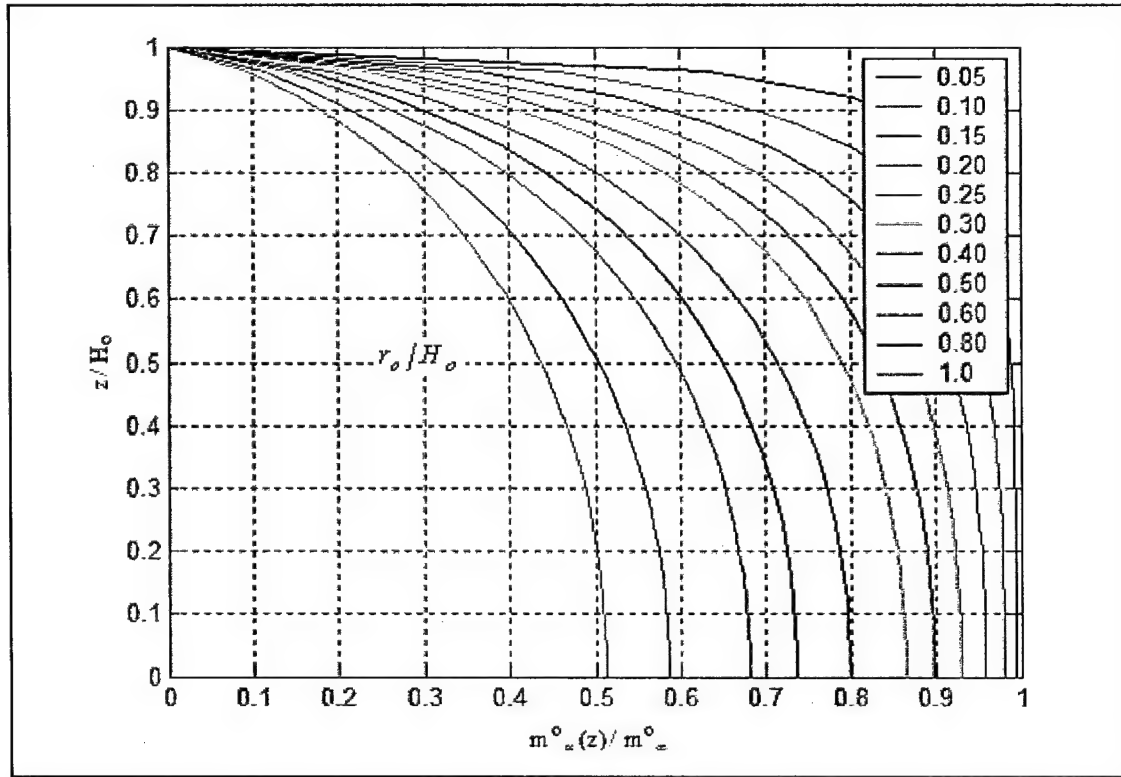


Figure 15. Plot for normalized outside hydrodynamic added mass for circular cylindrical towers

$$\frac{\bar{a}_o}{b_o} = \frac{a_o}{b_o} \quad (26)$$

where

$H_o$  = depth of surrounding water for both towers

$2\bar{a}_o$  = width of the elliptical tower perpendicular to the direction of ground motion

$2b_o$  = width of the actual tower parallel to the direction of ground motion

$2a_o$  = width of the actual tower perpendicular to the direction of ground motion

$2\bar{b}_o$  = width of the elliptical tower parallel to the direction of ground motion

Thus, if the quantity  $m_z^o/m_\infty^o$  were available for towers of elliptical cross section for a range of values of the ratio  $\bar{a}_o/\bar{b}_o$  and slenderness ratio  $H_o/\bar{a}_o$ , the normalized added mass could be readily determined for towers of arbitrary cross sections. However, Goyal and Chopra (1989b) judged this approach to be impractical because it would require a large number of graphs of normalized

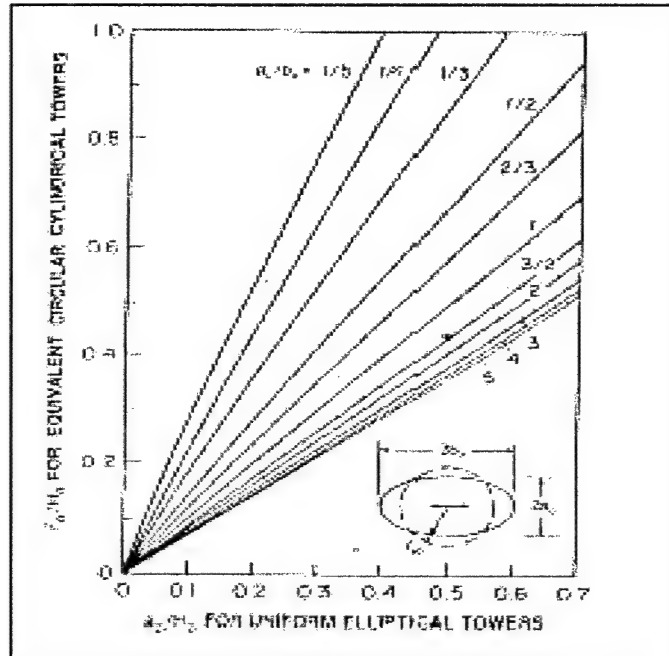


Figure 16. Properties of "equivalent" circular cylindrical towers corresponding to uniform elliptical towers associated with added hydrodynamic mass due to surrounding water (from Chopra and Goyal 1989a)

added mass to cover all the possible practical values of  $\bar{a}_o/\bar{b}_o$  and  $H_o/\bar{a}_o$ . They instead proposed to replace the elliptical tower by an equivalent circular tower. To this end, they developed a graph that gives the ratio  $\bar{r}_o/H_o$  as a function of the ratio  $\bar{a}_o/H_o$  of elliptical towers for different fixed values of  $\bar{a}_o/\bar{b}_o$ . This graph is displayed in Figure 16. Once an equivalent circular tower is defined in this way, Equation 22 or the graph in Figure 15 can be used to obtain the normalized added mass of the equivalent circular tower. Thus, the approach proposed by Goyal and Chopra requires defining two equivalent towers: first, one must define a tower with an elliptical cross section and, next, another with a circular cross section.

In summary, the procedure for defining the added hydrodynamic mass associated with the surrounding water for uniform towers of arbitrary cross section (with two axes of symmetry) consists of five steps:

- a. The parameters  $a_o$ ,  $b_o$ , and  $H_o$  of the actual tower are used in Equations 25 and 26 to determine the ratios  $H_o/\bar{a}_o$  and  $\bar{a}_o/\bar{b}_o$  of the equivalent elliptical tower. For a square cross section, these equations yield



$$\frac{H_o}{\bar{a}_o} = \frac{H_o}{a_o} \sqrt{\pi} \quad ; \quad \frac{\bar{a}_o}{b_o} = 1 \quad (27)$$

- b. Knowing  $\bar{a}_o/b_o$  and the inverse of the ratio  $H_o/\bar{a}_o$  determined in Step 1, Figure 16 provides the ratio  $r_o/H_o$  of an equivalent circular tower, where  $r_o$  is its equivalent radius.
- c. With the ratio  $r_o/H_o$ , Figure 15 allows us to evaluate the normalized added mass  $m_z^o(z)/m_\infty^o$  for the equivalent circular tower. Alternatively, the ratio  $m_z^o(z)/m_\infty^o$  can be directly defined from Equation 22 by setting the  $(\rho_w \pi r_o^2)$  equal to 1.
- d. The added hydrodynamic mass for an infinitely long tower with the arbitrary cross section  $m_\infty^o$  needs to be determined using a table presented by Goyal and Chopra (1989b–Table 1). This table contains  $m_\infty^o/(\rho_w A_o)$  for a few selected cross sections. Based on the data in this table, a graph depicting the relationship between the ratio  $a_o/b_o$  and the normalized added hydrodynamic mass  $m_\infty^o/(\rho_w A_o)$  for a rectangular section is presented in Figure 17. For a square cross section ( $a_o = b_o$ ), the ratio  $m_\infty^o/(\rho_w A_o)$  is 1.186.

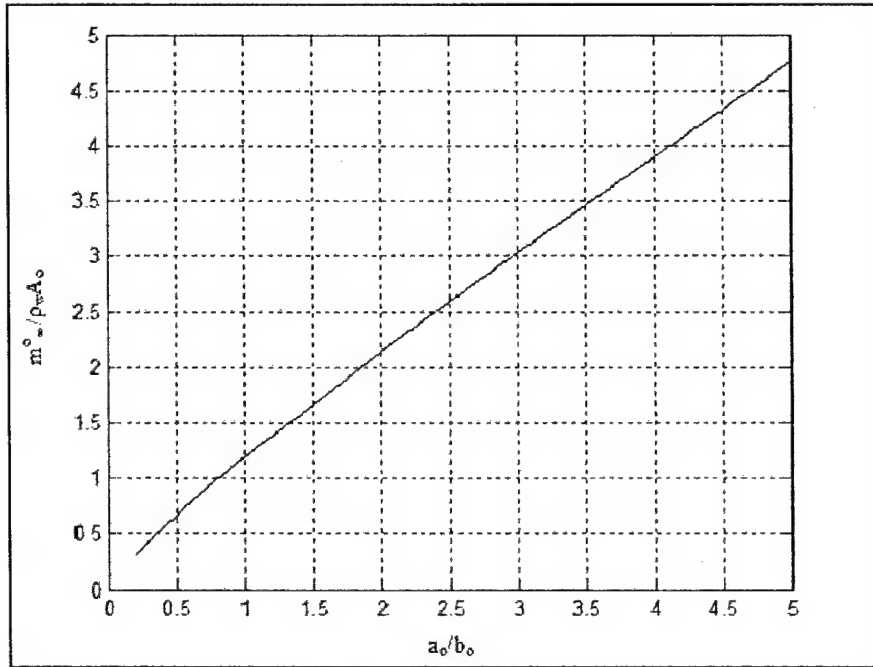


Figure 17. Normalized outside hydrodynamic added mass for an infinitely long tower

- e. Finally, the added hydrodynamic mass  $m_z^o(z)$  for the actual tower is computed by multiplying the normalized added mass  $m_z^o(z)/m_\infty^o$  calculated in Step 3 by  $m_\infty^o$  defined in Step 4.

Similarly to the expression for the case of the surrounding water, it can be shown that, from the solution of the Laplace equation for the inside water for circular cylindrical towers, one obtains

$$m_a^i(z) = (\rho_w \pi r_i^2) \left[ \frac{16 H_i}{\pi^2 r_i} \sum_{m=1}^{\infty} \frac{(-1)^{m-1}}{(2m-1)^2} D_m(\alpha_m r_i / H_i) \cos(\alpha_m z / H_i) \right] \quad (28)$$

where

$z$  = distance above the base of the tower

$r_i$  = radius of the inside surface of the tower,  $\alpha_m = (2m-1)\pi/2$

$H_i$  = depth of the inside water

and

$$D_m(\alpha_m r_i / H_i) = \frac{I_1(\alpha_m r_i / H_i)}{I_0(\alpha_m r_i / H_i) + I_2(\alpha_m r_i / H_i)} \quad (29)$$

in which  $I_n$  is the modified Bessel function of order  $n$  of the first kind.

The normalized added mass is obtained from Equation 28 dividing  $m_a^i(z)$  by  $m_\infty^i = \rho_w \pi r_i^2$ . Figure 18 displays the normalized added mass associated with the water contained inside the tower for a range of values of  $r_i/H_i$ , the ratio of the inside radius to inside water depth. When the ratio  $H_i/r_i$  tends to infinity (i.e., for an infinitely slender cylindrical tower), the normalized added mass is unity and it decreases as the tower becomes squatter (i.e., the ratio  $H_i/r_i$  decreases). Comparing the normalized added mass for outside water with the inside water masses, it is found that, for the same slenderness ratio, the normalized inside added mass is larger.

For a circular cylindrical tower, Equations 28 and 29 completely define the added hydrodynamic mass. The equations, however, are not directly applicable for towers with noncircular cross sections. Goyal and Chopra (1989b) also developed a simplified procedure to calculate the added hydrodynamic mass for towers with arbitrary cross section, provided they have two axes of symmetry. Let the  $2a_i$  and  $2b_i$  be, respectively, the interior dimensions of the actual tower perpendicular and along the direction of the ground motion  $H_i$  (the interior water depth), and  $A_i$ , the interior cross-section area of the tower. The methodology is similar to the one presented before and consists of the following steps:

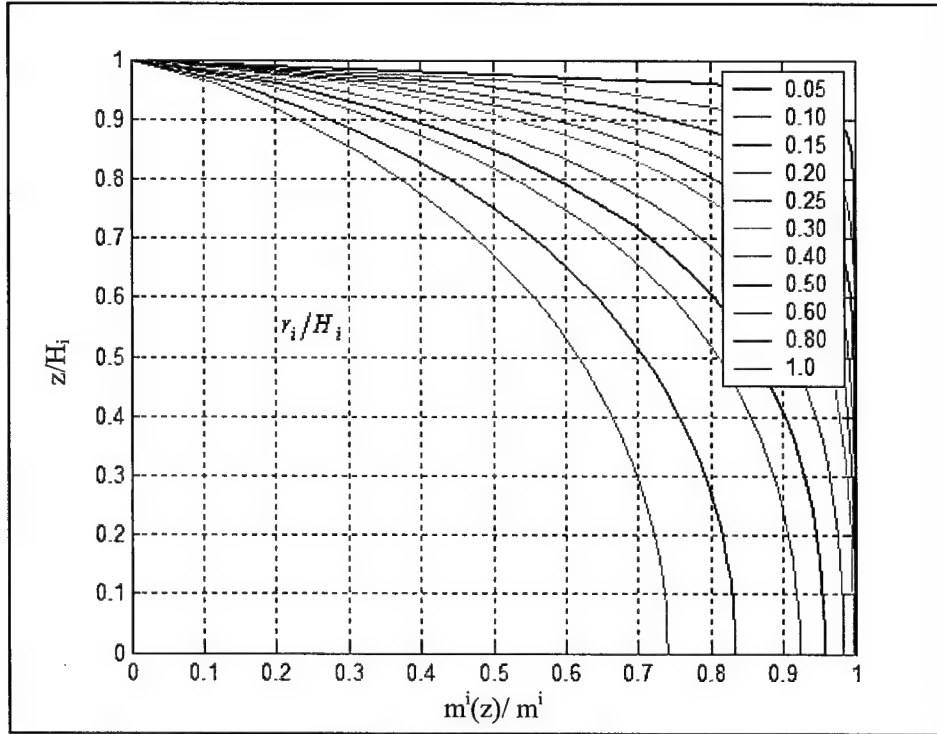


Figure 18. Plot for normalized inside hydrodynamic added mass for circular cylindrical towers

- a. Obtain the dimensions of an equivalent elliptical tower with interior cross-sectional dimensions  $2\bar{a}_i$  and  $2\bar{b}_i$  in terms of the dimensions of the actual tower, as follows:

$$\frac{H_i}{\bar{a}_i} = \frac{H_i}{\sqrt{A_i/\pi}} \sqrt{\frac{b_i}{a_i}} \quad (30)$$

$$\frac{\bar{a}_i}{\bar{b}_i} = \frac{a_i}{b_i} \quad (31)$$

For a tower with a square cross section, these equations yield

$$\frac{H_i}{\bar{a}_i} = \frac{H_i}{a_i} \pi \quad ; \quad \frac{\bar{a}_i}{\bar{b}_i} = 1 \quad (32)$$

- b. Calculate the slenderness ratio  $H_i/\bar{r}_i$  of an equivalent circular tower using the properties determined in Step 1. According to Goyal and Chopra (1989b), for the inside water analysis, the equivalent radius  $\bar{r}$  is given by the following simple formula, instead of a graph as in the case of the surrounding water:

$$\bar{r}_i = \sqrt{\frac{A_i \bar{b}_i}{\pi \bar{a}_i}} \quad (33)$$

and  $\bar{r}_i = \sqrt{A_i / \pi}$  for a tower with a square cross section.

- c. With  $H_i$  and  $\bar{r}_i$ , evaluate the normalized added mass  $m_a^i(z) / m_\infty^i$  for the equivalent cylindrical tower using Figure 18. In this case, the added hydrodynamic mass for the tower with arbitrary cross section is obtained by multiplying the normalized added mass by  $m_\infty^i = \rho_w A_i$ .
- d. As an alternative to Step c, the added hydrodynamic mass  $m_a^i(z)$  can be obtained directly from Equation 28.

Note that in the case of the inside water,  $m_\infty^i$  is the same regardless of the shape of the tower's cross section. In other words, it is not necessary to have available tables or graphs to determine the added hydrodynamic mass for an infinitely high tower with different cross sections, as in the case of the surrounding water.

Once the added hydrodynamic masses for the outside  $m_a^o(z)$  and inside  $m_a^i(z)$  water are obtained, the next step is to lump these distributed masses and add them to the discrete masses due to the inertia of the tower. The procedure varies depending on whether a shell or frame model is used to represent the tower. In the case of a frame model such as the one used in this study, the procedure is the following. A "tributary" length must be defined for each lumped mass along the tower height, say  $L_j$  for the mass at the  $j^{\text{th}}$  node. Suppose that the  $j^{\text{th}}$  node is at a height  $h_j$  measured from the base of the tower. Then, the lumped mass at the  $j^{\text{th}}$  node due to the outside and inside water is approximately given by

$$M_j = [m_a^o(h_j) + m_a^i(h_j)] L_j \quad (34)$$

A more accurate value would be obtained by using

$$M_j = \int_{h_j - L_j/2}^{h_j + L_j/2} [m_a^o(z) + m_a^i(z)] dz \quad (35)$$

However, this requires performing a very complicated integration involving special functions. Therefore, Equation 34 will be used in the present study.

## Soil-Structure Interaction

Another factor that has a strong influence on the seismic response of intake-outlet towers is the soil-interaction effect. Initially this effect was not going to be considered. It is well known that the soil-structure interaction effects are

important only for stiff and massive structures located on soft soils, and it was thought the intake tower did not comply with these characteristics. However, the discrepancies between the simplified frame model and the full finite element model of the tower plus dam (reported in Chapter 4) led to its inclusion.

The most common approach to the problem is to modify the dynamic properties of the structure and evaluate the response of the modified structure to the prescribed free-field ground motion (Building Seismic Safety Council, BSSC 2001). Among the approaches to achieve this, the simplest one involves considering the flexibility of the soil by means of translational and rotational springs. Moreover, because a substantial part of the structure's vibrational energy is dissipated into the supporting medium by radiation of energy and hysteretic behavior of the soil, translational and rotation dashpots are added to the model. The first effect, called radiation damping, is typically much more important than the second, which is referred to as material damping.

The method for incorporating the effects of soil-structure interaction based on springs and dashpots was thought to provide sufficient accuracy for the application at hand and, thus, was the approach adopted in this study. The coefficients of the springs and dashpots were calculated using the expressions described in Chapter 4 or the values obtained by using SAP2000 (explained in Chapter 6). As recommended by Newmark and Rosenblueth (1971), lumped masses were also attached to the degrees of freedom at the soil-structure interface. More elaborate procedures have their own approximations and do not eliminate the uncertainties that are inherent in the modeling of the structure-foundation-soil system, in the specifications of the ground motion, and in the estimation of the properties of the structure and, especially, the soil (BSSC 2001).

The effect of soil-structure interaction at the base of the tower and at the location of the bridge was introduced in the MATLAB program modifying the stiffness and mass matrices of the structural system. The values of the mass and stiffness coefficients defined in Chapter 4 were added to the degrees of freedom at the interface between the structure and the soil foundation. Because the springs representing the flexibility of the soil have one end attached to a fixed point, their stiffness coefficients are added to the diagonal terms of the stiffness matrix at the base of the tower and at one end of the bridge. The same occurs with the mass coefficients.

The radiation and material damping of the soils are accounted for by means of discrete dashpots. As explained in Chapter 4, these dashpots were defined only for the base of the tower because in the technical literature they are determined only for the case of an elastic half-space. In principle, the coefficients of the dashpots in the three directions (horizontal, vertical, and rotational or rocking) should be added to the damping matrix of the structure. However, there is a problem in this case: the damping matrix of the structure was not defined. Rather, the usual classical damping assumption was used, and the damping of the structure was introduced by means of modal damping ratios. In other words, if  $\Phi$  is the matrix of eigenvectors of the tower (or tower plus bridge, depending on the model considered) with a flexible foundation (i.e., with the springs at the base), it is assumed that the triple product

$$\Phi^T C \Phi = \text{diag}[\tilde{c}] = \begin{bmatrix} \ddots & & \\ & \tilde{c}_j & \\ & & \ddots \end{bmatrix} \quad (36)$$

leads to a diagonal matrix. Furthermore, for convenience, the diagonal terms are expressed in terms of the natural frequencies  $\omega_j$  and modal damping ratios  $\xi_j$ :

$$\tilde{c}_j = 2\xi_j\omega_j \quad ; \quad j = 1, \dots, n \quad (37)$$

If no other information is available, the values of the damping ratios  $\xi_j$  are usually considered to be equal to 0.05 in order to use design spectra specified in codes or seismic provisions. However, for consistency with the finite element model of the dam plus intake tower, the value of  $\xi_j$  was set equal to 0.245. It is recalled that this value accounts for the nonlinear behavior of the soil deposit and was derived by matching the surface accelerations calculated with QUAD4M and SAP2000.

When the dashpots are added to the base of the tower, the total damping matrix  $C_t$  is now the sum of two terms:

$$C_t = C + C_d \quad (38)$$

where  $C_d$  is a damping matrix with only three nonzero terms in correspondence with the two translational and rotational dofs at the base of the tower. When the new equations of motion are decoupled using the eigenvector matrix the usual way, the product

$$\Phi^T C_d \Phi = \tilde{c}_s \quad (39)$$

does not lead to a diagonal matrix. That is,  $\tilde{c}_s$  is, in general, a full matrix. In principle, this situation can be taken into account in an exact way by transforming the usual equations of motion into "state space" equations and solving them using complex eigenvalues and eigenvectors. However, the implicit uncertainties in the values of the damping coefficients and the assumptions and simplifications adopted so far do not warrant the complications introduced in the analysis by this procedure.

Taking into account that the diagonal terms of  $\tilde{c}_s$  are dominant with respect to the off-diagonal terms, it is proposed to neglect the latter terms and replace Equation 39 with

$$\Phi^T C_d \Phi = \text{diag}[\tilde{c}_s] = \begin{bmatrix} \ddots & & \\ & \tilde{c}_{sj} & \\ & & \ddots \end{bmatrix} \quad (40)$$

With this assumption, the total damping matrix  $C_t$  can now be decoupled using the modes of the tower with flexible base, that is

$$\Phi^T C_t \Phi = \text{diag}[\tilde{c}] + \text{diag}[\tilde{c}_s] = \begin{bmatrix} \ddots & & \\ & \tilde{c}_j + \tilde{c}_{sj} & \\ & & \ddots \end{bmatrix} \quad (41)$$

With the diagonal terms in Equation 30, one can define new equivalent modal damping ratios that approximately account for the presence of the dashpots, as follows:

$$\tilde{c}_j + \tilde{c}_{sj} = 2\tilde{\xi}_j \omega_j \quad ; \quad j = 1, \dots, n \quad (42)$$

And, using Equation 26, one can further write

$$\tilde{\xi}_j = \xi_j + \frac{\tilde{c}_{sj}}{2\omega_j} \quad ; \quad j = 1, \dots, n \quad (43)$$

The new modal damping ratios  $\tilde{\xi}_j$  are used in the traditional modal analysis to obtain the seismic response of the intake tower with soil-structure interaction effects included.

## Summary

A description of the formulation used in the MATLAB program was presented in this chapter. The following features are included in the program: the multiple-support excitation formulation and simplified procedures to define the added hydrodynamic masses and the soil-structure interaction effects. The program receives all the data related to the structure in an interactive way. The output of the program is the absolute acceleration and relative displacement time-history of any mode of interest.

The first step in considering the multiple-support excitations is the calculation of the pseudo-static displacements. These displacements are obtained by applying, in a pseudo-static way, prescribed displacements at each support of the structural system. In the case of multiple-support excitations, the prescribed displacements are those induced by the earthquake. Afterwards, the dynamic displacements are calculated using the usual modal analysis formulation. The total response is the sum of the pseudo-static and dynamic displacements.

Another feature included in the program is the simplified procedure to define the added hydrodynamic masses developed by Goyal and Chopra (1989b). This procedure is used to obtain the lumped masses that account for the presence of the water inside and outside the tower. The hydrodynamic added masses were added to the masses of the tower of the frame model and in the tower of all the finite element models.

The last feature included in the program is the soil-structure interaction effects. This effect is included in a simple way using springs, masses, and dashpots that represent the soil foundation beneath the tower and in the dam where the bridge is supported. The springs and masses are simply accounted for by modifying the appropriate terms of the stiffness and mass matrices. The addition of dashpots requires an additional assumption in order to avoid the use of complex eigenvalues and eigenvectors. The off-diagonal terms in the matrix obtained by pre- and post-multiplying the damping matrix containing the dashpots are neglected, and new modal damping ratios are calculated with diagonal terms.



## 6 Numerical Results

---

This chapter presents a summary of the results obtained during the investigation. The results are divided in two groups: those obtained with the finite element models and those obtained with the frame model developed in MATLAB. The results of the seismic analysis are displayed in graphical form. Only the relative displacement and absolute acceleration time-histories are presented. To reduce the number of plots presented in the report, only the response at the top of the tower is shown. However, the data are available for different points of the structural system. The results of an eigenvector analysis are presented in tables. A comparison of responses obtained with the different models and assumptions is also presented. Different results are obtained by either including or neglecting the factors that can affect the seismic response of the intake-outlet towers. These factors include the multiple-support excitation and the soil-structure interaction effects. A detailed discussion of the most important findings of this research is also presented.

### Seismic Input

The first step in any seismic analysis is the definition of the seismic input. In this study, the seismic input for all the finite element and frame models was defined in terms of an accelerogram applied at the base of the dam's foundation (at the bedrock). A response spectrum analysis was also carried out, and the results are presented at the end of the chapter. The results are first presented for two earthquakes. (Later on, more ground motions are considered.) The first one is the classical El Centro earthquake recorded in Imperial Valley, California, on 15 October 1940. Figure 19 shows a plot of the acceleration time-history of the El Centro earthquake used in this chapter. All the accelerations are presented as a fraction of  $g$  (the gravitational acceleration). For brevity, this is indicated in the vertical axes as "% $g$ ." The peak acceleration of the El Centro earthquake is 0.319  $g$ , and it has a total duration of 30 sec. This accelerogram was used because it became a standard input in most earthquake engineering studies and also because it represents a typical strong, broad-band motion. The other ground motion selected for the analyses is the Loma Prieta earthquake, recorded at the Gilroy Historic Building, in California, on 18 October 1989. Figure 20 presents its acceleration time-history, which has a total duration of 40 sec with a peak acceleration of 0.284  $g$ . This accelerogram was used because it has a different

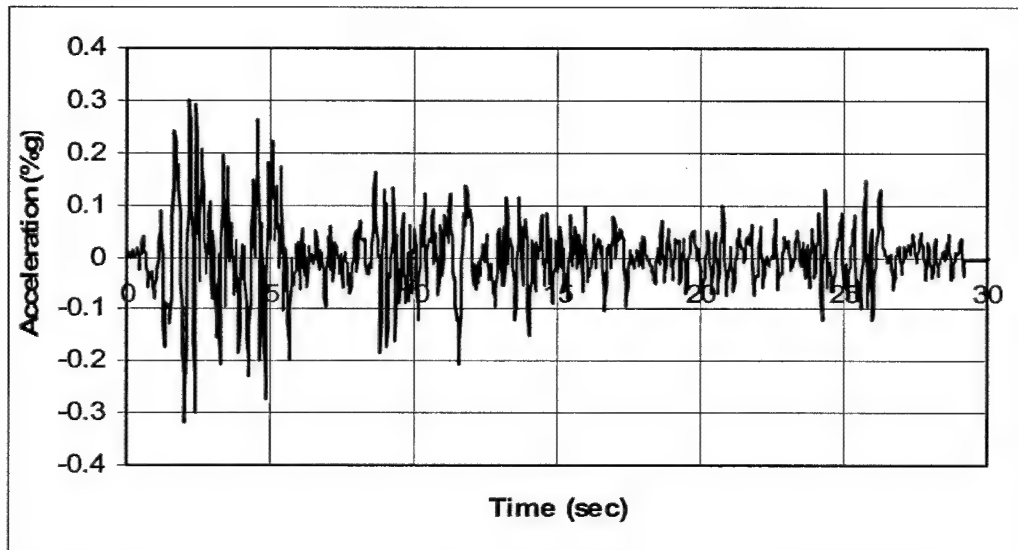


Figure 19. Acceleration time-history of the El Centro earthquake

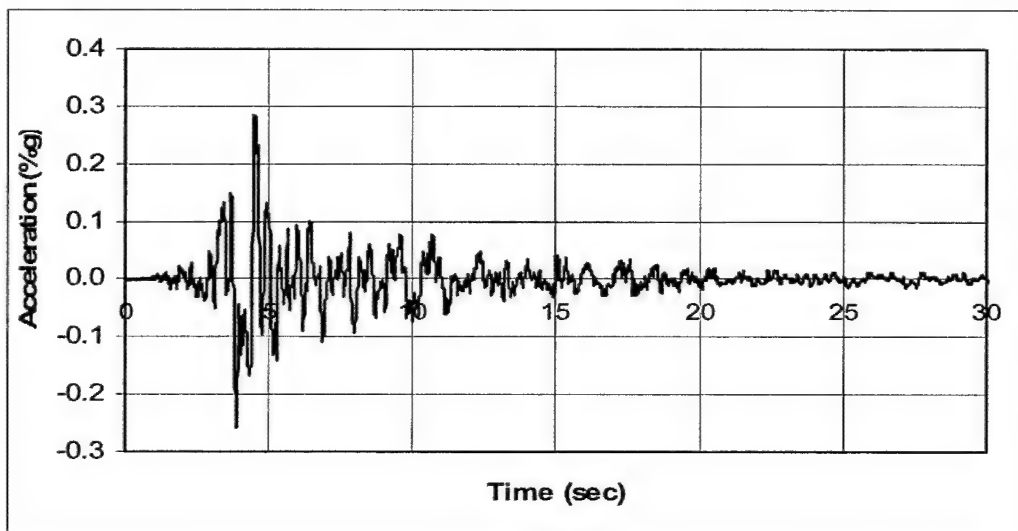


Figure 20. Acceleration time-history of the Loma Prieta earthquake at Gilroy Building

frequency content, a higher dominant period, and less strong motion duration compared with the El Centro earthquake (see Figures 21 through 26).

Figures 21 and 22 show the smoothed Fourier spectra for the El Centro and Loma Prieta accelerograms, respectively. Note that the Fourier spectrum is presented in terms of periods instead of frequencies as usual. Also shown in these figures is the predominant period for each earthquake. The El Centro earthquake has a lower predominant period than the Loma Prieta earthquake.

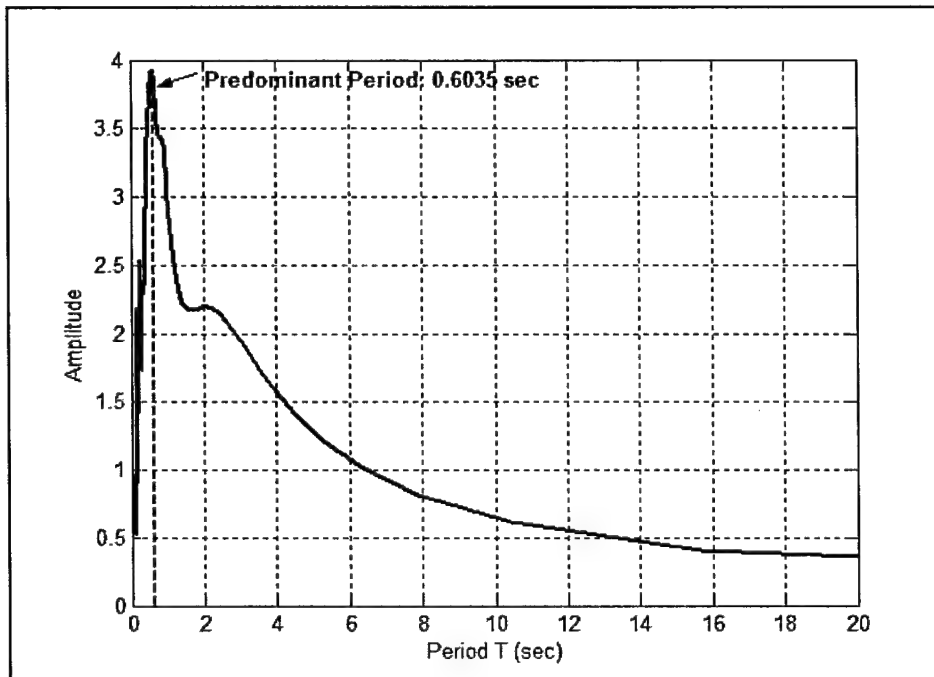


Figure 21. Smoothed Fourier spectrum of the El Centro earthquake

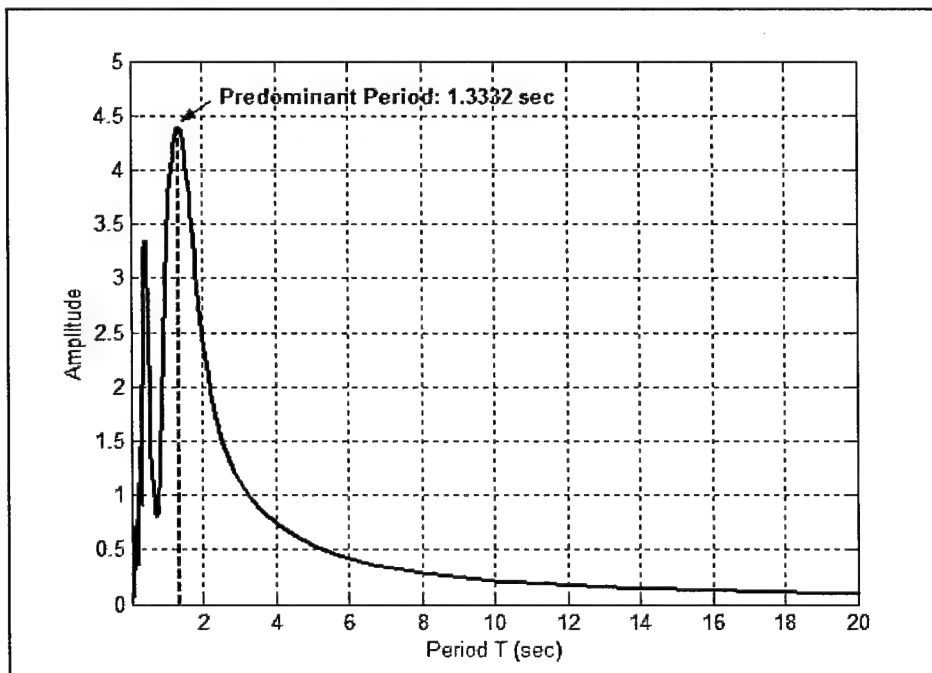


Figure 22. Smoothed Fourier spectrum of the Loma Prieta earthquake at Gilroy Building

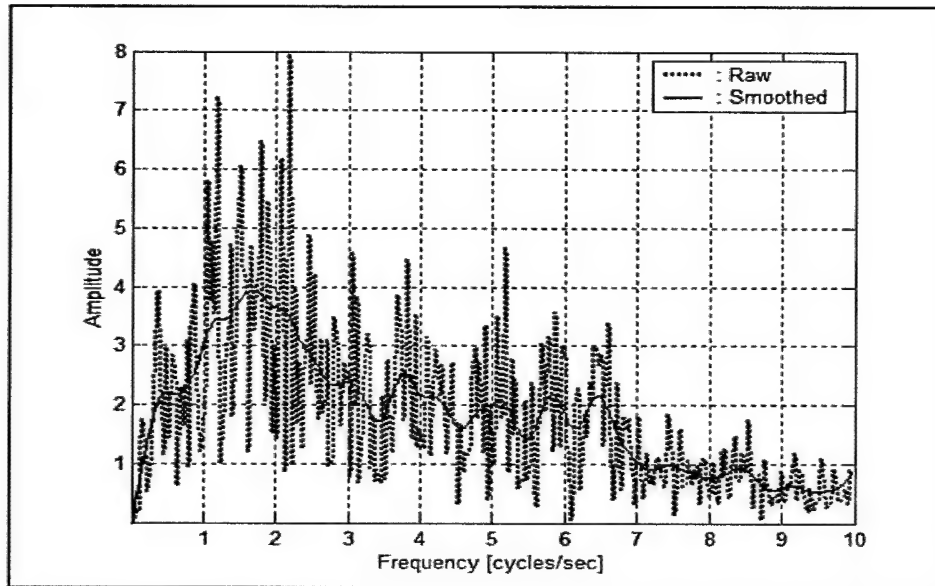


Figure 23. Raw and smoothed Fourier spectra for El Centro earthquake

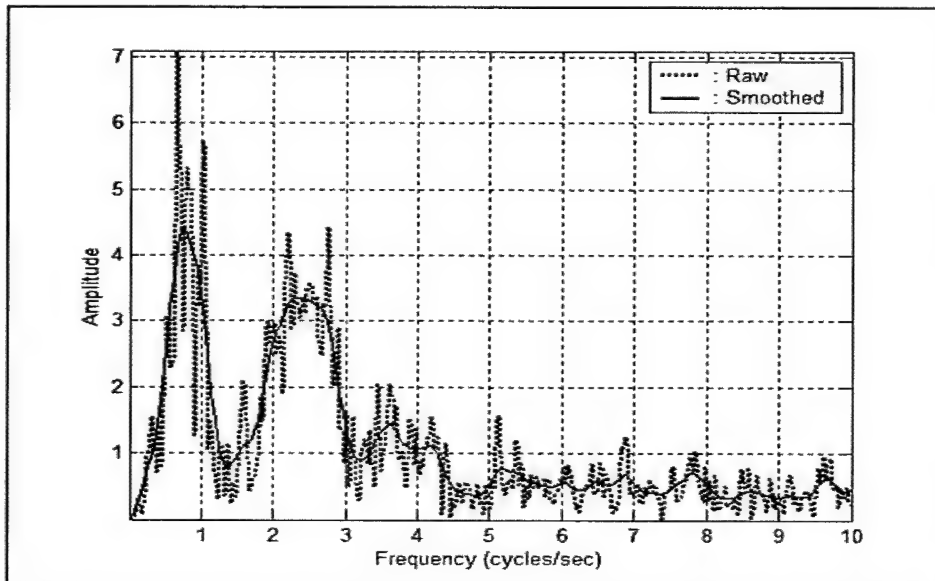


Figure 24. Raw and smoothed Fourier spectra for Loma Prieta earthquake at Gilroy Building

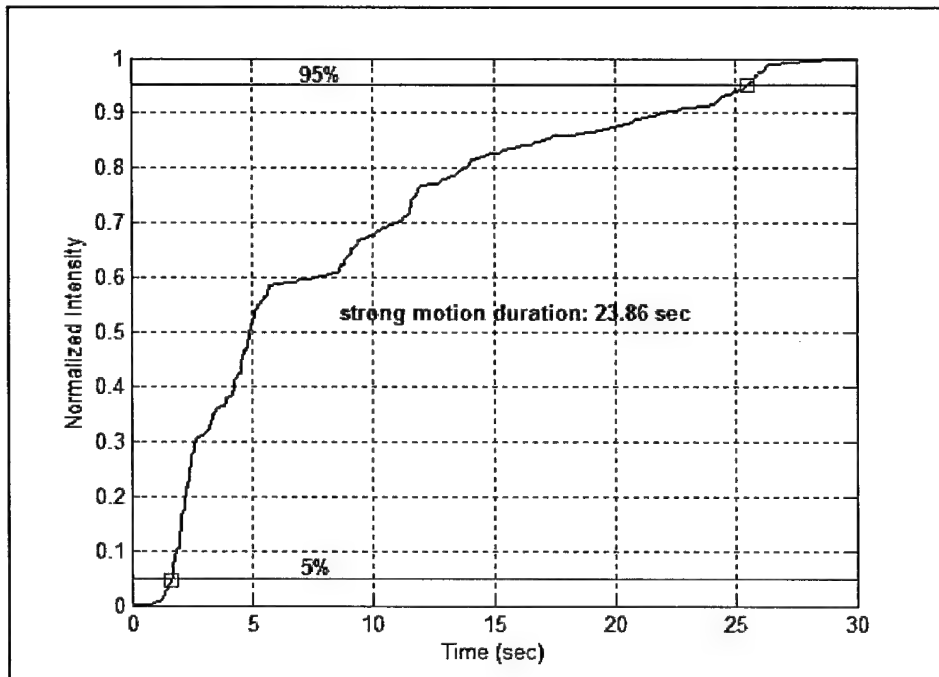


Figure 25. Arias intensity for El Centro earthquake

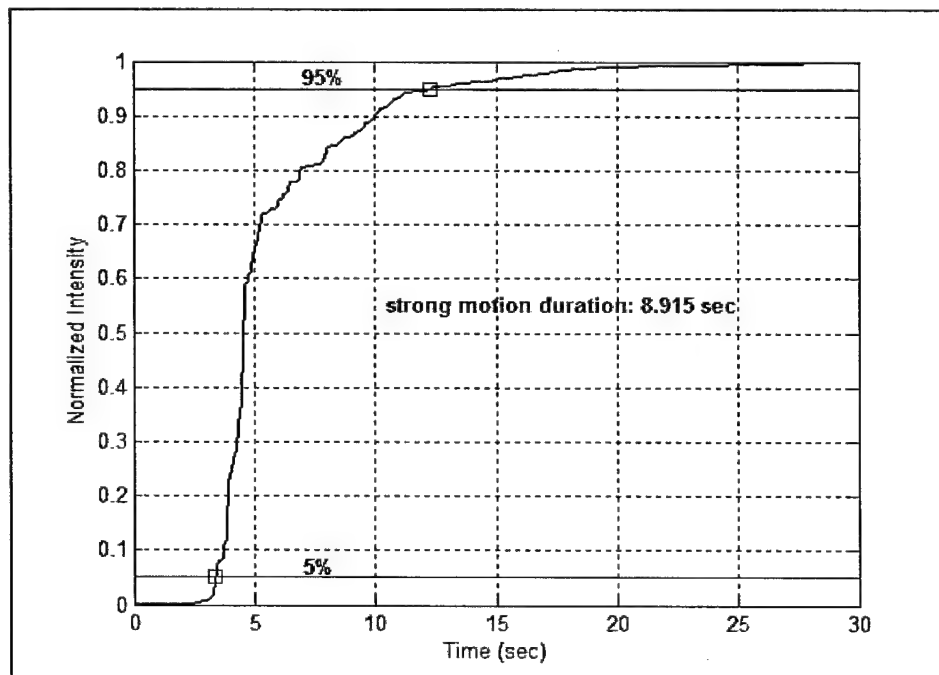


Figure 26. Arias intensity for Loma Prieta earthquake at Gilroy Building

Figures 23 and 24 display the raw and smoothed Fourier spectra in terms of frequency for the two accelerograms selected for this study. The original Fourier spectra of both earthquakes are very jagged, but when the smoothed spectra are plotted, the differences become apparent. Note that the Fourier spectrum for Loma Prieta has more pronounced peaks at low frequencies.

Figures 25 and 26 show the Arias intensity curves used for the calculation of the duration of the strong motion of each earthquake (El Centro and Loma Prieta). It can be seen that the El Centro earthquake has higher longer motion duration than the Loma Prieta earthquake.

## Multiple-Support Excitation Analysis

The multiple-support excitation effects in the intake-outlet tower and access bridge system were studied using the tools described in the previous chapters. The finite element model of the dam plus the intake tower and the frame model developed in MATLAB (using the formulation described in Chapter 5) were used in this phase of the study. The finite element model of the dam without the tower was used to obtain the absolute acceleration at the base of tower and at the point at which the access bridge is supported by the dam. The support of the bridge (i.e., the abutment) is assumed to be at the crest of the embankment. These acceleration time-histories were used as input for the MATLAB program. Figures 27 and 28 show a comparison between the acceleration time-histories at the base of the tower and at the access bridge for the El Centro and Loma Prieta earthquakes, respectively. These accelerograms were obtained from the finite element model of the dam plus foundation created in SAP2000.

The variability in the acceleration at the base of the tower and at the crest of the dam (at the abutment of the access bridge) is less than was expected, at the beginning of the study. There is, though, a slight amplification at the top (crest) of the dam. The lack of a more pronounced difference could be the result of the geometry and soil properties of the dam. The ratio between the dam's height and the width of its base is relatively small (0.14). The materials of the dam have shear wave velocities ranging from 450 to 700 ft/sec.

The two accelerograms for each earthquake (shown in Figures 27 and 28) were used as input to the tower plus bridge frame model. The acceleration at the base of the tower was then applied to a stick model, and the relative displacements at the top of the tower were compared for the two cases.

Figures 29 and 30 display the relative displacement time-histories at the top of the tower obtained by considering the multiple-support excitations (MSE) and a single excitation (SE). The two sets of results were obtained with the frame and column model of the intake tower implemented in MATLAB and using the formulation discussed in Chapter 5 for the MSE case. The results demonstrate that, at least for the case studied, the effect of multiple-support excitations is not significant because both displacements are very similar. The amplitudes of the

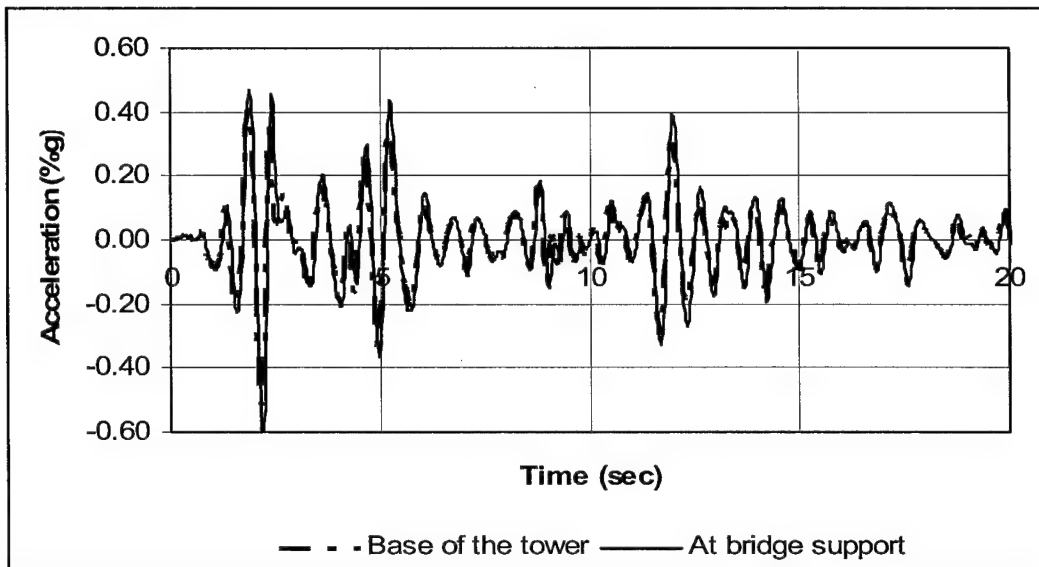


Figure 27. Acceleration at the tower base and bridge support (El Centro)

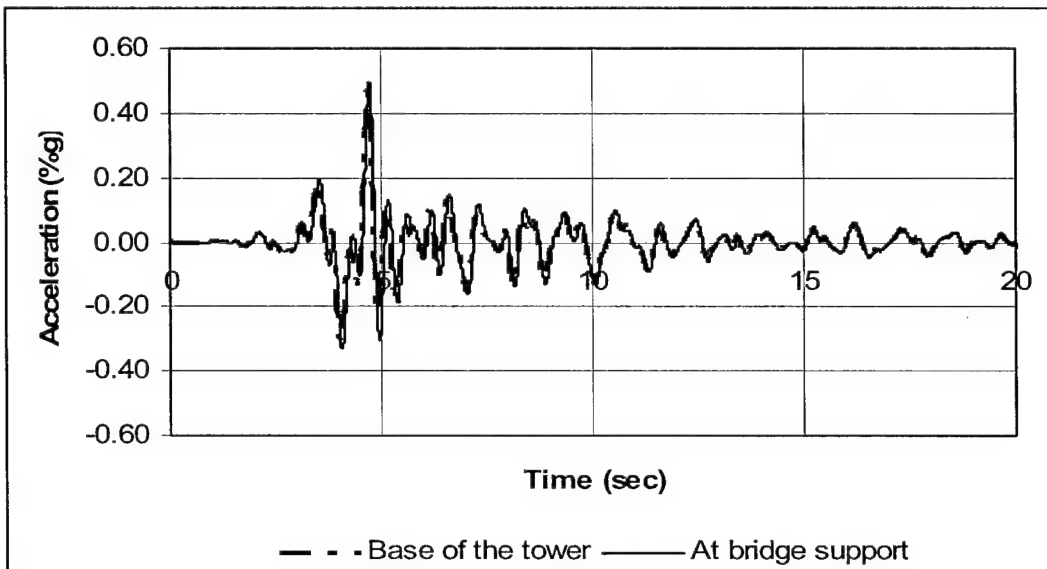


Figure 28. Acceleration at the tower base and bridge support (Loma Prieta)

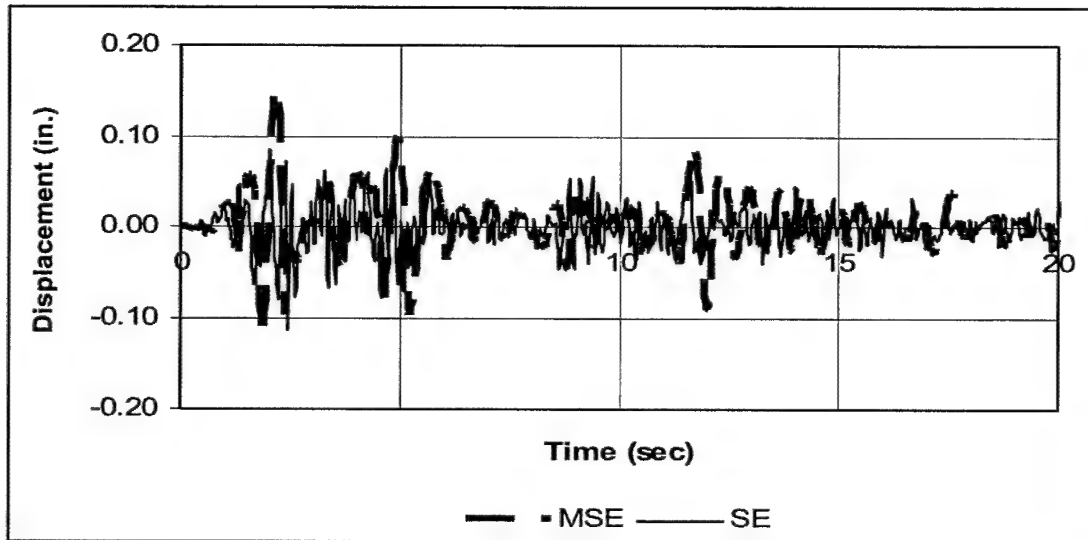


Figure 29. Relative displacements (El Centro)

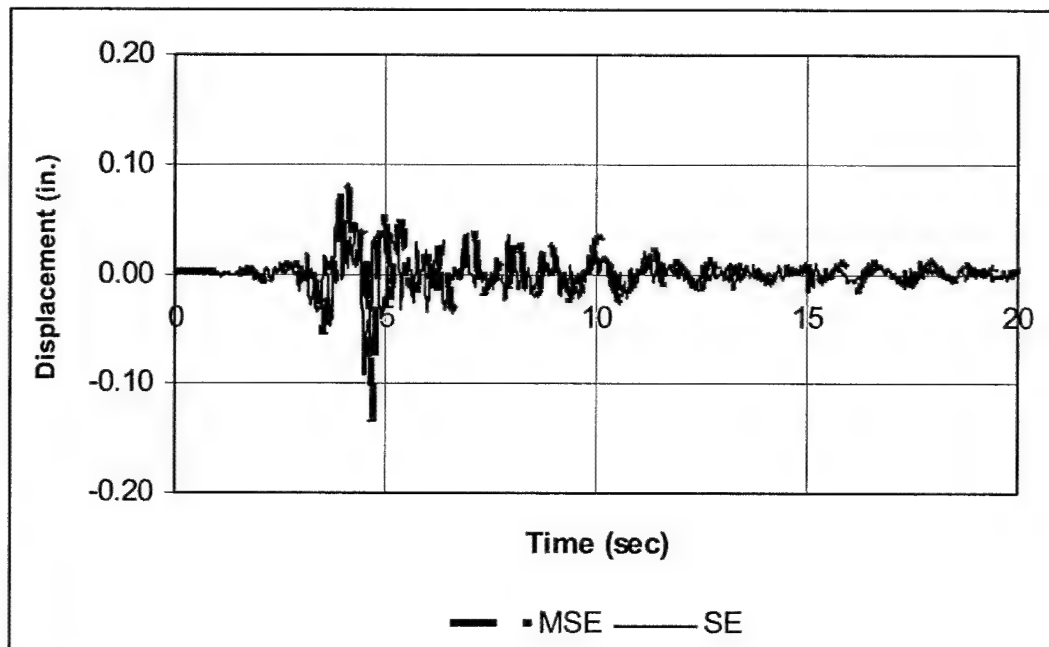


Figure 30. Relative displacements (Loma Prieta)



displacements calculated with the two models have a small variation along the complete time-history. Only a small difference in the frequency content of the response can be noted. Thus, at least for this particular case, the effect of the spatial variability of the ground motion at the supports is not important. This result was expected because of the small variation in the acceleration time-histories at each support. It is possible, of course, that in other situations in which the seismic motion at the top of the dam is significantly amplified and filtered, the consideration of the MSE effects could be important.

To gain further insight into the response of the structural system, the response was also calculated with the finite element model of the dam plus the intake tower and bridge. This permits verifying the results of the MSE analysis with a more accurate (but more complicated) model. Figures 31 and 32 show a comparison between the relative displacement time-histories at the top of the tower predicted by the dam plus tower finite element model and by the MATLAB-based frame model with the MSE.

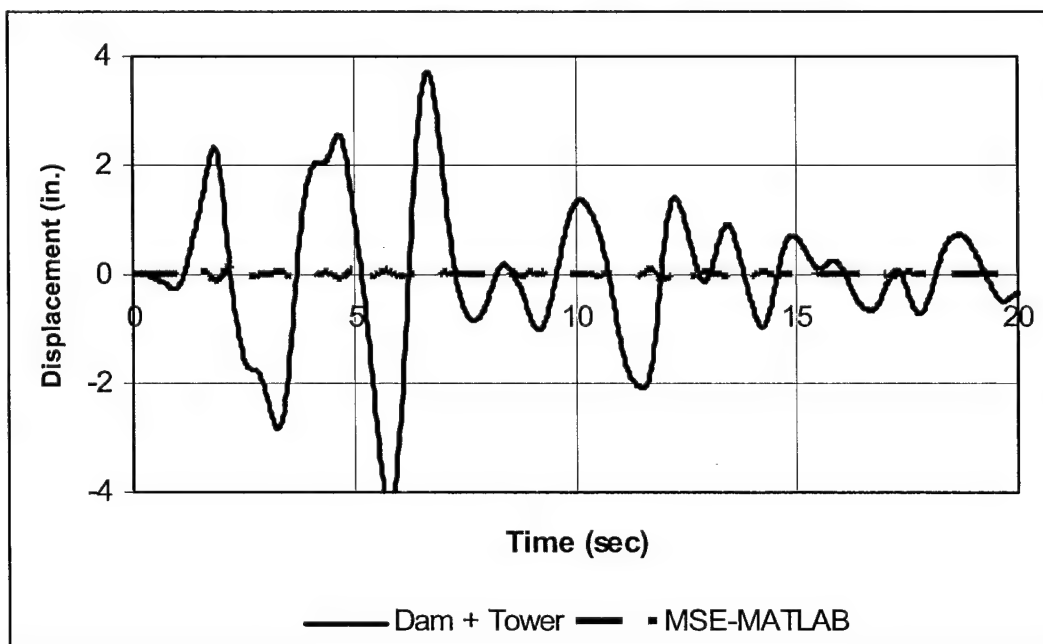


Figure 31. Relative displacements obtained with the frame model with MSE effects and with the dam plus tower finite element model (El Centro)

Obviously, the results are extremely different, almost of one order of magnitude. At first sight, these results were surprising since it was previously shown that the MSE effects were not important. These findings demonstrated the necessity of carrying out more analyses and extending the investigation.

To begin the investigation into the causes of the differences, the acceleration time-histories at the base of the tower and at the support of the bridge were now calculated using the finite element model of the dam with the intake tower included. It is recalled that the accelerations used as input to the frame model

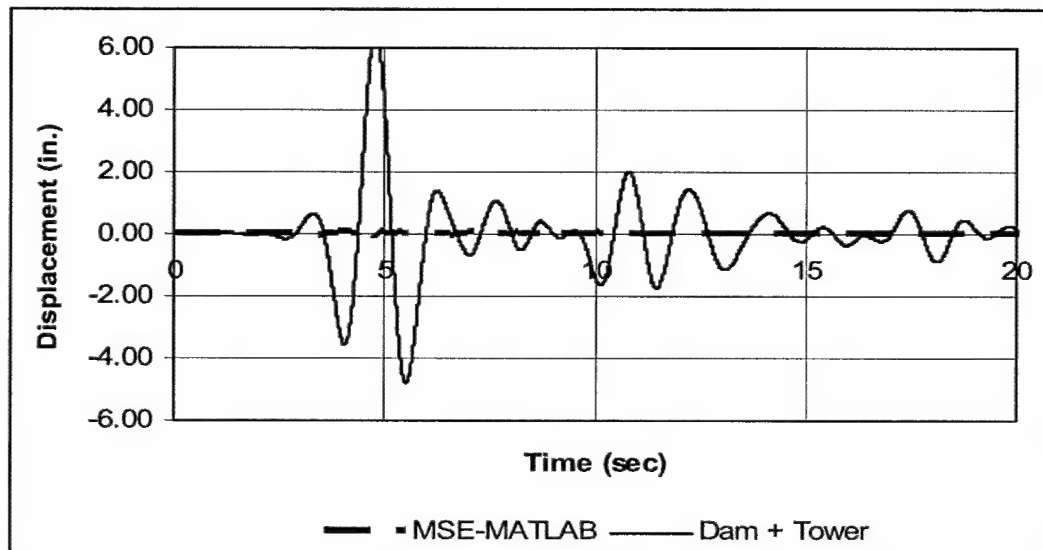


Figure 32. Relative displacements obtained with the frame model with MSE effects and with the dam plus tower finite element model (Loma Prieta)

were obtained from the finite element model of the dam alone (presented in Figures 27 and 28). The absolute accelerations at the base of the tower and at the bridge abutment (at the crest of the dam) computed with the combined model are displayed in Figures 33 and 34 for the El Centro and Loma Prieta earthquakes, respectively. It is very interesting to note the difference between the acceleration time-histories predicted by these two models (with and without the tower). The first difference that can be noticed is that the magnitudes of the accelerations are quite different. The accelerations will be compared in the following section, where additional discussion will also be presented. Here we would like to point out an interesting and unexpected phenomenon. The majority of the previous investigations dealing with dam response reported an amplification of the accelerations at the top. However, the results presented in Figures 33 and 34 reveal that the situation is different when the intake tower and the bridge are included in the model of the dam and its foundation. Here, there is a slight attenuation of the acceleration amplitudes at the crest of the dam. It can also be observed from the figures that the acceleration time-histories at the top of the dam (at bridge support) have the higher frequency components filtered out, as expected.

## Soil-Structure Interaction

To provide a better picture of the differences between the accelerations acting on the tower base obtained with finite element models of the dam alone and the dam plus tower, two comparative plots are presented. Figures 35 and 36 show the absolute acceleration time-histories at the base of the dam for the two finite element models and for the two earthquakes being considered. These plots indicate that there are significant differences between the accelerations at the

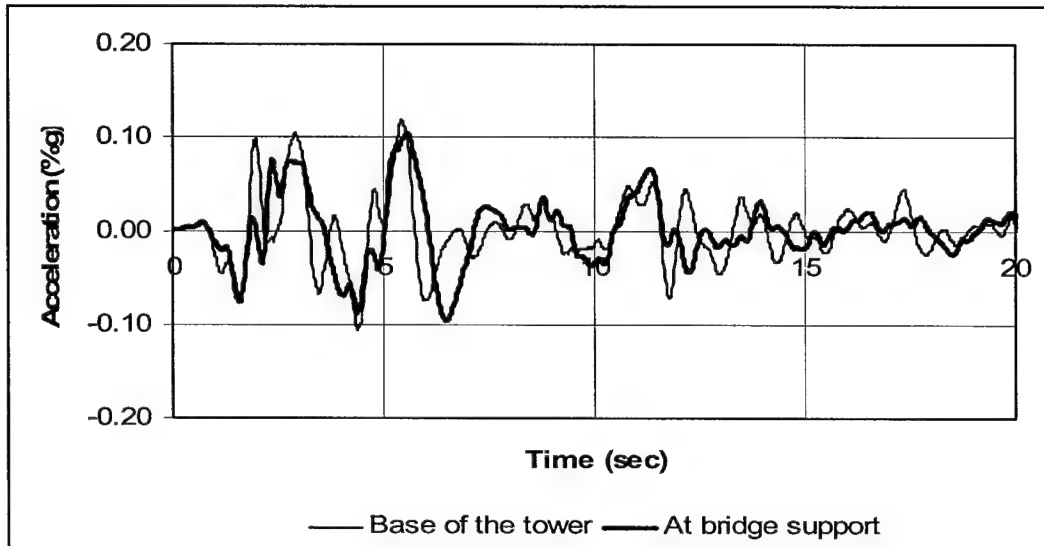


Figure 33. Accelerations at the tower base and bridge support obtained with the dam plus intake tower finite element model (El Centro)

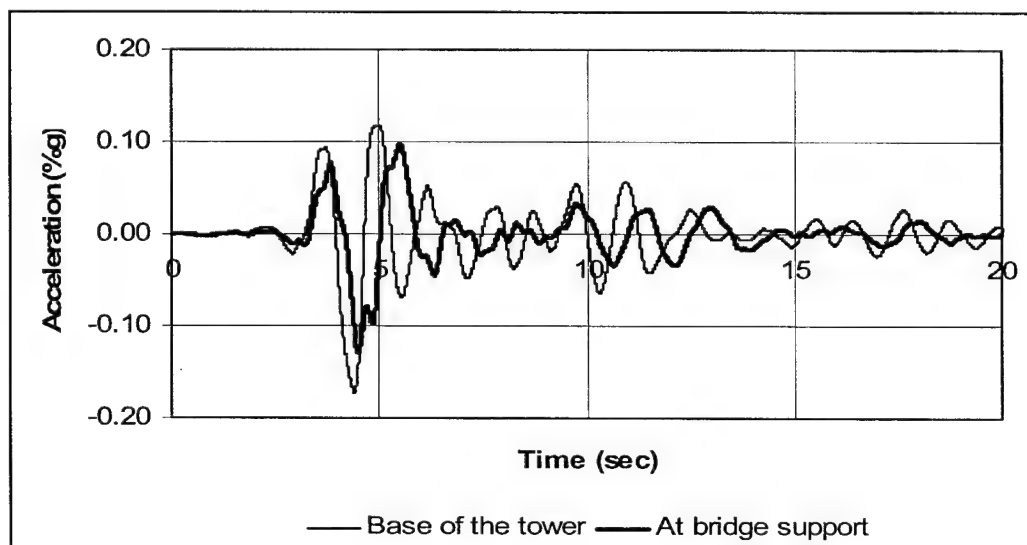


Figure 34. Accelerations at the tower base and bridge support obtained with the dam plus intake tower finite element model (Loma Prieta)

dam base when the tower is present and when it is not. The acceleration at the dam plus tower results demonstrates the importance of the dynamic interaction between the intake tower and the soil structure (the dam and the foundation). These findings explain the great differences in the previous results.

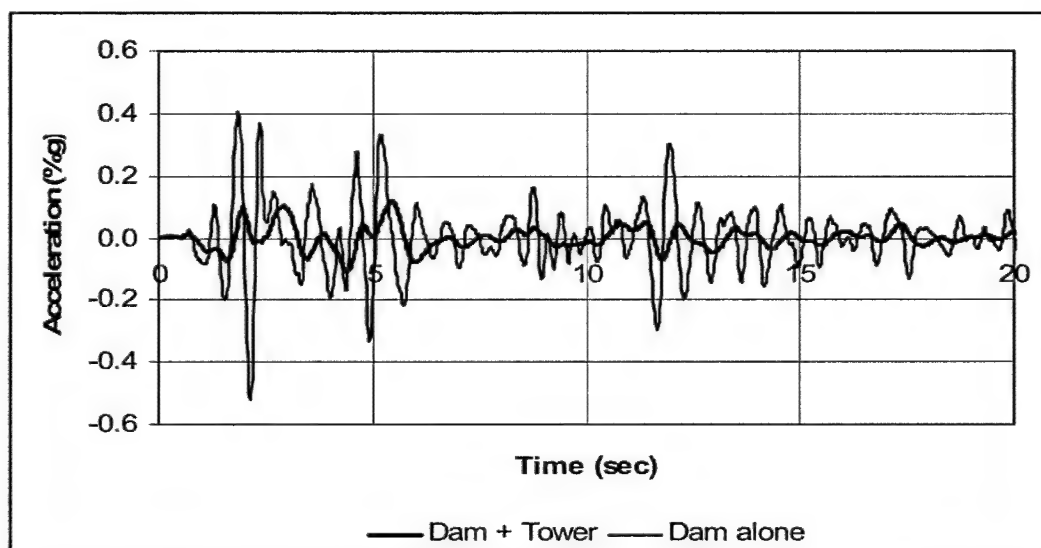


Figure 35. Accelerations at the base of the dam obtained with the dam plus intake tower and the dam alone finite element models (El Centro)

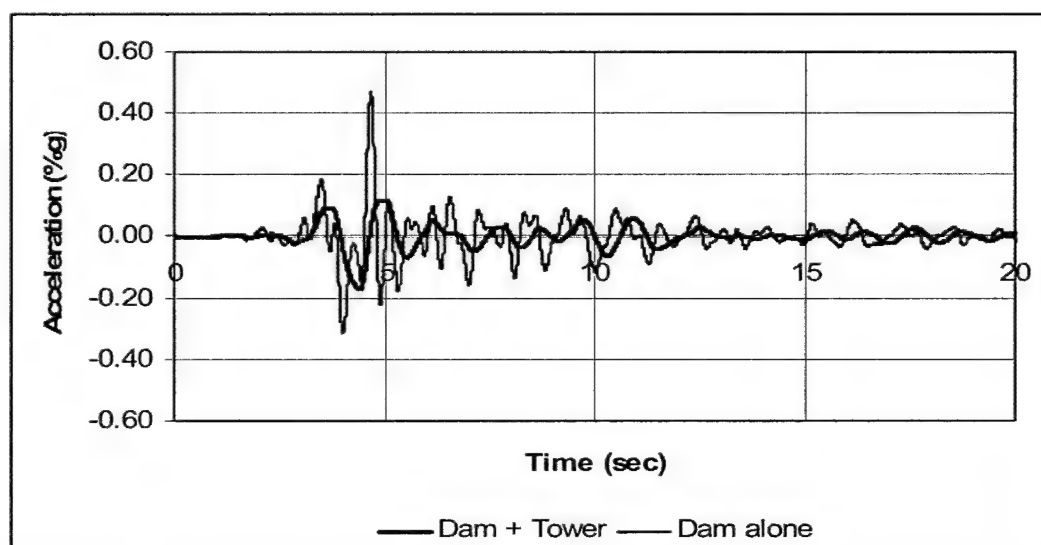


Figure 36. Accelerations at the base of the dam obtained with the dam plus intake tower and the dam alone finite element models (Loma Prieta)

Another result obtained with the model of the dam with the tower that can help to gain insight into the phenomenon is the variation of the free-field acceleration at different points along the free surface. Three points were selected to compute the acceleration; these are shown in Figure 37. Figures 38 and 39 show the acceleration time-histories at the three points in the free surface. The acceleration time-histories at nodes 1172 and 1055 shown in Figure 38 look very similar. These nodes are at the same elevation, but on opposite sides of the dam. This

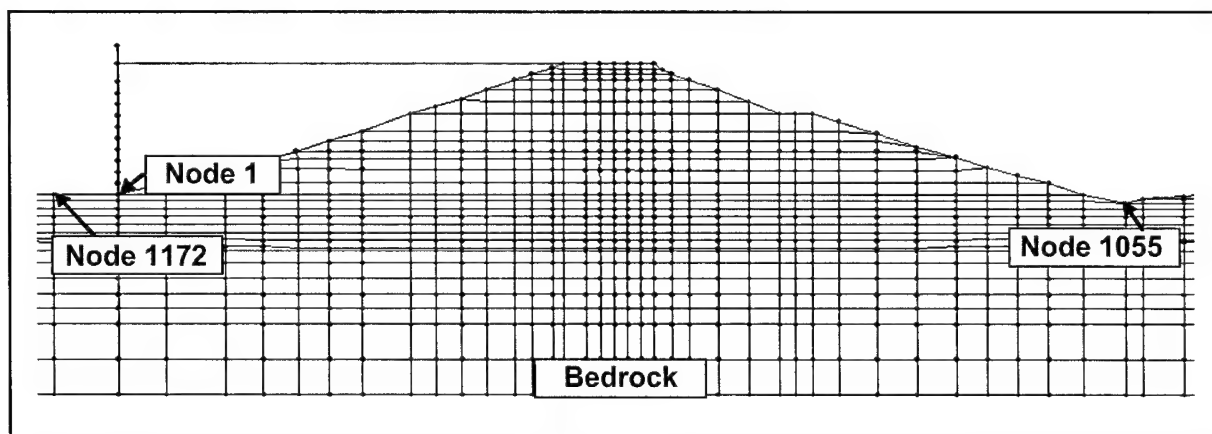


Figure 37. Nodes of the finite element model selected to calculate the acceleration

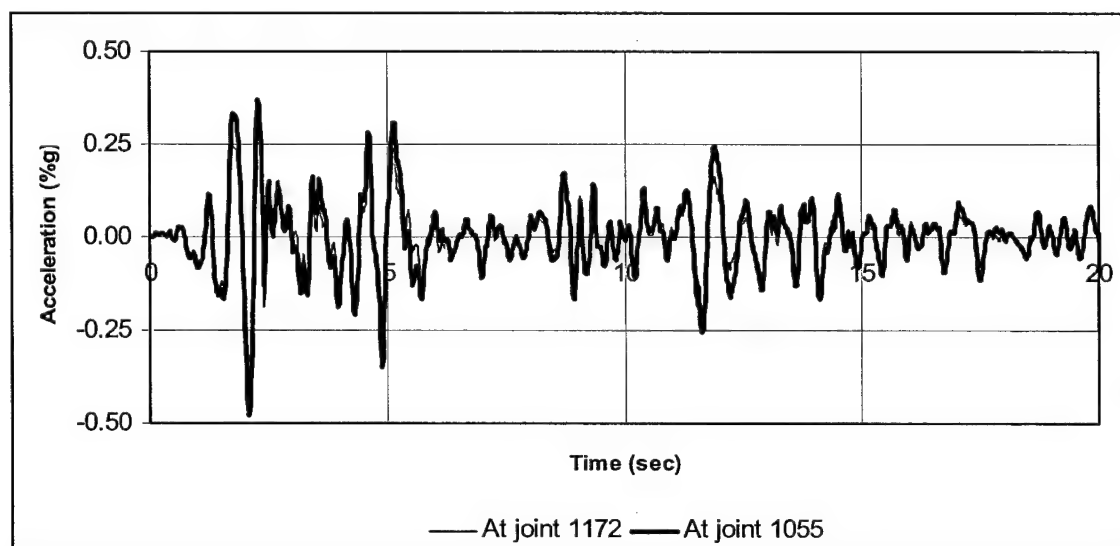


Figure 38. Acceleration time-histories at two nodes at the free surface on opposite sides of the dam

similarity was expected since the free-field accelerations at a point with the same elevation on a soil deposit with similar conditions should be very similar. However, as shown in Figure 39, the acceleration trace at node 1 looks very different from that at node 1172, which is located just to the side of it (see Figure 37). Node 1 is located at the interface of the dam and the intake tower. This result once again demonstrates the importance of the soil-structure interaction effects in this particular case study. The difference between the motions of the soil surface and of the base of the structure will result in a quite distinct response of the intake tower when its base is assumed fixed.

An additional numerical test was done to assess the importance of the soil structure-interaction effects in this particular case. The modulus of elasticity

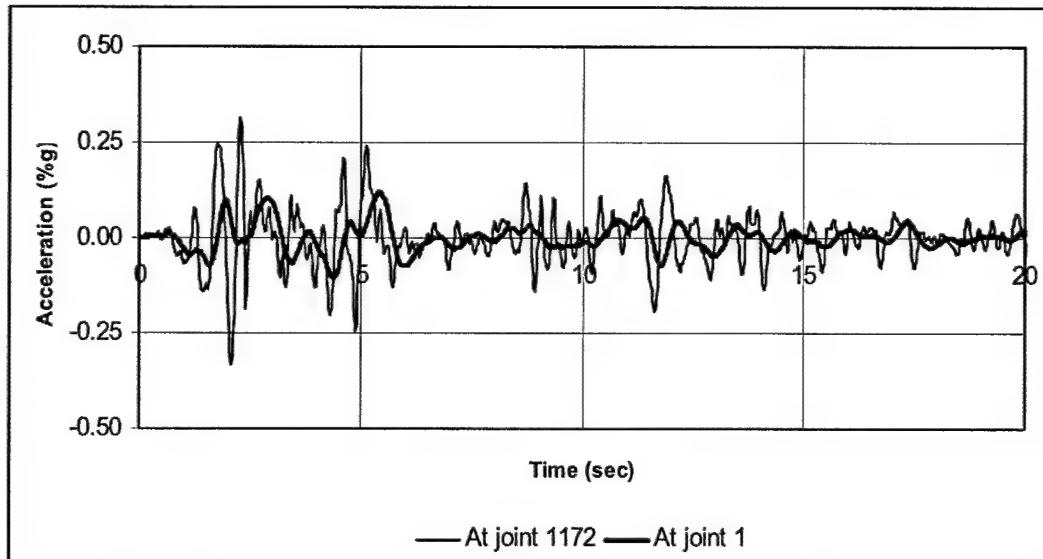


Figure 39. Acceleration time-histories at a node at the tower base and on the free surface

of each material that composes the embankment was increased so that the point of support of the tower and bridge become closer to a fixed-base condition in which the soil-structure interaction effects should diminish. As expected, as the moduli were increased, the acceleration time-histories became closer to those of the dam alone where no interaction occurs. The ample differences in the stiffness of the structure compared with the soil stiffness are responsible for the important soil-structure interaction effects. The values of the shear moduli of the different types of soils in the embankment are very small compared with those of more competent soils. The soils in the embankment classify as  $S_D$  or  $S_E$  according to the 1997 Uniform Building Code (ICBO 1997), where  $S_B$  is rock or competent soil. Moreover, it is recalled that the intake tower is made of a hollow concrete square section with outside dimensions of  $30 \times 30$  ft, wall thickness of 3 ft, and height of 75 ft. Therefore, the tower is very rigid compared with the soil deposit beneath it. As a result, the foundation will translate and rotate, causing the tower's displacements to increase with respect to those previously calculated (for example, those displayed in Figures 29 and 30).

To account for the soil-structure interaction effects, a simplified model of the intake-outlet tower was proposed in which the soil stiffness and damping were represented by translational and rotational springs and dashpots, respectively. As mentioned in Chapter 4, the stiffness and damping coefficients were calculated from the expressions presented in the SAP2000 reference manual (CSI 2000). These equations are similar to those first proposed by Lysmer (1965) and other authors (Gazetas 1991), which are independent of the frequency of the excitation. These formulas were used only at the base of the tower; i.e., they represent the soil below the foundation of the tower. The corresponding stiffness coefficients for the springs at the point where the bridge is lying on the dam were obtained in a different way. They were calculated using the approach based on the application of a unit force in a finite element model. Using SAP2000, a unit force was applied at the point where the bridge is connected to the dam. The force (or

moment) was applied once at a time in three directions (horizontal, vertical, and rotation), and the displacements and rotation along these directions were obtained. The stiffness coefficients were then calculated with the simple expression,

$$K = F/\Delta \quad (44)$$

in which  $F$  and  $\Delta$  represent the unit force (or moment) and displacement (or rotation) at each direction, respectively.

No dashpot was placed at the bridge support since the formulations available in the literature are based on a rigid disk in a semi-infinite half-space and thus they are not valid for the crest of the dam. The derivation of expressions for the damping coefficients for this particular case is out of the scope of this report. Thus, it was assumed that the springs-dashpots but without dashpots at the bridge location could approximate reasonably well the flexibility and energy radiation of the deposit below the tower and the dam below the bridge support. This is a reasonable assumption because the available damping coefficients represent the energy dissipation by radiation from the support into an elastic half-space with a plane interface. The crest of the dam where the bridge is supported cannot be considered as an elastic half-space, and thus the radiation damping should be smaller (albeit not zero, as it is being assumed here). Ignoring this damping will also lead to conservative results.

Using the values of the coefficients and the assumptions previously described, the frame model was analyzed again with the free-field acceleration as input. The displacements at the top of the tower were also calculated with the dam plus intake tower model to compare the results. Figures 40 and 41 present the relative displacement time-histories at the top of the tower for the frame with spring-dashpots and for the dam plus tower finite element model for the El Centro and Loma Prieta earthquakes.

Figures 40 and 41 show that the relative displacements of the proposed spring-dashpot model and the dam plus intake tower finite element model are in good agreement for both earthquakes. Therefore, based on these results one can preliminarily say that the simplified spring-dashpot model is reliable for this particular case. However, and in order to confirm the statement, additional tests are required. Both models were then analyzed by subjecting them to earthquakes with shorter and longer durations. Figures 42 and 43 show the relative displacements at the top of the tower for two short-duration earthquakes, namely Coalinga and Anza ground motions. The Coalinga accelerogram was recorded at Oil Fields Fire Station, California, on 2 May 1983 and the Anza record was measured at Pinyon Flat on 30 October 2001.

These figures show that again there are significant differences between the relative displacements at the top of the tower predicted by the two models. These results were unexpected because it was deemed that the spring-dashpot model would give a good approximation for all seismic motions. Thus, additional tests were performed to explain these findings.

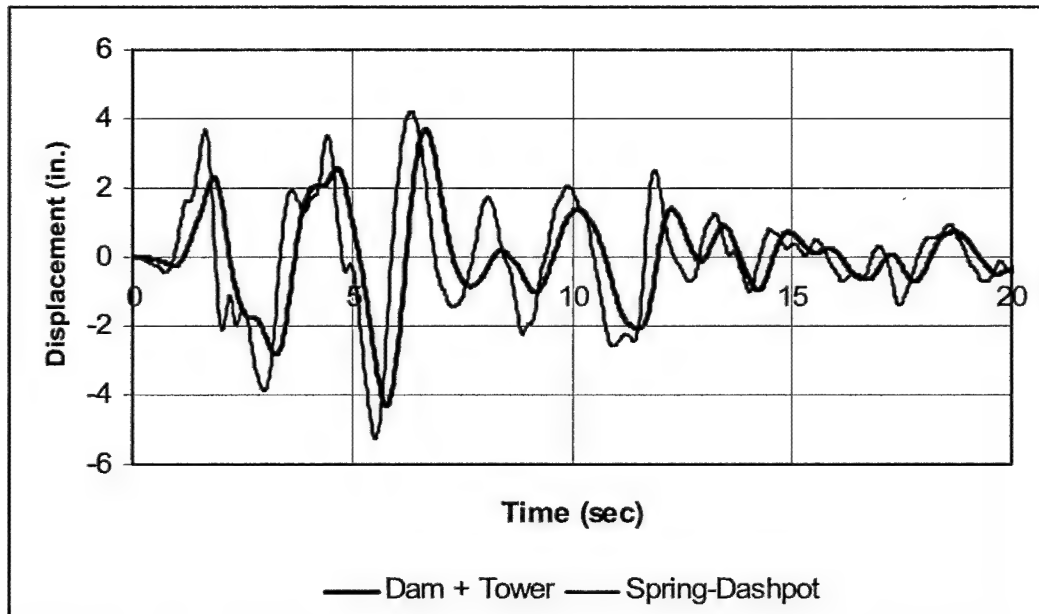


Figure 40. Displacements at the top of the tower for the dam plus tower and the frame with spring-dashpot models (El Centro)

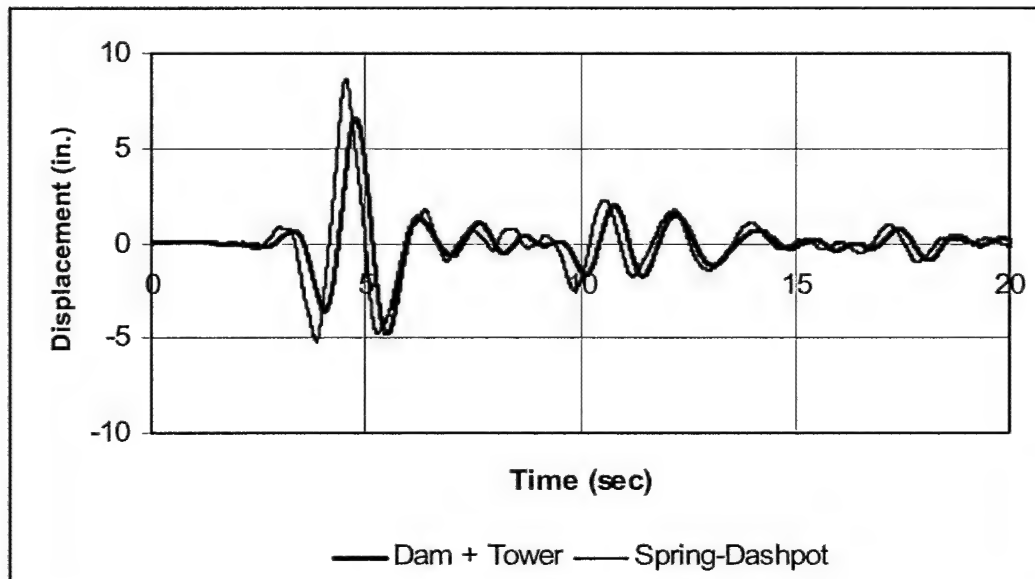


Figure 41. Displacements at the top of the tower for the dam plus tower and the frame with spring-dashpot models (Loma Prieta)



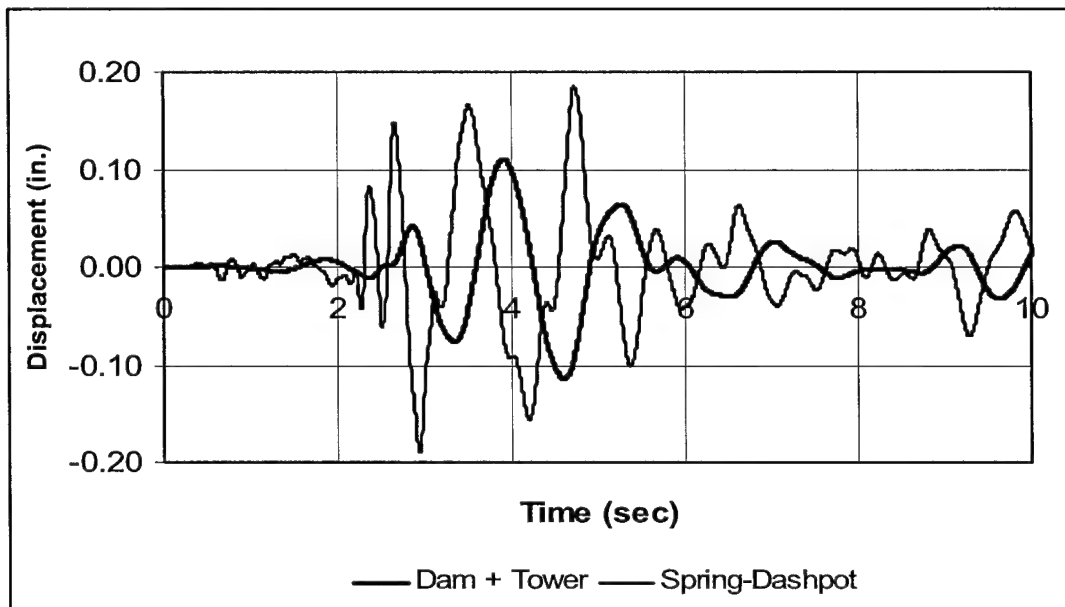


Figure 42. Displacements at the top of the tower for the dam plus tower and the frame with spring-dashpot models (Coalinga)

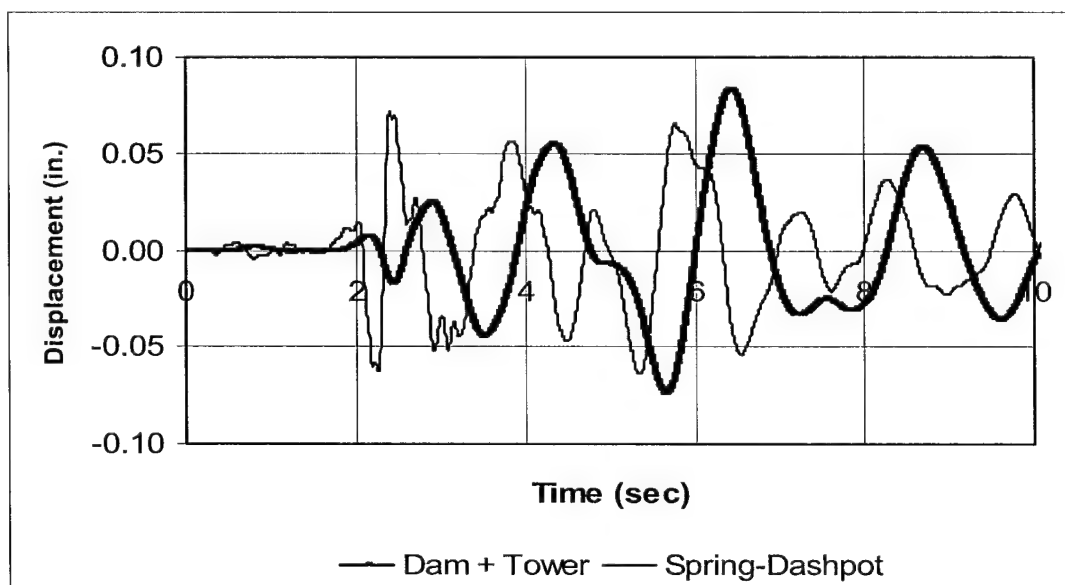


Figure 43. Displacements at the top of the tower for the dam plus tower and the frame with spring-dashpot models (Anza)

Fifteen additional earthquake time-histories were selected and applied to the frame model and dam plus tower finite element model. Some of the most relevant characteristics of these earthquakes are provided in Table 6. This information was obtained to have more data to clarify the problem. The Fourier spectrum was calculated to obtain the dominant period and frequency of the motion. The duration of the strong motion was also calculated. The dominant periods and frequencies, total duration, and duration of the strong motion ( $D_{strong}$ ) are displayed in the table. The first five earthquakes (in bold italics) are those for which the results of the frame with spring-dashpots and dam plus tower finite element model do not match very well. For the other 10 earthquakes listed in the table, the results are in good agreement. At first glance, the common characteristics of the first five earthquakes are their short durations (less than 11 sec except for the fifth one). Moreover, some of them have high dominant frequencies. The second observation would be that perhaps the problem is the frequency content of the acceleration time-history. Therefore, a series of tests using seismic input sinusoidal functions was performed to obtain some patterns and observe the trends. These results are not presented here for the sake of brevity. It was found that the sinusoidal functions with the higher dominant frequencies led to less similarity between the responses calculated with the two models.

**Table 6**  
**Strong Motion Duration, Predominant Periods, and Frequencies**  
**for Several Earthquakes**

Name	Duration sec	$D_{strong}$ sec	$T_p$ sec	$\omega_p$ rad/sec
<b><i>Round Valley</i></b>	6.85	3.605	0.0811	77.4745
<b><i>Anza</i></b>	10.32	2.10	0.0786	79.9387
<b><i>Coalinga</i></b>	10.30	2.34	0.1326	47.3845
<b><i>Anzap</i></b>	10.00	1.84	0.3567	17.6148
<b><i>Whittier Narrows</i></b>	20.00	4.42	0.2447	25.6771
Friuli	22.00	4.48	0.4073	15.4264
Trinidad	22.00	12.17	0.3191	19.6903
Imperial Valley	30.00	22.86	0.4122	15.2431
Pasadena	30.00	14.06	0.2090	30.0631
El Centro	31.00	23.86	0.6035	10.4112
Borrego	35.00	25.12	1.6614	3.7819
Loma Prieta at Gilroy Building	40.00	8.91	1.3320	4.7171
Loma Prieta at Anderson Dam	40.00	10.51	0.5506	11.4111
Cape Mendocino	44.00	18.66	2.4544	2.5600
Central California	40.00	25.20	0.8009	7.8452

Based on these results, the first conclusion obtained was that the stiffness and damping coefficients of the springs and dashpots needed verification. It is recalled that the values of these coefficients are only the function of the soil properties and main dimensions of the foundation. However, in theory these values also depend on the frequency of the excitation, even though for simplicity

this fact is often neglected in practice. Therefore, it was decided to use new coefficients that depend on the frequency of the seismic motion. These were calculated using the expressions developed by Gazetas et al. (1985). The equations proposed by Gazetas et al. (1985) are very similar to those used in the first analysis, but they are multiplied by a dynamic stiffness coefficient that depends on the excitation frequency. For nonharmonic excitations such as those due to real earthquakes, it is necessary to use the Frequency Response Method to fully account for the frequency dependency of the coefficients. However, the variation with frequency is not large, and it was deemed sufficient to set the frequency equal to the dominant frequency of the ground motion.

The relative displacement time-history (plotted for only the Coalinga earthquake, for the sake of brevity) is shown as Figure 44. This figure shows the responses obtained with the frame with spring-dashpots in which the coefficients are frequency independent and dependent on the frequency (the latter case is labeled as new spring-dashpot in the plot). These displacements are compared with those from the dam plus tower finite element model, which is regarded as the "exact" case. This plot shows no significant differences in the results between the two sets of springs and dashpots, indicating that disregarding the frequency dependency of the stiffness and damping coefficients is not the cause of the problem. Similar results were obtained for the other earthquakes, confirming again that there is no need to use frequency-dependent stiffness and dashpots coefficients, at least for this particular system. This statement should be reviewed on a case-by-case basis, however. One of the reasons why there is no need to consider frequency-dependent functions could be that the foundation block is very rigid and may not be sensitive to high-frequency excitation (Gazetas 1991).

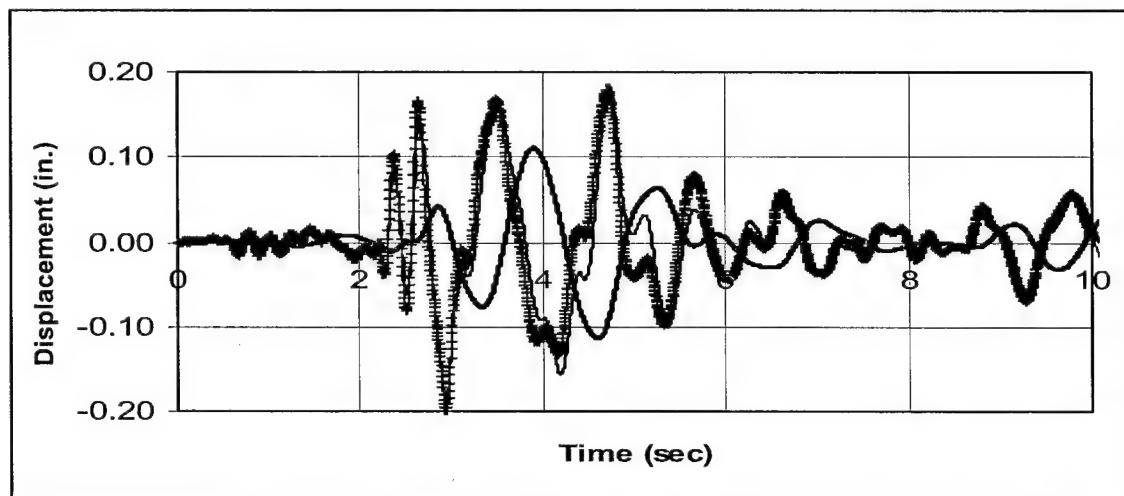


Figure 44. Displacements obtained with the dam plus tower and spring-dashpot models with frequency independent and dependent coefficients (Coalinga) [Note: — = Dam + Tower, --- = Spring-Dashpot, and —+— = Spring-Dashpot-new]

New sets of tests were performed to achieve good agreement between the response obtained with the simplified and full finite element model and to arrive at conclusions regarding the reasons for the discrepancies.

First, an eigenvalue analysis of the fixed-base intake tower modeled as a frame with and without the bridge was undertaken to observe the effect of the latter on the frequencies and periods. Next, the frame with spring-dashpots representing a flexible soil with and without the bridge was analyzed to obtain its natural frequencies and periods. Table 7 shows the natural periods for the simplified model of the intake tower with and without the service bridge and resting in a fixed and flexible soil foundation. Table 8 displays the natural frequencies for the

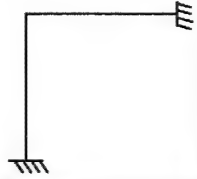
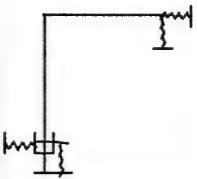

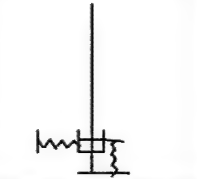

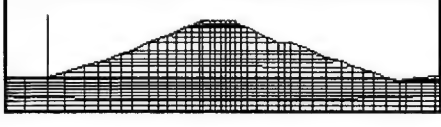
Table 7 Natural Periods of the Simplified Intake Tower Model				
	Fixed/Bridge	Flexible/Bridge	Fixed/No Bridge	Flexible/No Bridge
CASE				
MODE	Period sec	Period sec	Period sec	Period sec
1	0.1264	1.3859	0.1284	1.7816
2	0.0352	0.3502	0.0350	0.3495
3	0.0234	0.2658	0.0234	0.2659
4	0.0109	0.1237	0.0109	0.0252
5	0.0083	0.0509	0.0083	0.0196
6	0.0063	0.0252	0.0063	0.0091
7	0.0044	0.0197	0.0044	0.0090
8	0.0042	0.0091	0.0042	0.0057
9	0.0035	0.0090	0.0035	0.0045
10	0.0030	0.0057	0.0030	0.0042

Table 8 Modal Frequencies for the Simplified Intake Tower Model				
	Fixed/Bridge	Flexible/Bridge	Fixed/No Bridge	Flexible/No Bridge
MODE	Frequency rad/sec	Frequency rad/sec	Frequency rad/sec	Frequency rad/sec
1	49.7275	4.5338	48.9366	3.5268
2	178.7080	17.9409	179.4293	17.9774
3	268.6613	23.6393	268.8030	23.6270
4	576.1425	50.8007	577.0503	249.2425
5	755.5220	123.5330	755.5436	320.4843
6	1001.2780	249.0922	1001.6660	692.0222
7	1419.8940	319.6271	1419.9200	695.8858
8	1489.9280	691.2986	1491.2250	1097.3350
9	1816.4410	695.8807	1816.7210	1387.7560
10	2088.3500	1097.0620	2096.8810	1511.9260

same cases. The cases on rigid foundation were analyzed to obtain a measure of the flexibility of the springs on the spring-dashpot or flexible foundation model. It can be noticed that, when a fixed-base condition is used, the presence of the bridge has almost no effect on the periods and frequencies. For the flexible foundation models, the periods increased as expected when compared with the fixed-base cases. It can be noticed here a small increase in the lower periods of the model of the tower without the bridge. These results seem to indicate that the springs at the base of the tower are very rigid in all or some directions, since a greater increase in the periods for the flexible-base case was expected. This is so because the dominant vibration periods in the response calculated with the finite element model of the dam plus tower (shown in Figures 42 and 43) are larger than those of the spring-dashpots models. To verify this preliminary conclusion, the periods and frequencies of the dam plus intake tower finite element model were computed.

Table 9 summarizes the natural periods and frequencies obtained with the finite element model of dam plus intake tower with and without the access bridge. These results should be compared with the previously obtained periods and frequencies corresponding to the simplified intake tower model resting on flexible foundation (the spring-dashpot model) shown in Tables 7 and 8. Table 9 also contains natural periods and frequencies associated with the vibration of the dam itself; thus, these results cannot be compared on a one-to-one basis with those in Tables 7 and 8. Rather, the comparison should be made examining the mode shapes. Nevertheless, in general, the results confirm that the finite element model consisting of the dam and tower is more flexible than the spring-dashpot

**Table 9**  
**Natural Periods and Frequencies for the Dam Plus Tower Model**

Bridge			No Bridge		
					
Mode	No Bridge Period sec	Bridge Period sec	Mode	No Bridge Frequency rad/sec	Bridge Frequency rad/sec
1	19.7359	2.3753	1	0.3184	2.6452
2	1.6888	1.7573	2	3.7204	3.5755
3	1.2536	1.2940	3	5.0122	4.8556
4	0.6309	0.5776	4	9.9588	10.8776
5	0.5643	0.5642	5	11.1349	11.1362
6	0.5445	0.5432	6	11.5399	11.5674
7	0.5165	0.5155	7	12.1647	12.1896
8	0.5050	0.5055	8	12.4424	12.4304
9	0.4566	0.4566	9	13.7603	13.7611
10	0.4312	0.4340	10	14.5724	14.4764

model. Note also that when the bridge is taken out, the periods increase more dramatically than in the case of the spring-dashpot model. These findings demonstrate that, for the present system, the values of the spring constants used to represent the flexible soil foundation are not adequate to get a good approximation with the simple model. They underestimate the flexibility of the soil.

Before proceeding to deal with this situation, it is very instructive to examine the mode of vibration corresponding to the lowest natural period of the two finite element models considered in Table 9. These are shown in Figures 45 and 46. Note that, as shown in Figure 46, the very high period (19.7 sec) corresponds to a rigid body rotation of the intake tower caused by the rocking flexibility of the soil. The situation is similar when the bridge is included in the model (Figure 45), but the value of the period is now restricted by the presence of the bridge.

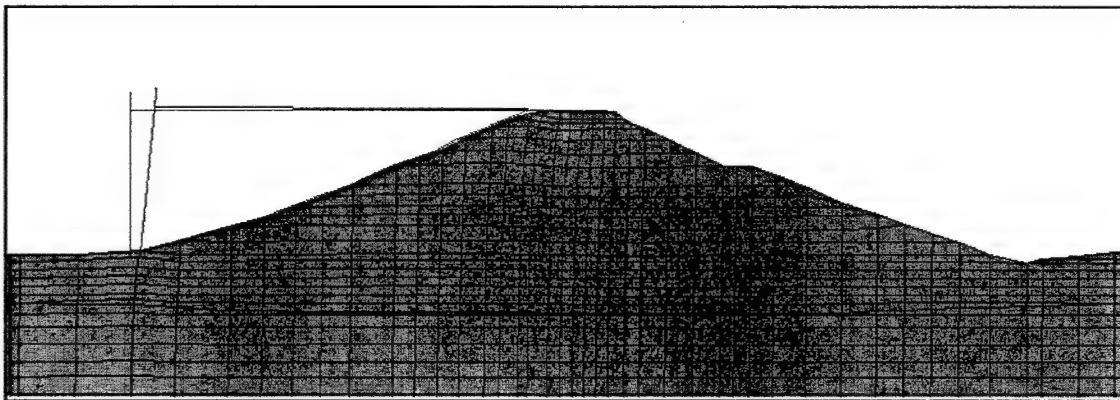


Figure 45. Mode shape obtained with the dam plus tower and bridge finite element model

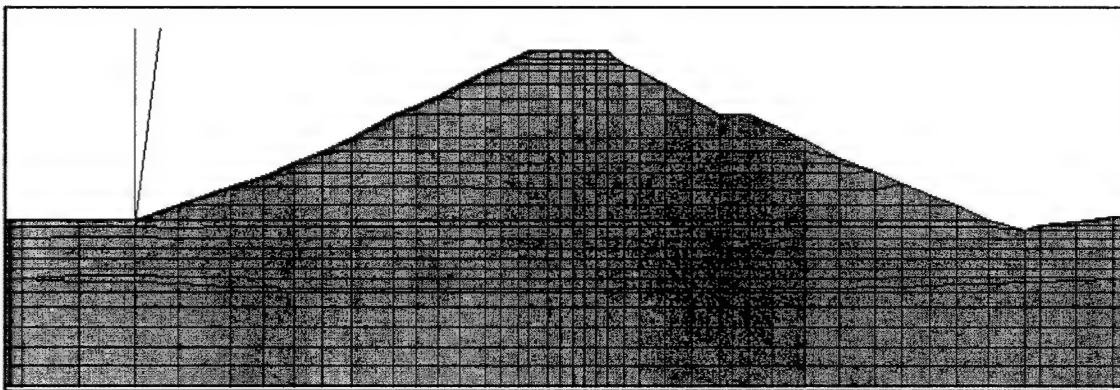


Figure 46. Mode shape obtained with the dam plus tower finite element model without the bridge

It was decided to evaluate the stiffness coefficients of the springs at the tower base using another method. Ideally, the coefficients should be determined using an analytical method so that they can be later applied to other situations.

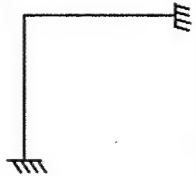
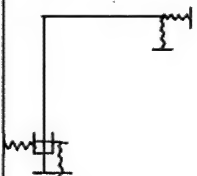
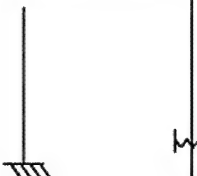
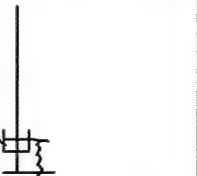
However, this is a task well beyond the scope of this report. Moreover, it is not clear what assumptions used to define the coefficients currently available are not appropriate and cause the problem previously described. Therefore, it was decided to perform a numerical simulation. As was done to determine the springs at the support of the access bridge, the stiffness coefficients were calculated using the unit force method and SAP2000. Table 10 shows the values for the stiffness coefficients obtained with this approach. The unit load was applied in the horizontal and vertical directions, and a unit moment was applied along the axis perpendicular to the plane of analysis. The values identified as "Equations" correspond to those obtained using the formulas in Chapter 4; i.e., they were calculated with the equations published in the literature. These values were used in the first spring-dashpot model.  $K_x$  and  $K_y$  represent the stiffness of the soil in the horizontal and vertical directions, respectively, and  $K_r$  is the coefficient of the rocking spring. It can be noticed that the coefficients calculated with the two methods show substantial differences.

<b>Table 10</b> <b>Stiffness Coefficients for the Spring-Dashpot Model</b>			
<b>Method</b>	<b><math>K_x</math> kip/ft</b>	<b><math>K_y</math> kip/ft</b>	<b><math>K_r</math> kip-ft/rad</b>
Equations	47,367	49,691	6,245,753
Unit-Force	1,265	2,406	44,763

Several tests were done varying the three original stiffness coefficients. The results demonstrated that the major factor influencing the response of this structural system is the rocking stiffness. The best agreement between the dam plus tower finite element model and the frame with spring-dashpots was obtained when the rocking stiffness calculated from the unit-force method was used. The periods and frequencies from the eigenvalue analysis were calculated and examined for a second time. The first 10 new natural periods and frequencies are presented in Tables 11 and 12, respectively. These should be compared with those in Table 9. It is evident that, using the new stiffness coefficients, the periods and frequencies of the frame with spring-dashpots are much closer to those of the dam plus tower finite element model. The natural periods obtained with the new rocking coefficient in Table 10 increased and are now closer to the corresponding periods of the dam plus tower model.

Once the natural periods were in better agreement, the displacements of the intake tower with the new stiffness coefficients were calculated again. The results of the new time-history analyses are presented in Figures 47 through 52. These figures show a comparison between the relative displacements at the top of the tower obtained by using the dam plus tower finite element model and the frame with spring-dashpots. The tower response is presented for several earthquakes with different durations and frequency contents. For a same earthquake, the displacements were calculated in two ways: first, all the vibration modes were used to calculate the response; next, the response was obtained by considering only the contribution of the first mode.

**Table 11**  
**Natural Periods for the Simplified Intake Tower Model with the New Coefficients**

CASE	Fixed/Bridge	Flexible/Bridge	Fixed/No Bridge	Flexible/No Bridge
				
MODE	Period sec	Period sec	Period sec	Period sec
1	0.1264	2.1446	0.1284	20.4082
2	0.0352	0.3502	0.0350	0.3495
3	0.0234	0.2729	0.0234	0.2731
4	0.0109	0.1237	0.0109	0.0253
5	0.0083	0.0509	0.0083	0.0196
6	0.0063	0.0253	0.0063	0.0091
7	0.0044	0.0197	0.0044	0.0090
8	0.0042	0.0091	0.0042	0.0057
9	0.0035	0.0090	0.0035	0.0045
10	0.0030	0.0057	0.0030	0.0042

**Table 12**  
**Natural Frequencies for the Simplified Intake Tower Model with the New Coefficients**

MODE	Fixed/Bridge	Flexible/Bridge	Fixed/No Bridge	Flexible/No Bridge
	Frequency rad/sec	Frequency rad/sec	Frequency rad/sec	Frequency rad/sec
1	49.7275	2.9298	48.9366	0.3079
2	178.7080	17.9409	179.4293	17.9775
3	268.6613	23.0200	268.8030	23.0080
4	576.1425	50.8011	577.0503	248.7022
5	755.5220	123.5316	755.5436	320.4843
6	1001.2780	248.5518	1001.6660	692.0222
7	1419.8940	319.6271	1419.9200	695.3091
8	1489.9280	691.2986	1491.2250	1097.3350
9	1816.4410	695.3041	1816.7210	1387.2050
10	2088.3500	1097.0620	2096.8810	1511.9260



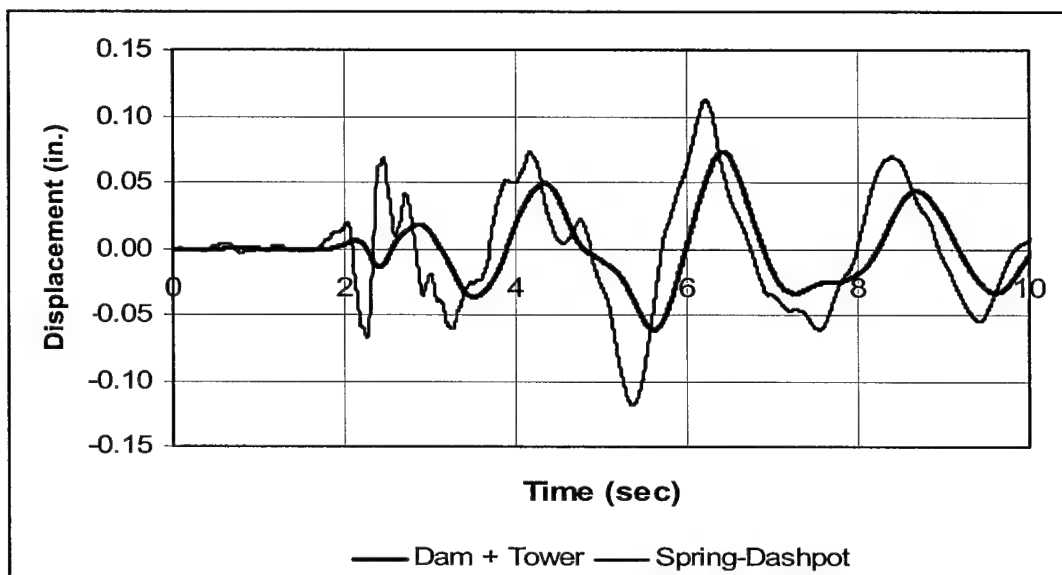


Figure 47. Relative displacements obtained with the dam plus tower and the new spring-dashpot models including all modes (Anza)

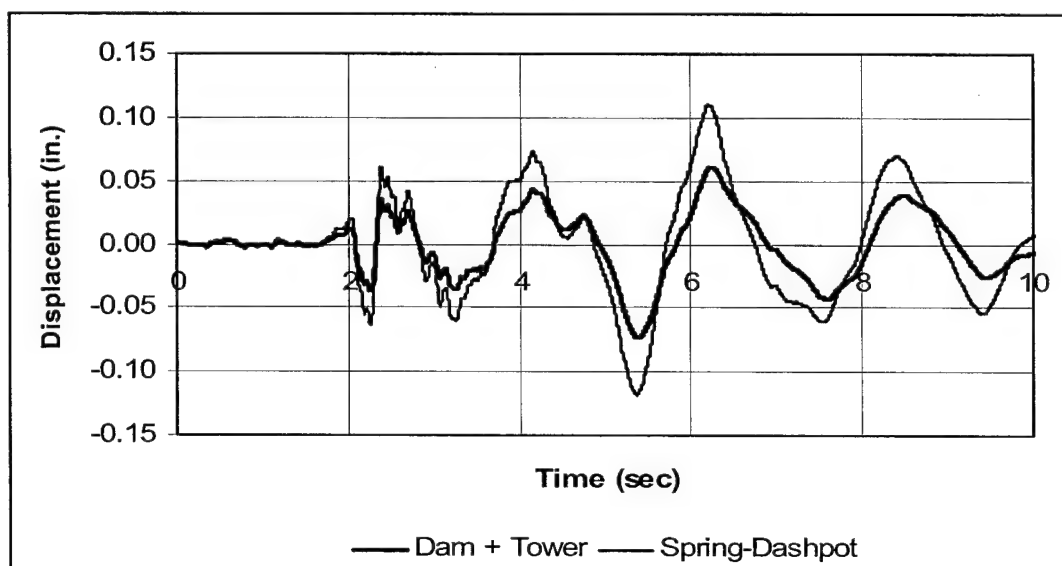


Figure 48. Relative displacements obtained with the dam plus tower and the new spring-dashpot models considering only the first mode of vibration (Anza)

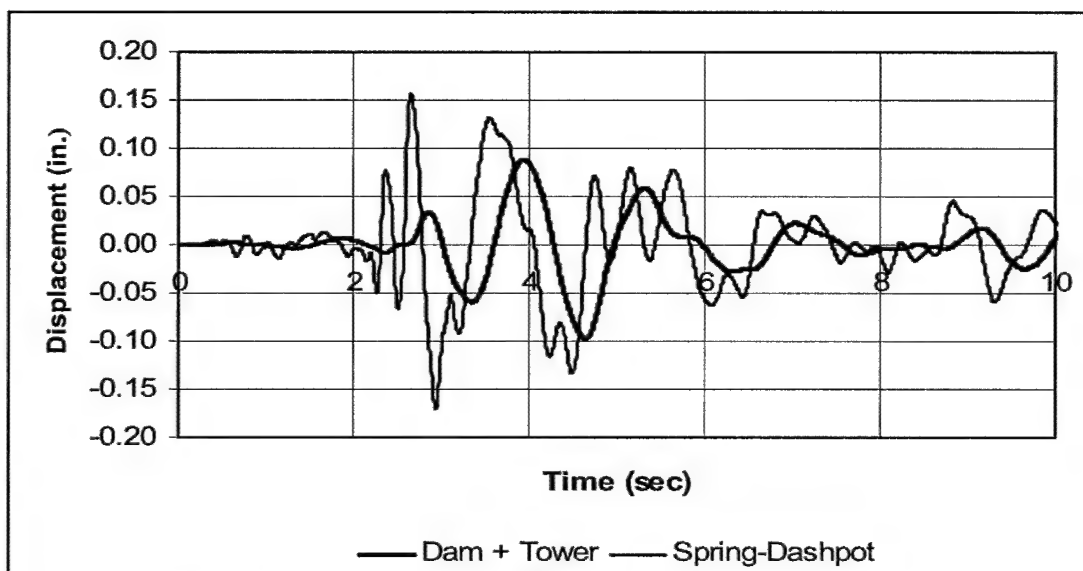


Figure 49. Relative displacements obtained with the dam plus tower and the new spring-dashpot models including all modes (Coalinga)

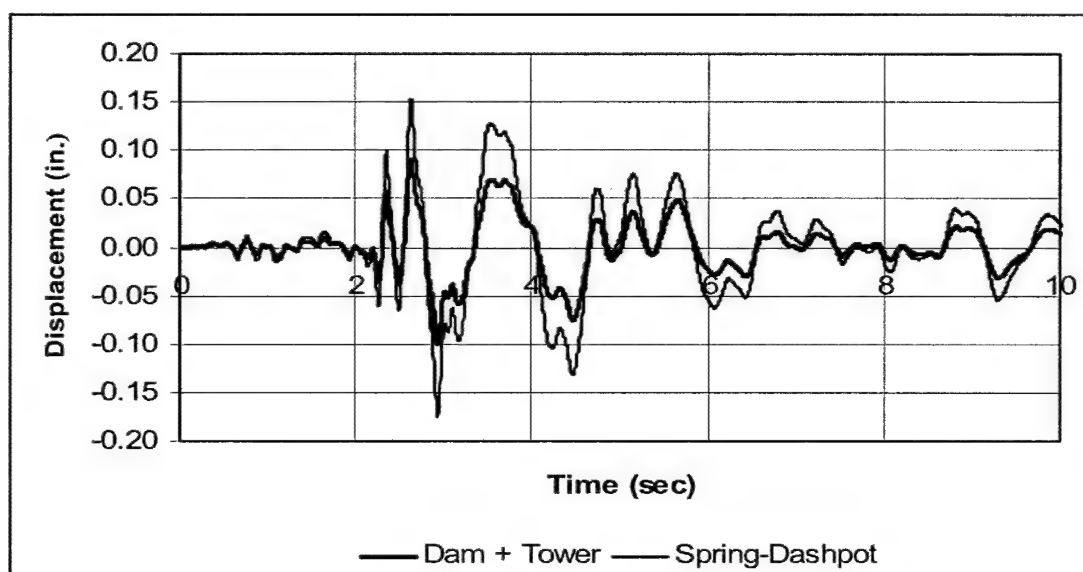


Figure 50. Relative displacements obtained with the dam plus tower and the new spring-dashpot models considering only the first mode of vibration (Coalinga)

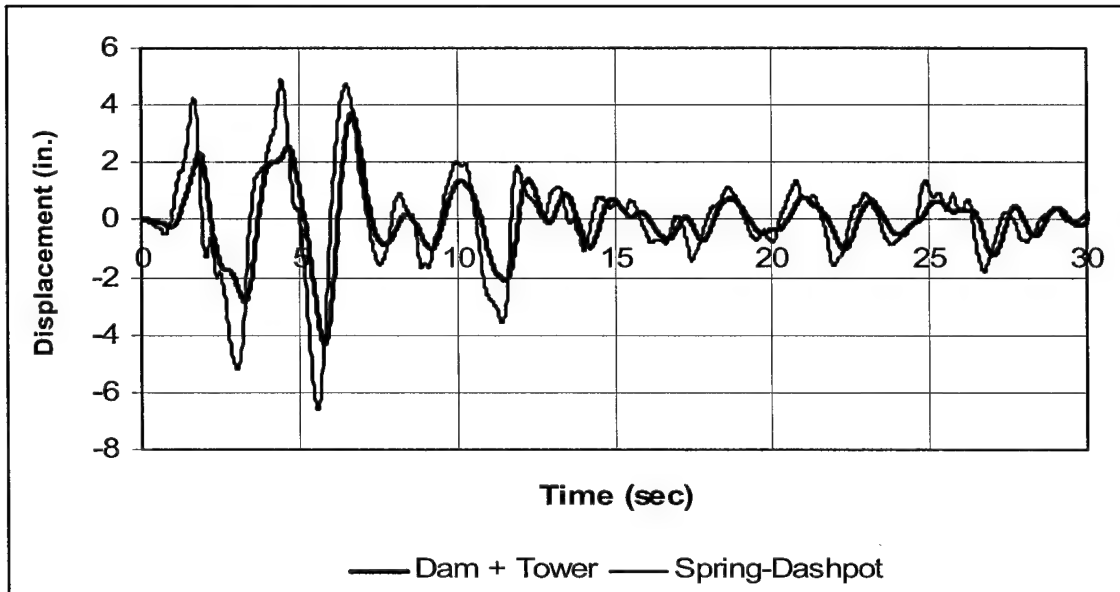


Figure 51. Relative displacements obtained with the dam plus tower and the new spring-dashpot models including all vibration modes (El Centro)

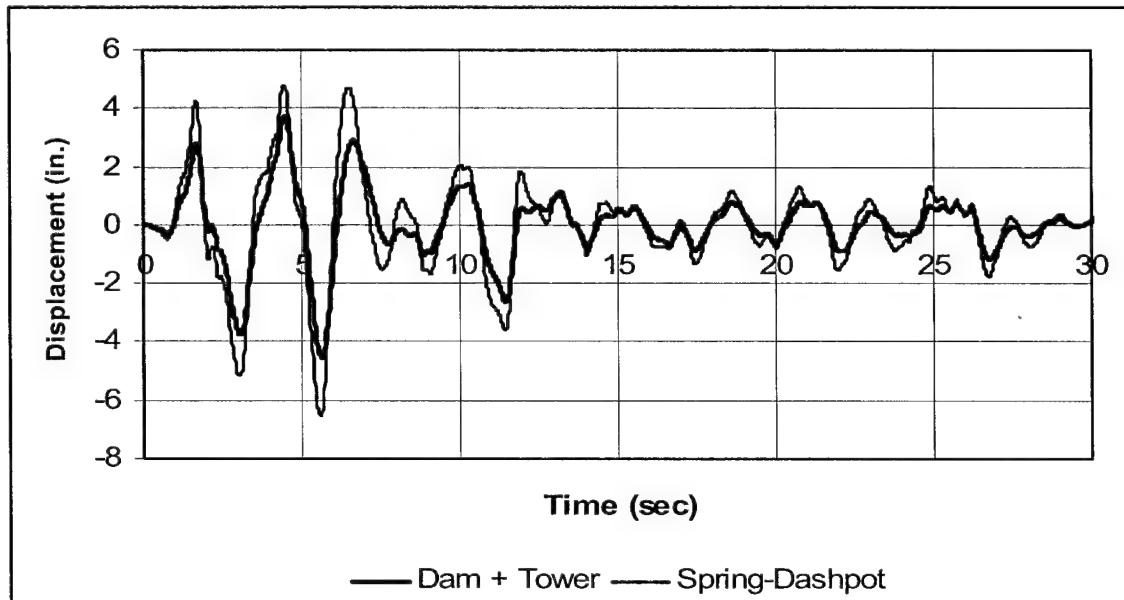


Figure 52. Relative displacements obtained with the dam plus tower and the new spring-dashpot models considering only the first mode of vibration (El Centro)

The first four plots (Figures 47 through 50) correspond to the short-duration earthquakes (Anza and Coalinga). These graphs are presented first, since it was for these earthquakes that the larger differences between the results of the spring-dashpot model and the finite element analysis were observed. The last two plots (Figures 51 and 52) show the displacements at the top of the tower for the El Centro earthquake, for which reasonable results were obtained with the original spring coefficients. A better agreement between the two models was now achieved.

It is evident that now all the plots show a good agreement between the responses calculated with both models. This fact verifies the importance of the soil rocking stiffness in the seismic analysis of intake towers founded in soft soils. Moreover, the results indicate the need of refining the definitions of the spring coefficients so that they more accurately represent the stiffness of the soil.

Comparing the time-histories computed with several modes and with the lowest mode, one can conclude that a good approximation can be achieved by using only the first mode of vibration. This occurs because the soil-structure interaction accentuates the importance of the first mode of vibration, i.e., the rigid body rotation of the tower.

The last set of results demonstrates that the proposed frame with spring-dashpots model is acceptable for calculating the approximate seismic response of the intake tower and bridge system, provided that the proper spring coefficients are adopted. Note that the frame model slightly overestimates the magnitude of the displacements. These differences could be lessened by changing the values of the damping coefficients. However, in this study, the coefficients of the dashpots were not modified; i.e., the original expressions in Table 5 were used to define them.

The importance of the rocking stiffness in this case study could be the result of many factors. Some studies confirm that, for tall structures such as the pylons of tall bridges, the most important mode of foundation behavior is the rocking stiffness term (Po Lam and Law 2000). The intake tower of this study is a relatively tall structure founded on soft soil causing the increase of the displacements and rotation at its base. Thus, perhaps for this reason, the rocking stiffness has a great influence in the overall response of this particular case study. Also, with regard to the subject of rocking in buildings, another author (Bard 1988) conducted a study measuring the transverse and rocking components of the motion at the base of several tall buildings. The buildings of this study have between 3 and 12 stories. Bard (1988) confirmed that if the building is founded on a flexible base, the rocking motion should be larger than for the same building founded on a fixed base. He stated that the large amount of rocking proved the existence of a very strong soil-structure interaction. These two studies verified the importance of having a good approximation of the rocking stiffness to properly account for the soil-structure interaction phenomenon.

## Response Spectrum Analysis

A response spectrum analysis was performed to directly obtain the maximum responses of the intake-outlet tower under study. The base shear and overturning moment were calculated by implementing the formulation described below into a MATLAB-based program.

First, the maximum modal forces for a frame model were calculated as follows:

$$(F_j)_{max} = K \Phi_j \frac{T_j^2}{4\pi^2} PSA_j \quad (45)$$

where

$K$  = stiffness matrix

$\Phi_j$  =  $j^{th}$  mode of vibration ( $j^{th}$  column of the eigenvector matrix)

$T_j$  = corresponding period

$PSA_j$  = spectral acceleration obtained from the response spectrum for the period  $T_j$

For a plane frame model, Equation 45 gives forces in the horizontal and vertical directions as well as moments. However, if a lumped mass model is used, the rotations (and moments) are condensed out; i.e., only the translational dofs are used. Adding the horizontal components of the forces in Equation 45, one obtains the modal base shear for a given mode  $j$  with

$$V_j = \sum_{i=1,3,5,\dots}^N F_{ij} \quad ; j=1..N \quad (46)$$

in which  $N$  is the total number of dofs. In Equation 6.3 it is assumed that the horizontal forces are those with odd subindices, and a lumped mass model was used.

The total maximum base shear can be approximately computed by using the SRSS (square root of the sum of the squares) modal combination rule:

$$V = \sqrt{\sum_{j=1}^N V_j^2} \quad (47)$$

The modal overturning moments are calculated using the horizontal modal forces:

$$M_j = \sum_{i=1,3,5,\dots}^N F_{ij} h_i \quad ; j=1..N \quad (48)$$

where  $h_i$  is the distance from the point of application of the force  $F_{ij}$  to the base. Using the SRSS modal combination rule, the total maximum overturning moment at the base is obtained as follows:

$$M = \sqrt{\sum_{j=1}^N M_j^2} \quad (49)$$

The base shear and overturning moment were calculated using a design spectrum for a soil type  $S_D$  and damping ratio of 24.5 percent. It is recalled that this is the equivalent damping ratio that accounts for the nonlinear behavior of the soil and was obtained by matching the responses from QUAD4M and SAP2000. These results were compared with those obtained from a time-history analysis using earthquakes compatible with the design spectrum. To obtain a design spectrum for 24.5 percent damping ratio, the reduction factors developed by Newmark and Hall (1982) were applied to the spectral acceleration spectrum for 5 percent of damping. The reduction factor used is

$$SR_A = \frac{3.21 - 0.68 \ln(\zeta_{eff})}{2.12} \quad (50)$$

where  $\zeta_{eff}$  is the desired damping ratio (in this case, 0.245) and the constant "2.12" in the denominator is the corresponding amplification factor with respect to the 5 percent damped elastic design spectrum. The design spectrum selected for the study was the one specified in the 1997 Uniform Building Code (ICBO 1997) for seismic zone 3 and soil profile type  $S_D$ .

A set of compatible earthquakes was produced by Luis A. Montejo, graduate student at the University of Puerto Rico at Mayagüez. He generated two compatible earthquakes for a UBC-97 design spectrum with 24.5 percent damping and soil type  $S_D$ . The process for the generation of compatible accelerograms is based on the modification of recorded acceleration time-histories using the wavelet transform (Montejo 2004). The El Centro and Loma Prieta earthquakes were used as starting or seed accelerograms to implement the process. In addition to the analysis using the UBC-97 design spectrum and to the spectrum-compatible accelerograms, a response spectrum analysis using the ground response spectra of the El Centro and the Loma Prieta earthquakes was undertaken.

Figures 53 and 54 show the pseudo-acceleration response spectra for the El Centro and Loma Prieta earthquakes, respectively. Each figure contains three spectra: the 5 percent damping spectrum of the original earthquake, the 24.5 percent of the original accelerogram, and the spectrum compatible with the UBC-97 for 24.5 percent damping.

Tables 13 through 16 present the base shear and overturning moment calculated with the response spectrum or time-history analysis. Two models of the tower were used: the frame model previously described and a shear building model. Shear building models are not commonly used to study structures such as towers because the deformation pattern of the latter structural systems is governed by bending. However, it was considered interesting to examine how well

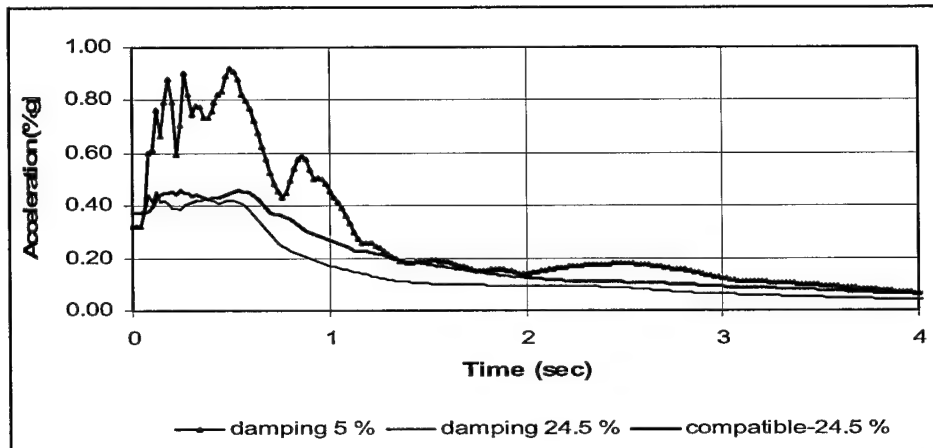


Figure 53. Acceleration response spectra for the El Centro earthquake

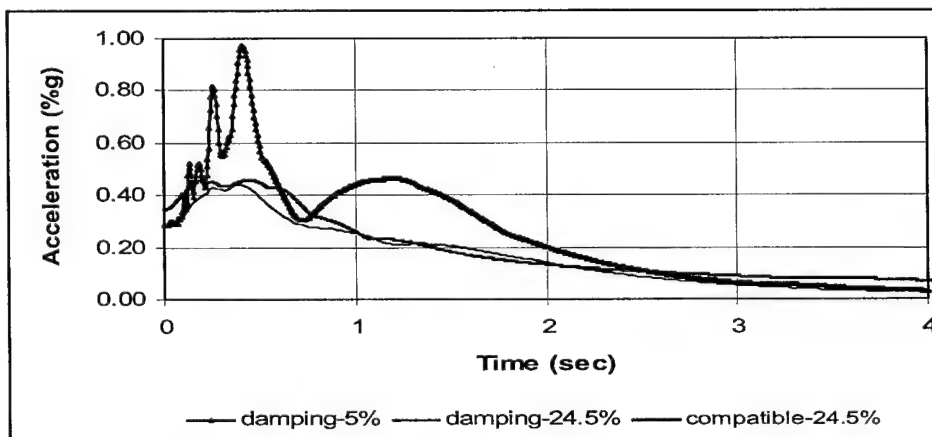


Figure 54. Acceleration response spectra for the Loma Prieta earthquake

<b>Table 13</b> <b>Base Shears and Overturning Moments for El Centro and Loma Prieta Earthquakes (Response Spectrum Analysis)</b>					
Earthquake	Type of Analysis	Shear Building Model		Frame Model	
		$V_{base}$ kip	$M_{base}$ kip-ft	$V_{base}$ kip	$M_{base}$ kip-ft
Loma Prieta	Spectrum (24.5 %)	1445.50	35315.00	1442.90	24675.00
El Centro	Spectrum (24.5 %)	1300.00	28159.00	1597.00	26664.00

<b>Table 14</b> <b>Base Shears and Overturning Moments for El Centro and Loma Prieta Earthquakes (Time-History Analysis)</b>			
Earthquake	Type of Analysis	Frame Model	
		$V_{base}$ kip	$M_{base}$ kip-ft
Loma Prieta	Time-history	1099.25	39379.25
El Centro	Time-history	1222.78	30033.13

<b>Table 15</b> <b>Base Shears and Overturning Moments for El Centro and Loma Prieta Spectrum-Compatible Accelerograms (Response Spectrum Analysis)</b>					
Earthquake	Type of Analysis	Shear Building Model		Frame Model	
		$V_{base}$ kip	$M_{base}$ kip-ft	$V_{base}$ kip	$M_{base}$ kip-ft
Loma Prieta	Spectrum (24.5 %)	1486.40	35911.00	1732.20	28845.00
El Centro	Spectrum (24.5 %)	1474.00	34297.00	1849.80	29984.00

<b>Table 16</b> <b>Base Shears and Overturning Moments for El Centro and Loma Prieta Spectrum-Compatible Accelerograms (Time-History Analysis)</b>			
Earthquake	Type of Analysis	Frame Model	
		$V_{base}$ kip	$M_{base}$ kip-ft
Loma Prieta	Time-history	1293.13	39862.25
El Centro	Time-history	1548.90	29426.00

the shear building model approximated the seismic response of intake towers. The advantage of this model is its simplicity.

The agreement between the results of the time-history and spectrum analyses is quite reasonable for both earthquakes, and for the original and spectrum-compatible accelerograms. It is interesting to observe from the values in the tables that the agreement between the time-history and spectrum analyses is better when the shear building model is used. This could be because the errors introduced when a shear building model is used are somehow compensating for the approximations inherent in the response spectrum approach.

## Summary

This chapter presented numerical examples of the seismic analysis of intake-outlet towers and their evaluation. The numerical tools used for the analysis of the towers that accounts for the multiple-support excitation and soil-structure interaction effects were two finite element programs and a MATLAB-based program. A typical intake-outlet tower from the USACE inventory was selected for all the analyses. Thus, this study can help to establish a behavioral pattern of the dynamic response of comparable towers founded on similar soil conditions.

The response of the towers, including the access bridge and multiple-support excitations, indicates that these effects are not significant, at least for this case study. The amplification of the ground acceleration at the bridge support was not significant, probably due to the particular soil conditions and geometry of the dam. Another important finding of the study is that the dynamic response of this intake tower is mainly influenced by the soil-structure interaction effects. The soil-structure interaction in this system was very strong due to the large



differences between the stiffness of the soil and the tower. That is, the intake tower is very rigid compared with the soft soil beneath it. The results also indicate that the rocking stiffness is the parameter that plays the most important role in the dynamic response of the structural system studied. Therefore, it is crucial to have accurate expressions to evaluate the stiffness of the spring associated with the rocking motion.

The values obtained with commonly used formulas did not provide satisfactory results in the present study. To overcome this problem, new values of the stiffness coefficients were obtained by applying a unit force (or moment) to the finite element model at the location of the foundation and calculating the displacement (or rotation). It is realized, however, that this approach is not practical and thus more research is needed on this subject. Finally, it is important to emphasize that the effects of multiple-support excitation and soil-structure interaction should be reviewed on a case-by-case basis. It may happen that, for other towers and dams, the importance of these two effects, or the lack of it, could be reversed.

## 7 Conclusions and Recommendations

---

### Summary and Conclusions

This report presented the seismic analysis of a typical intake-outlet tower considering the multiple-support excitations and soil-structure interaction effects. The intake-outlet was selected based on data available from the USACE inventory. The Arkabutla Dam located in northern Mississippi, 30 miles south of Memphis, TN, was chosen for the analysis because it is of particular interest for the Corps of Engineers. The geometry of the original intake tower was changed so that it became relatively simple to permit a simplification of the analysis. The analyses were performed using several two-dimensional finite element models and a frame model. A computer program was also developed for this investigation using MATLAB. Two finite element computer programs were used: QUAD4M and SAP2000. The finite element models developed are the Arkabutla Dam (using QUAD4M and SAP2000) and the Arkabutla Dam plus the intake tower (using SAP2000). The models implemented in the MATLAB program are two plane frame models of the intake tower with and without the bridge, and the same systems with springs and dashpots at the supports. Included in the MATLAB program are the formulation for multiple-support excitation effects, the soil-structure interaction problem, and the simplified procedure for the calculation of the added hydrodynamic masses.

The finite element model of the dam plus the intake tower with the access bridge was regarded as the "exact" model for the comparison with the simplified models. The main response quantity used for the comparison is the relative displacement at the top of the tower. The results are presented in terms of plots of the top relative displacement as function of time. The base shear and overturning moments were calculated when a response spectrum analysis was done.

One of the principal findings of this report was that the effect of the multiple-support excitation in the response of the tower and service bridge is not important and it can be disregarded. The slight variation in the soil properties between the base of the tower and the location of the bridge, combined with low aspect ratio of earth dam geometry, may have contributed to this result. Due to the similar soil properties and geometry of the dam, the acceleration at the base of the tower was similar to that at the bridge support. Before undertaking the study, it was

expected that there would be significant differences between the acceleration time-histories at the two supports, but the results demonstrated otherwise.

Another important result obtained from this research is the demonstration of the important influence of the soil-structure interaction effects in the response of the tower. Initially, this effect was not going to be included in the study because it was not deemed to be important. However, the completely different responses obtained with the model of the tower plus bridge with fixed bases and those from the "exact" finite element model led to the authors investigating this effect. By examining the response of the tower from the finite element model, it could be seen that the displacements were the sum of those due to the bending deformation plus those due to the rotation of the tower as a rigid body. To confirm that the soil-structure interaction was responsible for the differences observed, the accelerations at the interface between the tower and the soil with the tower included in the finite element model were compared with those obtained at the free surface of the model of the dam without the tower. As was suspected, the accelerations were quite different.

It was then decided to account for the soil-structure interactions by simple means so that they can be incorporated in the frame model of the tower and bridge system. The simplest way to consider the soil-structure interaction is by means of springs and dashpots at the base of the structure. This idea was originally developed for the study of vibration of machine foundations. Then the following problem emerged: the formulas that define the stiffness and damping coefficients of the springs and dashpots cannot be applied at the end of the bridge that lies on the dam. Indeed, these coefficients were obtained under the premise that a harmonic force was applied to a rigid circular disk resting on top of an elastic half-space. Clearly, the crest of a dam is far from this assumption. Therefore, it was decided to obtain the stiffness coefficients by applying a unit force at the top of the dam, one at a time in two directions (horizontal and vertical). Moreover, it was also decided not to place any dashpots there (a conservative assumption).

To obtain more accurate values for the stiffness coefficients, as well as to determine the dashpot coefficients, one has to apply a force of the form  $e^{i\omega t}$  and obtain the steady-state response for different excitation frequencies  $\omega$ . This option was not pursued because it was beyond the scope of the report. The coefficients for the springs and dashpots in three directions (horizontal, vertical, and rotation about an axis normal to the plane) at the tower base were taken from the technical literature. When the response of the frame with the springs and dashpots was compared with the finite element model, the matching was acceptable for certain earthquakes but inaccurate for others. Additionally, a comparison of the tower's natural periods detected that the periods of the finite element model were larger than those predicted by the frame with springs and dashpots. By varying the values of the spring coefficients to try to obtain a better agreement, it was found that the coefficient of the rocking spring was responsible for the mismatch. This is another finding of the research: at least for the case studied in this investigation, the coefficient associated with the rocking motion of the foundation does not well represent the flexibility of the soil. Therefore, it was concluded that the value of the rocking stiffness would have to be determined by applying a

unit moment at the free surface. When used with the frame model, the value obtained in this way allowed a very good agreement with the results from the full finite element model of the dam-tower-bridge-foundation system.

It can be argued that the soil underneath the reservoir of the case studied was soft and that in other cases the soil-structure interaction will not be important. However, to establish if this is indeed the case, a brief parametric study was undertaken in which the stiffness of the soil deposit (the shear wave velocity or elastic moduli) was gradually increased. It was found that the effect remained important except for a material that could be characterized as a hard rock.

## Recommendations for Further Studies

Although this study tried to be as comprehensive as possible within the time constraints, there are a number of topics or ideas that were not addressed or explored because of time limitations or because they fall outside the scope of the study. However, it is believed that studying these topics is worthwhile and can complement the results of this work. The subjects recommended for further studies are listed below in no specific order.

- a. A nonlinear analysis of the intake-outlet should be performed to examine the dynamic behavior of this kind of structure until failure or when the tower begins to degrade during a severe earthquake.
- b. The nonlinear analysis can be extended to include the model of the dam plus the intake tower. When the nonlinear behavior of the soil is considered, the stiffness of the soil changes with time, depending on the level of strains (Kumar and Prakash 1997). Thus, at any particular time, the strains in soil and thus the foundation stiffness will not be the same for any two different base input motions. It will be very interesting to study this phenomenon for intake-outlet towers. To do that, it will be necessary to use another computer program with the capabilities to perform nonlinear analysis of soil structures in addition to conventional ones.
- c. The same methodology used in this study can be applied to other towers with typical dimensions but for taller dams. The multiple-support excitation effects could be important in these cases, especially if the material of the dam is quite different from the soil beneath the tower.
- d. The accuracy of the stiffness coefficients of the springs representing the rocking motion should be examined. To properly account for the soil-structure interaction effects in tall, slender structures such as intake towers and chimneys, it is crucial to have reliable values of these coefficients.
- e. It will be useful for future analysis of tower-bridge systems to have spring and dashpot coefficients obtained for a wedge-like soil structure

such as an earthen dam. This could, in principle, be done in an analytical fashion following a procedure similar to that for the elastic half-space case. However, due to the complexity of the geometry, it is more likely that the study will have to be done numerically. In this case, many geometrical configurations of the dam will have to be studied in order to obtain coefficients that are a function of the aspect ratio of the dam (height/base length) and the properties of the predominant soil type ( $G$ ,  $\rho$ , and  $\nu$ ).

- f.* The survey conducted by the U.S. Army Corps of Engineers in which they identified the typical properties of the intake-outlet towers under their jurisdiction should be extended to include the typical configurations of the service bridges. An inventory of the service bridges could be very useful in identifying the typical bridge supports, sections, and other details that are necessary in the modeling process of this kind of system.
- g.* It would be interesting to include the effects of the conduits or tunnels in the seismic analysis of the intake-outlet towers. These conduits or tunnels are very large and could play an important role in the response of the tower with the dam.
- h.* Extending the analysis of the tower and bridge systems in the perpendicular direction, i.e., along the longitudinal axis of the dam, should be done. This could be very useful in identifying the effect of the torsion produced by the bridge in the tower and its influence in the overall response of the system.
- i.* Special attention should be paid to the support of the bridge. Depending on the type of foundation, the bridge might slide along the foundation as the result of a strong earthquake.

# References

---

- Bard, P. Y. (1988). "The importance of rocking in building motion: An experimental evidence." *Proceedings of Ninth World Conference on Earthquake Engineering*, August 1988, Tokyo, Japan. Vol VIII, 333-38.
- Building Seismic Safety Council. (2001). "NEHRP recommended provisions (National Earthquake Hazards Reduction Program) for seismic regulations for new buildings and other structures," Washington, DC.
- Chang, F. (1990). "Earthquake response spectral analysis of Arkabutla Dam, Mississippi: Report 1," U.S. Army Engineer Division, Vicksburg, Vicksburg, MS, 1-17.
- Chopra, A., and Liaw, C-Y. (1975). "Earthquake resistant design of intake-outlet towers." *Proceedings of the American Society of Civil Engineers*, July 1975. *Journal of the Structural Division* 101(ST7), 1349-66.
- CSI. (2000). "SAP2000 analysis reference manual," Computers and Structures, Inc., Berkeley, CA.
- Daniell, W. E., and Taylor, C. A. (1994). "Full-scale dynamic testing and analysis of a reservoir intake tower," *Earthquake Engineering and Structural Dynamics* 23, 1219-37.
- Der Kiureghian, A., and Neuenhofer, A. (1991). "A response spectrum method for multiple-support seismic excitations," Technical Report UCB/EERC-91/08, College of Engineering, University of California, Berkeley.
- Dove, R. (1996). "Structural parameter analysis of U.S. Army Corps of Engineers existing intake tower inventory," Technical Report SL-96-1, U.S. Army Engineer Waterways Experiment Station, Vicksburg, MS.
- Dove, R. (1998). "Performance of lightly reinforced concrete intake towers under selected loading," Technical Report SL-98-1, U.S. Army Engineer Waterways Experiment Station, Vicksburg, MS.
- \_\_\_\_\_. (2000). "Ultimate deflection response of lightly reinforced concrete intake towers," Technical Report SL-00-06, U.S. Army Engineer Waterways Experiment Station, Vicksburg, MS.

- Dove, R., and Matheu, E. (2002a). "Seismic performance evaluation of intake towers," *Proceedings, 34th Joint Meeting UJNR Panel on Wind and Seismic Effects*, 13-15 May 2002, Gaithersburg, MD.
- \_\_\_\_\_. (2002b). "Dynamic response of lightly reinforced concrete intake towers," *Proceedings, 3d U.S.-Japan Workshop on Advanced Research on Earthquake Engineering for Dams*, 22-23 June 2002, San Diego, CA.
- Gazetas, G. (1991). "Formulae and charts for impedance functions of surface and embedded foundations," *Journal of Geotechnical Engineering (ASCE)* 117(9), 1363-81.
- Gazetas, G., Dobry, R., and Tassoulas, J. (1985). "Vertical response of arbitrarily-shaped embedded foundations," *Journal of Geotechnical Engineering (ASCE)* 111(GT6), 750-771.
- Goyal, A., and Chopra, A. (1989a). "Simplified evaluation of added hydrodynamic mass for intake towers," *Journal of Engineering Mechanics* 115(7), 1393-1435.
- \_\_\_\_\_. (1989b). "Hydrodynamic and foundation interaction effects in dynamics of intake towers: Frequency response functions," *Journal of Structural Engineering* 115(6), 1371-85.
- \_\_\_\_\_. (1989c). "Earthquake response spectrum analysis of intake-outlet towers," *Journal of Engineering Mechanics* 115(7), 1413-31.
- Harichandran, R., and Wang, W. (1988). "Response of simple beam to spatially varying earthquake excitation," *Journal of Engineering Mechanics* 114(9), 1526-41.
- \_\_\_\_\_. (1989). "Response of indeterminate two-span beam to spatially varying seismic excitation," *Earthquake Engineering and Structural Dynamics* 19, 173-87.
- Headquarters, U.S. Army Corps of Engineers. (2003). "Structural design and evaluation of outlet works," Engineer Manual 1110-2-2400, Washington, DC.
- Hudson, M., Idriss, I. M., and Beikae, M. (1994). *User's manual for QUAD4M*. University of California, Davis.
- Idriss, I. M., Lysmer, J., Hwang, R., and Seed, H. B. (1973). "QUAD4: A computer program for evaluating the seismic response of soil structures by variable damping finite element procedures," Report No. EERC 73-16, University of California, Berkeley.
- International Conference of Building Officials (ICBO). (1997). "Uniform building code," Vol 2, Whittier, CA.

- Kramer, S. (1996). *Geotechnical earthquake engineering*. Prentice Hall, New Jersey, 294-303.
- Kumar, S., and Prakash, S. (1997). "Natural frequency response of structures considering soil-structure interaction." *Proceedings of Discussion, Special Technical Session on Earthquake Geotechnical Engineering*, Fourteenth International Conference on Soil Mechanics and Foundation Engineering. Hamburg, Germany. 225-33.
- Liaw, C.-Y., and Chopra, A. K. (1974). "Dynamics of tower surrounded by water," *Earthquake Engineering and Structural Dynamics* 1(3), 33-49.
- Loh, C.-H. (1991). "Stochastic response of lifeline to spatial variation of seismic waves." *Proceedings of the Second International Conference on Recent Advances in Geotechnical Earthquake Engineering and Soil Dynamics*. St. Louis, MO. Paper No. 5.9, 711-17.
- Loh, C.-H., and Ku, B.-D. (1995). "An efficient analysis of structural response for multiple support seismic excitations." *Engineering Structures* 17(1), 15-26.
- Lysmer, J. (1965). "Vertical motion of rigid footings," Ph.D. diss., University of Michigan, Ann Arbor, MI.
- (The) MathWorks. (2000). "MATLAB: The language of technical computing," The MathWorks, Inc., Natick, MA.
- Montejo, L. A. (2004). "Generation and analysis of spectrum-compatible earthquakes time-histories using wavelets." M.S. thesis, University of Puerto Rico, Mayagüez.
- Newmark, N. M., and Hall, W. J. (1982). "Earthquake spectra and design." *Earthquake Engineering Research Institute*. Berkeley, CA.
- Newmark, N. M., and Rosenblueth, E. (1971). *Fundamentals of earthquake engineering*. Prentice Hall, Englewood Cliffs, NJ, 93-100.
- Paz, M. (1997). *Structural dynamics: Theory and computation*. 4th ed., Chapman and Hall, New York, 399-430.
- Po Lam, I., and Law, H. (2000). "Soil structure interaction of bridge for seismic analysis," MCEER Report No. 00-0008, State University of New York at Buffalo.
- Rutenberg, A., and Heidebrecht, A. C. (1988). "Approximate spectral multiple support seismic analysis: Traveling wave approach." *Proceedings of the Institution of Civil Engineers*, Part 2, 85, 223-236.
- Safak, E. (1995). "Simulation of earthquake motions at soil sites." *Proceedings for the Fifth U.S. National Conference on Earthquake Engineering*, Chicago, IL. III, 35-44.



- Schnabel, P. B., Lysmer, J., and Seed, H. B. (1972). "SHAKE: A computer program for earthquake response analysis of horizontally layered sites," Report No. 72-12, Earthquake Engineering Research Center, University of California, Berkeley.
- Seed, H. B. J., and Idriss, I. M. (1970). "Soil moduli and damping factors for dynamic response analyses." Report No. EERC 70-10, Earthquake Engineering Research Center, University of California, Berkeley.
- Shaw, D. E. (1975). "Seismic structural response analysis for multiple support excitations." *Proceedings, 3<sup>rd</sup> International Conference on Structural Mechanics in Reactor Technology (SMIRT)*, London. Part K, 4, 1-8.
- Sun, J. I., Golesorkhi, R., and Seed, H. B. (1988). "Dynamic moduli and damping ratios for cohesive soils," Report No. EERC 88/15, Earthquake Engineering Research Center, University of California, Berkeley.
- Westergaard, H. M. (1933). "Water pressures on dams during earthquakes," *Transactions, ASCE* 98, 418-33.
- Williams, A. N. (1990). "Analysis of the base-excited response of intake-outlet towers by a Green's function approach," *Engineering Structures* 13, 43-53.
- Yamamura, N., and Tanaka, H. (1990). "Response analysis of flexible MDF systems for multiple-support seismic excitations," *Earthquake Engineering and Structural Dynamics* 19(3), 345-57.
- Zembaty, Z., and Rutenberg, A. (2002). "Spatial response spectra and site amplification effects," *Engineering Structures* 24, 1485-96.
- Zerva, A. (1988). "Effects of spatial variation of ground motions on bridges." *Proceedings of the 5<sup>th</sup> ASCE Specialty Conference*, Blacksburg, VA. 253-56.
- \_\_\_\_\_. (1991). "Effects of spatial variability and propagation of seismic ground motions on the response of multiple supported structures," *Probabilistic Engineering Mechanics* 6(3-4), 212-21.
- \_\_\_\_\_. (1992). "Seismic ground motion simulations from a class of spatial variability models," *Earthquake Engineering and Structural Dynamics* 21(4), 351-61.



**REPORT DOCUMENTATION PAGE**Form Approved  
OMB No. 0704-0188

Public reporting burden for this collection of information is estimated to average 1 hour per response, including the time for reviewing instructions, searching existing data sources, gathering and maintaining the data needed, and completing and reviewing this collection of information. Send comments regarding this burden estimate or any other aspect of this collection of information, including suggestions for reducing this burden to Department of Defense, Washington Headquarters Services, Directorate for Information Operations and Reports (0704-0188), 1215 Jefferson Davis Highway, Suite 1204, Arlington, VA 22202-4302. Respondents should be aware that notwithstanding any other provision of law, no person shall be subject to any penalty for failing to comply with a collection of information if it does not display a currently valid OMB control number. PLEASE DO NOT RETURN YOUR FORM TO THE ABOVE ADDRESS.

<b>1. REPORT DATE (DD-MM-YYYY)</b> September 2004		<b>2. REPORT TYPE</b> Final report		<b>3. DATES COVERED (From - To)</b>	
<b>4. TITLE AND SUBTITLE</b>  Seismic Analysis of Intake Towers Considering Multiple-Support Excitation and Soil-Structure Interaction Effects				<b>5a. CONTRACT NUMBER</b>	
				<b>5b. GRANT NUMBER</b>	
				<b>5c. PROGRAM ELEMENT NUMBER</b>	
<b>6. AUTHOR(S)</b>  Aidcer L. Vidot, Luis E. Suárez, Enrique E. Matheu, and Michael K. Sharp				<b>5d. PROJECT NUMBER</b>	
				<b>5e. TASK NUMBER</b>	
				<b>5f. WORK UNIT NUMBER</b> 33013	
<b>7. PERFORMING ORGANIZATION NAME(S) AND ADDRESS(ES)</b>  Department of Civil and Environmental Engineering, University of Puerto Rico, Mayagüez Campus, Mayagüez, PR 00681; Geotechnical and Structures Laboratory, U.S. Army Engineer Research and Development Center, 3909 Halls Ferry Road, Vicksburg, MS 39180-6199				<b>8. PERFORMING ORGANIZATION REPORT NUMBER</b>  ERDC/GSL TR-04-16	
<b>9. SPONSORING / MONITORING AGENCY NAME(S) AND ADDRESS(ES)</b>  U.S. Army Corps of Engineers Washington, DC 20314-1000				<b>10. SPONSOR/MONITOR'S ACRONYM(S)</b>	
				<b>11. SPONSOR/MONITOR'S REPORT NUMBER(S)</b>	
<b>12. DISTRIBUTION / AVAILABILITY STATEMENT</b> Approved for public release; distribution is unlimited.					
<b>13. SUPPLEMENTARY NOTES</b>					
<b>14. ABSTRACT</b>  This report investigates the seismic response of intake-outlet towers. The effect of different ground accelerations at the supports of the tower and inspection bridge is examined. The water outside and inside the tower is accounted for by added masses. The accelerations at the bridge support and tower base are obtained from a finite element model of the dam and soil foundation. The other effect examined is the soil-structure interaction. First, a direct approach based on a finite element model of the tower, bridge, and dam with the earthquake motion applied at the bedrock is used. The second approach uses a frame model of the tower and bridge with springs and dashpots accounting for the soil-structure interaction. This simple model provides reasonable results if adequate values of the torsional spring are used. The effects of the soil-structure interaction proved to be much more important than the multiple support excitation.					
<b>15. SUBJECT TERMS</b> Dynamic stress analysis                      Ground motions                      Multiple-support excitation Dynamic stresses                              Intake towers                          Soil-structure interaction					
<b>16. SECURITY CLASSIFICATION OF:</b>			<b>17. LIMITATION OF ABSTRACT</b>	<b>18. NUMBER OF PAGES</b>  104	<b>19a. NAME OF RESPONSIBLE PERSON</b> Enrique E. Matheu
<b>a. REPORT</b> UNCLASSIFIED	<b>b. ABSTRACT</b> UNCLASSIFIED	<b>c. THIS PAGE</b> UNCLASSIFIED			<b>19b. TELEPHONE NUMBER (include area code)</b> (601) 634-3235